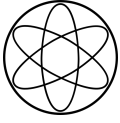


Technische Universität München

**Nucleon-Nucleon Interaction
with Coupled Nucleon-Delta Channels
in Chiral Effective Field Theory**

Susanne Strohmeier

April, 2020



Technische Universität München
Physik Department
Lehrstuhl für Theoretische Physik T39



Nucleon-Nucleon Interaction
with Coupled Nucleon-Delta Channels
in Chiral Effective Field Theory

Susanne Brigitte Strohmeier

Vollständiger Abdruck der von der Fakultät für Physik der Technischen Universität München zur Erlangung des akademischen Grades eines

Doktors der Naturwissenschaften (Dr. rer. nat.)

genehmigten Dissertation.

Vorsitzende: Prof. Dr. Laura Fabbietti

Prüfer der Dissertation: 1. apl. Prof. Dr. Norbert Kaiser
2. Prof. Dr. Andreas Weiler

Die Dissertation wurde am 11.05.2020 bei der Technischen Universität München eingereicht und durch die Fakultät für Physik am 03.07.2020 angenommen.

This thesis contains material which has previously been published in

S. Strohmeier and N. Kaiser, “Nucleon-Nucleon Scattering with Coupled Nucleon-Delta Channels in Chiral Effective Field Theory,” [arXiv:2004.12964](https://arxiv.org/abs/2004.12964) [nucl-th].



This work has been supported in part by the DFG and the NSFC through funds provided to the Sino-German CRC 110 “Symmetries and the Emergence of Structure in QCD”, the Excellence Cluster UNIVERSE, the Excellence Cluster ORIGINS, the TUM Graduate School, and the Wilhelm und Else Heraeus-Stiftung.

ABSTRACT

In this work the potential for elastic scattering of two nucleons is calculated in chiral effective field theory at next-to-leading order with coupled $N\Delta$ - and $\Delta\Delta$ -channels. To solve the coupled channel scattering equation one needs the potentials of all possible combinations of initial and final states (NN , $N\Delta$, ΔN , $\Delta\Delta$) up to this order. We give analytic expressions for the spectral functions of the two-pion exchange for all contributing one-loop diagrams. The contact potentials at leading and next-to-leading order and the corresponding low energy constants are determined. The rich coupling of the $N\Delta$ and $\Delta\Delta$ contact potentials to the nucleon-nucleon channels is investigated. We perform a fit of the low energy constants, which arise from the $NN \rightarrow NN$ contact potential and contribute at next-to-leading order to the NN S- and P-waves only. The influence of the Δ -isobar dynamics entering through the coupled channels is studied in detail.

ZUSAMMENFASSUNG

In dieser Arbeit wird das Potential für die elastische Streuung zweier Nukleonen in chiraler effektiver Feldtheorie bis zur nächst führenden Ordnung mit gekoppelten $N\Delta$ - und $\Delta\Delta$ -Kanälen berechnet. Um die Streugleichung mit gekoppelten Kanälen zu lösen, werden die Potentiale aller möglichen Kombinationen aus Anfangs- und Endzustand (NN , $N\Delta$, ΔN , $\Delta\Delta$) bis zu dieser Ordnung benötigt. Wir geben analytische Ausdrücke für die Spektralfunktionen des Zweipionenaustausches für alle möglichen Einschleifendiagramme an. Die Kontaktpotentiale in führender und nächst führender Ordnung und die dazugehörigen Parameter werden bestimmt. Die umfangreiche Kopplung der $N\Delta$ - und $\Delta\Delta$ -Kontaktpotentiale an die Nukleon-Nukleon-Kanäle wird untersucht. Wir führen einen Fit der Niederenergiekonstanten, die aus dem $NN \rightarrow NN$ Kontaktpotential stammen und auf nächst führender Ordnung zu den NN S- und P-Wellen beitragen, durch. Der dynamische Einfluss des Δ -Isobars, der durch die gekoppelten Kanäle entsteht, wird detailliert untersucht.

*Daß ich erkenne, was die Welt
Im Innersten zusammenhält*
— J. W. von Goethe, *Faust*

CONTENTS

1	INTRODUCTION	1
2	QUANTUM CHROMODYNAMICS AND CHIRAL EFFECTIVE FIELD THEORY	5
2.1	Quantum chromodynamics	5
2.1.1	QCD Lagrangian	5
2.1.2	Symmetries of QCD	6
2.2	Chiral effective field theory	7
2.2.1	Chiral effective Lagrangian	7
2.2.2	Δ -isobar as explicit degree of freedom	9
2.2.3	Effective Lagrangian in heavy baryon limit	10
2.2.4	Propagators and vertices in non-relativistic limit	13
2.2.5	Power counting in chiral effective field theory	13
3	NUCLEON NUCLEON POTENTIAL	15
3.1	Scattering equations	16
3.2	Treatment of principle value integrals	19
3.3	Regularization	20
3.4	Partial wave projection	21
4	ONE- AND TWO-PION EXCHANGE	23
4.1	One-pion exchange potentials	23
4.2	Two-pion exchange potentials	23
4.2.1	Lorentz tensors and pertinent projectors	27
4.2.2	Phase space integral including spin matrices	31
4.2.3	Irreducible 2π -exchange from planar box diagrams	32
4.3	Contributions of two-pion exchange box diagrams	34
4.4	Triangle and bubble diagrams	43
5	CONTACT POTENTIAL	47
5.1	Definition of contact potential and low-energy constants	47
5.2	Fits of low-energy constants	53
5.2.1	Fits to Nijmegen phase shifts	53
5.2.2	Fits of leading order contact potentials in coupled channel approach	54
5.2.3	Influence of contact interactions involving deltas	57
6	PHASE SHIFTS	61
6.1	Peripheral phase shifts	61
6.1.1	F-waves	61

6.1.2	G-waves	62
6.1.3	H-waves	63
6.1.4	I-waves	65
6.2	Phase shifts in low partial waves	66
6.2.1	S-waves	66
6.2.2	P-waves	66
6.2.3	D-waves	68
6.3	Influence of the $N\Delta$ -coupled channels	70
6.4	Comparison of results for two scattering equations	71
6.5	Next-to-next-to-leading order effects	73
7	SUMMARY AND CONCLUSION	75
A	CONVENTIONS	77
A.1	General conventions	77
A.2	Spin and isospin matrices and relations	78
A.3	Isospin matrix elements	80
A.4	Non-relativistic expansion	80
A.5	Projectors entering two-pion phase space integrals	81
B	QUANTUM NUMBERS OF COUPLED CHANNELS	83
C	RELATIONS FOR LOW ENERGY CONSTANTS	87
C.1	Definition of LECs in spectroscopic notation	87
C.2	Relations for LECs in spectroscopic notation	92
	BIBLIOGRAPHY	95

INTRODUCTION

The theoretical description of nuclear forces started in 1935 with Yukawa's meson exchange theory [1]. The one-pion exchange led to promising results, whereas multi-pion exchanges rendered the perturbative expansion uncontrollable because of the large pion-nucleon coupling constant. Many models of nuclear forces came up before the formulation of quantum chromodynamics (QCD) as the fundamental theory of strong interactions. However, QCD is highly nonperturbative in the energy regime of nuclear forces. This issue has been bypassed by the concept of a low-energy effective field theory. As Weinberg suggested, one should write down the most general Lagrangian consistent with the symmetries of the underlying theory [2]. In the case of QCD this is the spontaneously and explicitly broken chiral symmetry. The effective degrees of freedom in chiral effective field theory (ChEFT) are then pions, nucleons and other hadrons (e.g. vector mesons and baryon resonances), instead of quarks and gluons. Heavier degrees of freedom are understood to be integrated out.

In some sense, one is back to Yukawa's meson theory but with chiral symmetry now incorporated into the theory as a guiding principle. The classification of the nuclear potential by Taketani et al. [3] is still valid, but it has been refined over the years. The NN-potential can be divided into three parts where different types of interactions dominate, see Fig. 1.1. The long distance region III is described by one-pion exchange. The force at intermediate distances (region II) is dominated by two-pion exchange. The short-distance part in region I is then described in chiral effective field theory by a unresolved contact interaction. In absence of other information, the unknown low-energy constants of this contact interaction are then fitted to scattering data.

The calculations within chiral effective field theory started with the calculation of $\pi\pi$ and πN scattering to one loop order by Gasser and Leutwyler [5,6]. Weinberg's approach to the nuclear force [7,8] suggested to calculate the nucleon-nucleon potential perturbatively and then iterate it to all orders by a scattering equation. Applications of the chiral Lagrangian to the two-nucleon system using time ordered perturbation theory were performed in Refs. [9,10] and to the πN -observables in Ref. [11].

The NN potential up to next-to-leading order (NLO) was derived in Ref. [12] using dimensional regularization. Single and double Δ -isobar excitations were included in Ref. [13] as well as next-to-next-to-leading order (N2LO) contributions. In Refs. [14,15] the two nucleon potential was calculated up to N2LO with the method of unitary transformations, including also the Δ -isobar as an explicit degree of freedom in intermediate states for the two-pion exchange. Further improvements of the NN potential with and without the

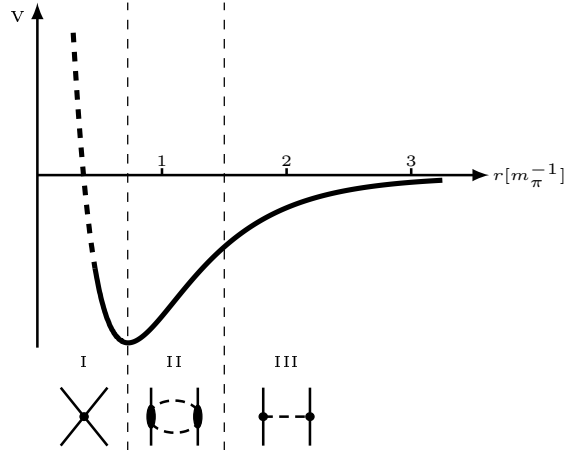


FIGURE 1.1: Schematic picture showing the nucleon-nucleon potential divided into three regions where different types of interactions dominate. The distance r is given in units of the pion Compton wavelength $m_\pi^{-1} = 1.4$ fm. Adapted from Refs. [3, 4]

Δ -isobar were derived by different groups e.g. in Refs. [16–22] up to dominant N5LO contributions in Ref. [23] or a N4LO potential including N5LO contact interactions in Ref. [24].

A coupled $N\Delta$ -channel approach was used for a phenomenological potential in Refs. [25–27] and as an extension of the so-called CD-Bonn potential [28] in Refs. [29, 30]. The structure of the chiral effective Lagrangian for pions, nucleons and Δ -isobars was derived in detail in Ref. [31] and some parts of this Lagrangian have been worked out in Ref. [32].

In this work, we include the coupled $N\Delta$ - and $\Delta\Delta$ -channels in the calculation of the two nucleon S-matrix in chiral effective field theory in order to investigate the influence of the dynamics of the Δ -isobar. For this purpose, we derive the interaction potential among nucleons and Δ -isobars at leading and next-to-leading order and make use of a coupled channel scattering equation.

In Chapter 2 a brief introduction of quantum chromodynamics and chiral effective field theory is given. The power counting scheme of ChEFT is discussed. We summarize the Lagrangians for the interactions among pions, nucleons and deltas in the non-relativistic heavy baryon limit.

In Chapter 3 we give the general structure of the NN-potential and discuss different types of scattering equations. The derivation of the so-called local regularization is summarized. The chapter closes with the method used to perform partial wave projections most conveniently. In Chapter 4 the LO and NLO potentials are derived in detail. The NLO potentials are given in terms of spectral functions and dispersion integrals. We derive the relevant projectors for the decomposition of 2π phase space integrals that contain specific Lorentz tensors appearing in the calculation of two-pion exchange. The irreducible part of 2π exchange from planar box diagrams is determined by considering the pertinent integrals over the loop-energy.

In Chapter 5 the contact terms at LO and NLO are worked out. The contact potential is projected onto the partial waves for the (NN, N Δ , Δ N, $\Delta\Delta$)-system and the relations between these two descriptions of the contact-potentials are worked out. The fitted values of the NN low-energy constants are given. The influence of contact interactions involving up to four Δ -isobars is discussed. Only a limited part of these can be determined by the fit routine.

In Chapter 6 we show our results for the NN-phase shifts and mixing angles. Results for scattering equations are compared, namely the Kadyshevsky equation and the Lippmann-Schwinger equation. The results in the coupled channel approach are compared to those obtained with the next-to-next-to-leading order potential in the delta-less case.

The entire thesis is concluded in Chapter 7.

QUANTUM CHROMODYNAMICS AND CHIRAL EFFECTIVE
FIELD THEORY

The Standard Model of particle physics describes three of the four fundamental forces in nature. Among them, the strong force between quarks and gluons is described by the theory of quantum chromodynamics (QCD). Due to its non-abelian nature the coupling α_s decreases at high energies and QCD can be treated perturbatively in this regime. This weak coupling leads to asymptotic freedom of quarks and gluons. However, at low momentum transfer the coupling gets very strong and the quarks and gluons are confined into color neutral hadrons. QCD is highly non-perturbative at these low energies. The nuclear force is part of the QCD dynamics in this low-energy domain. Its description on the quark level is quite complex, but it can be investigated non-perturbatively with lattice QCD, where numerical simulations of full QCD are performed on a discretized finite Euclidean space-time lattice. Another possibility consist of utilizing color confinement. The substructure of hadrons is not resolved at sufficiently low energies. So one can build an effective field theory for point-like hadrons obeying the symmetries of QCD, called chiral effective field theory. Due to the presence of a small expansion parameter and a power counting, a perturbative expansion of the nuclear force in this low-energy regime becomes possible.

In this chapter, we give a short overview of QCD and its symmetries. A short derivation of chiral effective field theory (ChEFT) is presented, together with the inclusion of the Δ -isobar as additional degree of freedom and the resulting power counting scheme. This chapter follows closely Refs. [11, 31, 33–35].

2.1 QUANTUM CHROMODYNAMICS

2.1.1 QCD Lagrangian

QCD is the gauge field theory describing the strong interactions with the non-abelian group $SU(3)_{\text{color}}$ as the underlying gauge group. The fundamental degrees of freedom in QCD are quarks and gluons. Quarks are spin- $\frac{1}{2}$ fermions and gluons are massless vector bosons. The QCD Lagrangian is given by

$$\mathcal{L}_{\text{QCD}} = \sum_{f=u,d,s,c,b,t} \bar{q}_f (i\gamma^\mu \mathcal{D}_\mu - m_f) q_f - \frac{1}{4} G_{\mu\nu,a} G_a^{\mu\nu} \quad (2.1)$$

with the quark fields q_f (in six flavors: *up*, *down*, *charm*, *strange*, *top*, *bottom*), the Dirac matrices γ^μ , and the quark masses m_f . Each quark field q_f is a color triplet, i. e. $q_f = (q_f^{\text{red}}, q_f^{\text{green}}, q_f^{\text{blue}})$. The gauge-covariant derivative is given by

$$\mathcal{D}_\mu = \partial_\mu - ig \frac{\lambda_a}{2} A_{\mu,a} , \quad (2.2)$$

and the gluon field strength tensor reads

$$G_{\mu\nu,a} = \partial_\mu A_{\nu,a} - \partial_\nu A_{\mu,a} + gf_{abc} A_{\mu,b} A_{\nu,c} . \quad (2.3)$$

Here, $A_{\mu,a}$ are the eight gluon fields, g is the strong coupling constant, λ_a are the Gell–Mann matrices, and the f_{abc} are the structure constants of the $\mathfrak{su}(3)$ Lie algebra satisfying the commutation relations $[\lambda_a, \lambda_b] = 2if_{abc}\lambda_c$.

2.1.2 Symmetries of QCD

In the following we consider only the two lightest types of quarks $f = u, d$. The quark fields can be decomposed into their right- and left-handed components,

$$q_R = P_R q \qquad q_L = P_L q \quad (2.4)$$

with the projection operators

$$P_R = \frac{1}{2}(1 + \gamma_5) \qquad P_L = \frac{1}{2}(1 - \gamma_5) . \quad (2.5)$$

In the so-called chiral limit, i. e. the limit of vanishing quark masses $m_u = m_d = 0$, the right- and left-handed quark fields decouple in the QCD Lagrangian

$$\mathcal{L}_{QCD}^0 = \bar{q}_R i\gamma^\mu \mathcal{D}_\mu q_R + \bar{q}_L i\gamma^\mu \mathcal{D}_\mu q_L - \frac{1}{4} G_{\mu\nu,a} G_a^{\mu\nu} . \quad (2.6)$$

This Lagrangian is invariant under the separate unitary transformations

$$q_R = \begin{pmatrix} u_R \\ d_R \end{pmatrix} \longrightarrow \mathcal{U}_R q_R = \exp\left(i\xi_a^R \tau^a\right) \begin{pmatrix} u_R \\ d_R \end{pmatrix} \quad (2.7)$$

and

$$q_L = \begin{pmatrix} u_L \\ d_L \end{pmatrix} \longrightarrow \mathcal{U}_L q_L = \exp\left(i\xi_a^L \tau^a\right) \begin{pmatrix} u_L \\ d_L \end{pmatrix} . \quad (2.8)$$

The matrices τ^a generate the $\mathfrak{su}(2)$ Lie algebra and \mathcal{U}_R and \mathcal{U}_L are elements of the flavor transformation groups $SU(2)_R$ and $SU(2)_L$, respectively. The QCD Lagrangian of massless u- and d-quarks possesses a $SU(2)_R \times SU(2)_L$ -symmetry, which is called the chiral symmetry. Noether's theorem states that there are six conserved currents. These can be written as three vector currents

$$J_V^{\mu,a} = \bar{q} \gamma^\mu \tau^a q \quad (2.9)$$

and three axial vector currents

$$J_A^{\mu,a} = \bar{q}\gamma^\mu\gamma_5\tau^a q. \quad (2.10)$$

By adding the (small) quark mass term $-m_u\bar{u}u - m_d\bar{d}d$ to the Lagrangian in Eq. (2.6), chiral symmetry gets explicitly broken, as the right- and left-handed quark fields are now mixing. In this case the axial-vector currents are not conserved any longer. However, the vector currents remain conserved for equal quark masses $m_u = m_d$, which corresponds to the usual isospin $SU(2)$ symmetry.

If a symmetry of the Lagrangian (or Hamiltonian) is not present in the ground state, this symmetry is called spontaneously broken. The non-observation of parity-doublets in the (low-energy) hadron spectrum implies that $SU(2)_R \times SU(2)_L$ is broken down to $SU(2)_V$. Therefore, the QCD ground state is invariant only under vector transformations but not under axial transformations. According to the Goldstone theorem, there have to exist three massless Goldstone bosons. These are identified with the isospin triplet of the pseudoscalar pions. In fact, the pions are not massless, because the chiral symmetry is also explicitly broken by (small) non-zero quark masses.

2.2 CHIRAL EFFECTIVE FIELD THEORY

To obtain an effective field theory of QCD, the soft and hard scales have to be identified. One chooses the soft scale to be given by the pion mass $Q \sim m_\pi$ and the hard scale as the chiral symmetry breaking scale $\Lambda_\chi \approx 1 \text{ GeV}$. If $\nu = Q/\Lambda_\chi$ is small, a perturbative expansion in this parameter can be applied. First, we have to construct the effective Lagrangian.

2.2.1 Chiral effective Lagrangian

The effective Lagrangian of chiral perturbation theory can be split into a pionic part $\mathcal{L}_{\pi\pi}$, the pion-nucleon interaction part $\mathcal{L}_{\pi N}$, and interactions between more nucleons (and pions):

$$\mathcal{L}_{eff} = \mathcal{L}_{\pi\pi} + \mathcal{L}_{\pi N} + \dots, \quad (2.11)$$

where $\mathcal{L}_{\pi\pi}$ and $\mathcal{L}_{\pi N}$ are sorted by the number of derivatives of the pion and nucleon fields:

$$\mathcal{L}_{\pi\pi} = \mathcal{L}_{\pi\pi}^{(2)} + \mathcal{L}_{\pi\pi}^{(4)} + \dots, \quad (2.12)$$

$$\mathcal{L}_{\pi N} = \mathcal{L}_{\pi N}^{(1)} + \mathcal{L}_{\pi N}^{(2)} + \dots. \quad (2.13)$$

The leading order $\pi\pi$ - and πN -Lagrangians, given in Refs. [5, 6], read

$$\mathcal{L}_{\pi\pi}^{(2)} = \frac{f_\pi^2}{4} \left(\text{Tr} \left[\partial_\mu U \partial^\mu U^\dagger \right] + m_\pi^2 \text{Tr} \left[U + U^\dagger \right] \right), \quad (2.14)$$

$$\mathcal{L}_{\pi N}^{(1)} = \bar{\psi} \left(i\gamma^\mu \mathcal{D}_\mu - M_N + \frac{g_A}{2} \gamma^\mu \gamma_5 u_\mu \right) \psi. \quad (2.15)$$

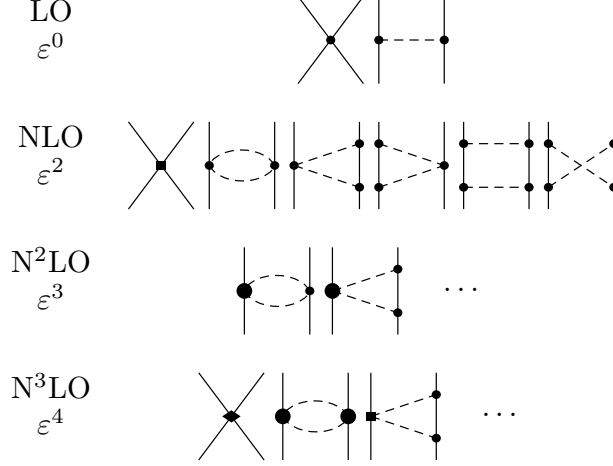


FIGURE 2.1: Contributions to the two- and three-nucleon force ordered by the power-counting scheme $\varepsilon = Q/\Lambda_\chi$. Solid and dashed lines denote nucleons and pions, respectively.

The $SU(2)$ matrix U collects the pion fields in the form

$$U = \frac{1}{f_\pi} \left(\sqrt{f_\pi^2 - \boldsymbol{\pi}^2} + i\boldsymbol{\tau} \cdot \boldsymbol{\pi} \right) \quad (2.16)$$

and the chirally covariant derivative reads

$$\mathcal{D}_\mu = \partial_\mu + \Gamma_\mu . \quad (2.17)$$

The so-called chiral connection Γ_μ is defined as

$$\Gamma_\mu = \frac{1}{2} [\xi^\dagger, \partial_\mu \xi] = \frac{1}{2} (\xi^\dagger \partial_\mu \xi + \xi \partial_\mu \xi^\dagger) = \frac{i}{4f_\pi} \boldsymbol{\tau} \cdot (\boldsymbol{\pi} \times \partial_\mu \boldsymbol{\pi}) + \mathcal{O}(\boldsymbol{\pi}^4) , \quad (2.18)$$

where

$$\xi = \sqrt{U} = 1 + \frac{i}{2f_\pi} \boldsymbol{\tau} \cdot \boldsymbol{\pi} - \frac{1}{8f_\pi^2} \boldsymbol{\pi}^2 + \frac{i}{16f_\pi^3} (\boldsymbol{\tau} \cdot \boldsymbol{\pi})^3 + \dots , \quad (2.19)$$

which has the property, $\xi \xi^\dagger = 1$, and therefore $\partial_\mu (\xi \xi^\dagger) = (\partial_\mu \xi) \xi^\dagger + \xi \partial_\mu \xi^\dagger = 0$. The axial vector quantity u_μ is defined as

$$\begin{aligned} u_\mu &= i \left\{ \xi^\dagger, \partial_\mu \xi \right\} = i \left(\xi^\dagger \partial_\mu \xi - \xi \partial_\mu \xi^\dagger \right) \\ &= -\frac{1}{f_\pi} \boldsymbol{\tau} \cdot \partial_\mu \boldsymbol{\pi} - \frac{1}{2f_\pi^3} (\boldsymbol{\tau} \cdot \boldsymbol{\pi}) (\boldsymbol{\tau} \cdot \partial_\mu \boldsymbol{\pi}) + \mathcal{O}(\boldsymbol{\pi}^5) . \end{aligned} \quad (2.20)$$

The leading interaction terms with one and two pion fields read [34]

$$\mathcal{L}_{\pi N}^{(1)} = \bar{\psi} \left(i\gamma^\mu \partial_\mu - M_N - \frac{g_A}{2f_\pi} \gamma^\mu \gamma_5 \boldsymbol{\tau} \cdot \partial_\mu \boldsymbol{\pi} - \frac{1}{4f_\pi^2} \gamma^\mu \boldsymbol{\tau} \cdot (\boldsymbol{\pi} \times \partial_\mu \boldsymbol{\pi}) + \dots \right) \psi . \quad (2.21)$$

Here, $M_N = 938.9$ MeV is the average nucleon mass, $m_\pi = 138.03$ MeV the average pion mass, $f_\pi = 92.4$ MeV the weak pion decay constant and $g_A = 1.29$ the nucleon axial vector coupling constant. To account for the Goldberger-Treiman discrepancy we do not use the experimental value $g_A = 1.2723(23)$ [36] determined in neutron β -decay. Our shifted value of g_A yields $g_{\pi N}^2/(4\pi) = 13.6$ for the charged pion-nucleon coupling constant $g_{\pi N} = g_A M_N / f_\pi$. This value of $g_{\pi N}$ is consistent with the determination from πN -scattering data based on the Goldberger-Miyazawa-Oehme sum rule $g_{\pi N}^2/(4\pi) = 13.69 \pm 0.20$ [37].

2.2.2 Δ -isobar as explicit degree of freedom

The $\Delta(1232)$ isobar is the lowest excited state of the nucleon. The mass splitting between the nucleon and the Δ -isobar is $\Delta = M_\Delta - M_N = 293$ MeV. Due to the small mass splitting and the strong coupling to the pion-nucleon system, the Δ -isobar should also be included in the effective field theory and this way the set of small scales gets extended [31, 34],

$$\varepsilon \in \left\{ \frac{q}{\Lambda_\chi}, \frac{m_\pi}{\Lambda_\chi}, \frac{\Delta}{\Lambda_\chi} \right\}. \quad (2.22)$$

This set defines to the so-called small scale expansion (SSE). The latter is a phenomenological extension, since the mass difference Δ does not vanish in the chiral limit. In the purely nucleonic or Δ -less theory the effects of the Δ -isobar are hidden in the constants of the higher order interactions, as it is shown in Fig. 2.2. Out of the four πN -low-energy constants at N²LO three (c_2, c_3, c_4) are shifted, if the Δ -isobars are treated explicitly [38].

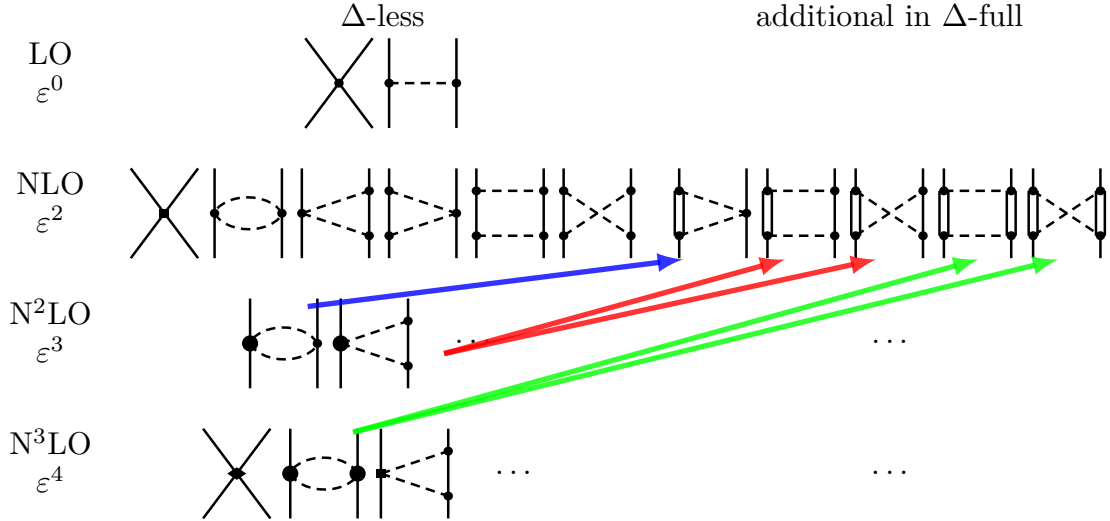


FIGURE 2.2: Power counting without and with explicit Δ -isobar degrees of freedom. The double lines denote Δ -isobars. The arrows indicate where the Δ is hidden in the Δ -less theory.

2.2.3 Effective Lagrangian in heavy baryon limit

The nucleon mass M_N is not small compared to the chiral symmetry breaking scale $\Lambda_\chi \approx M_N$ and it does not vanish in the chiral limit ($m_\pi \rightarrow 0$). Moreover, the time-derivative of the relativistic baryon field yields a factor of order $E \simeq M_N$. This feature destroys the strict correspondence between the expansion in pion loops and the expansion in small external momenta. The heavy baryon chiral effective theory (HBChEFT) [39] solves the issue by following an approach developed originally for systems containing heavy quarks [40]. In the extreme non-relativistic limit the baryons are treated as static sources. Then, the energy exchange between baryons is small compared to their momenta. This restores the one-to-one correspondence between the loop and the small momentum expansion, i.e. a consistent power counting scheme emerges [11].

The expansion in the heavy baryon limit for nucleons and deltas has been developed in detail in Refs. [31, 32]. We summarize the main steps here.

The nucleon four-momentum p_μ can be decomposed as

$$p_\mu = M_N v_\mu + k_\mu , \quad (2.23)$$

where the four-velocity v_μ satisfies $v^2 = 1$ and $k_\mu \ll M_N, \Lambda_\chi$. One defines the projection operators

$$P_\pm = \frac{1}{2}(1 \pm \not{v}) \quad (2.24)$$

giving rise to the light N -components and the heavy h -components of the nucleon field ψ_N via the relations

$$N(x) := \exp(iM_N v \cdot x) P_+ \psi_N(x) , \quad (2.25)$$

$$h(x) := \exp(iM_N v \cdot x) P_- \psi_N(x). \quad (2.26)$$

The nucleon sector

The heavy baryon projection can be combined with path integral methods as outlined in Ref. [41]. The transitions between the light and heavy components of the nucleon fields are then described by operators \mathcal{A} , \mathcal{B} and \mathcal{C} and yield the following Lagrangian,

$$\mathcal{L}_{\pi N} = \bar{N} \mathcal{A}_N N + \bar{h} \mathcal{B}_N N + \bar{N} \gamma_0 \mathcal{B}_N^\dagger \gamma_0 h - \bar{h} \mathcal{C}_N h. \quad (2.27)$$

These operators can be expanded chirally, i.e. $\mathcal{A} = \mathcal{A}^{(1)} + \mathcal{A}^{(2)} + \dots$. At their lowest orders, they read

$$\mathcal{C}_N^{(0)} = 2M_N , \quad (2.28)$$

$$\mathcal{A}_N^{(1)} = i v \cdot D + g_A S \cdot u , \quad (2.29)$$

$$\mathcal{B}_N^{(1)} = -\gamma_5 (2i S \cdot D + \frac{g_A}{2} v \cdot u) , \quad (2.30)$$

$$\mathcal{C}_N^{(1)} = i v \cdot D + g_A S \cdot u , \quad (2.31)$$

with the nucleon four-velocity v_μ and the Pauli-Lubanski spin-vector $S_\mu = \frac{i}{2}\gamma_5\sigma_{\mu\nu}v^\nu$, where $\sigma_{\mu\nu} = \frac{i}{2}[\gamma_\mu, \gamma_\nu]$. For the common choice $v^\mu = (1, \mathbf{0})$ one has $S^\mu = (0, \boldsymbol{\sigma})/2$. For the second order operators, Ref. [32] gives the following expressions,

$$\mathcal{A}_N^{(2)} = c_1\langle\chi_+\rangle + c_2(v\cdot u)^2 + c_3u^2 + c_4[S^\mu, S^\nu]u_\mu u_\nu, \quad (2.32)$$

$$\mathcal{B}_N^{(2)} = -c_4\gamma_5[v\cdot u, S\cdot u], \quad (2.33)$$

$$\mathcal{C}_N^{(2)} = -\left[c_1\langle\chi_+\rangle + c_2(v\cdot u)^2 + c_3u^2 + c_4[S^\mu, S^\nu]u_\mu u_\nu \right], \quad (2.34)$$

where $\chi_\pm = u^\dagger\chi u^\dagger \pm u\chi^\dagger u$. According to Eq. (2.20) u_μ includes the pion fields and $\langle\dots\rangle$ denotes a trace in flavor space, such that $\langle\chi_+\rangle = 2m_\pi^2(U^\dagger + U)$.

The nucleon delta sector

The technology for the heavy baryon projection in the nucleon-delta sector has been developed in Ref. [31]. One has to work with appropriate spin and isospin projection operators. Using a simplified notation that suppresses Lorentz and isospin indices, the effective Lagrangian has the form,

$$\mathcal{L}_{\pi N\Delta} = \bar{T}\mathcal{A}_{N\Delta}N + \bar{G}\mathcal{B}_{N\Delta}N + \bar{T}\gamma_0\mathcal{D}_{N\Delta}^\dagger\gamma_0h + \bar{G}\gamma_0\mathcal{C}_{N\Delta}^\dagger\gamma_0h + \text{h.c.}, \quad (2.35)$$

where T_i^μ describes the light delta and G_i^μ stands for the heavy delta. The field G has five components. It contains the heavy spin- $\frac{3}{2}$ component and the heavy and light parts of the two off-shell spin- $\frac{1}{2}$ components. The transition operators read in this case

$$\mathcal{A}_{N\Delta,\mu}^{(1),i} = P_+g_{\pi N\Delta}{}_3P_{\mu\alpha}w_\alpha^iP_+, \quad (2.36)$$

$$\mathcal{B}_{N\Delta,\mu}^{(1),i} = g_{\pi N\Delta} \begin{pmatrix} 0 \\ -\frac{4(1+3z_0)}{3}P_+S_\mu S\cdot w^iP_+ \\ 2z_0P_-\gamma_5v_\mu S\cdot w^iP_+ \\ -2z_0P_-\gamma_5S_\mu v\cdot w^iP_+ \\ (1+z_0)P_+v_\mu v\cdot w^iP_+ \end{pmatrix}, \quad (2.37)$$

$$\mathcal{D}_{N\Delta,\mu}^{(1),i} = 0, \quad (2.38)$$

$$\mathcal{C}_{N\Delta,\mu}^{T(1),i} = g_{\pi N\Delta} \begin{pmatrix} P_-\omega_\alpha^i{}_3P_{\alpha\mu}P_- \\ 2z_0P_-\omega_\alpha^i S_\mu\gamma_5P_+ \\ (1+z_0)P_-\omega_\alpha^i v_\mu P_- \\ -\frac{4(1+3z_0)}{3}P_-\omega_\alpha^i S_\mu P_- \\ -2z_0P_-\omega_\alpha^i v_\mu\gamma_5P_+ \end{pmatrix}, \quad (2.39)$$

with $w_\alpha^i = \frac{1}{2}\langle\tau^i u_\alpha\rangle$, ${}_3P_{\mu\nu} = g_{\mu\nu} - v_\mu v_\nu - \frac{4}{1-d}S_\mu S_\nu$ in d space-time dimensions and the P_\pm are the velocity projection operators defined above. There appear two parameters, the leading pion-nucleon-delta coupling constant $g_{\pi N\Delta}$ and a so-called off-shell parameter z_0 .

The delta sector

If one now performs simultaneously the $1/M$ expansion of the nucleon and delta fields, the Δ -N mass splitting remains in the propagator. This is a quantity of order ϵ , so it must be kept in the expansion. In the heavy baryon approach, the delta Lagrangian takes the form

$$\mathcal{L}_{\pi\Delta} = \bar{T}\mathcal{A}_{\Delta}T + \bar{G}\mathcal{B}_{\Delta}T + \bar{T}\gamma_0\mathcal{B}_{\Delta}^{\dagger}\gamma_0G - \bar{G}\mathcal{C}_{\Delta}G, \quad (2.40)$$

where the operator between two light delta fields reads

$$\mathcal{A}_{\Delta,\mu\nu}^{(1),ij} = -(iv \cdot D^{ij} - \Delta\delta^{ij} + g_1S \cdot u^{ij})g_{\mu\nu}. \quad (2.41)$$

We omit the lengthy expressions of $\mathcal{B}_{\Delta}^{(1)}$ and $\mathcal{C}_{\Delta}^{(1)}$ here. They can be found in Ref. [32].

Elimination of heavy components

In order to integrate out the heavy components, one just needs to shift the corresponding heavy fields. For the heavy nucleon component this variable shift reads according to Ref. [41]

$$h \rightarrow h' + \mathcal{C}_N^{-1}\mathcal{B}_N^{(1)}N, \quad (2.42)$$

and Ref. [31] specifies the variable shift for the $G^{\mu}(x)$ fields as

$$G \rightarrow G' + \mathcal{C}_{\Delta}^{-1}\mathcal{B}_{\Delta}^{(1)}T + \mathcal{C}_{\Delta N}^{-1}\mathcal{B}_{\Delta N}^{(1)}N. \quad (2.43)$$

After integrating out the heavy components h' and G' one arrives at Lagrangians for the light components

$$\tilde{\mathcal{L}}_{\pi N} = \bar{N}\mathcal{A}_N N + \bar{N}\left[\gamma_0\tilde{\mathcal{B}}_N^{\dagger}\gamma_0\tilde{\mathcal{C}}_N^{-1}\tilde{\mathcal{B}}_N + \gamma_0\mathcal{B}_{N\Delta}^{\dagger}\gamma_0\mathcal{C}_{\Delta}^{-1}\mathcal{B}_{N\Delta}\right]N, \quad (2.44)$$

$$\tilde{\mathcal{L}}_{\pi\Delta} = \bar{T}\mathcal{A}_{\Delta}T + \bar{T}\left[\gamma_0\mathcal{B}_{\Delta}^{\dagger}\gamma_0\mathcal{C}_{\Delta}^{-1}\mathcal{B}_{\Delta} + \gamma_0\tilde{\mathcal{D}}_{N\Delta}^{\dagger}\gamma_0\tilde{\mathcal{C}}_N^{-1}\tilde{\mathcal{D}}_{N\Delta}\right]T, \quad (2.45)$$

$$\tilde{\mathcal{L}}_{\pi N\Delta} = \bar{T}\mathcal{A}_{N\Delta}N + \bar{T}\left[\gamma_0\tilde{\mathcal{D}}_{N\Delta}^{\dagger}\gamma_0\tilde{\mathcal{C}}_N^{-1}\tilde{\mathcal{B}}_N + \gamma_0\mathcal{B}_{\Delta}^{\dagger}\gamma_0\mathcal{C}_{\Delta}^{-1}\mathcal{B}_{N\Delta}\right]N + \text{h.c.}, \quad (2.46)$$

where

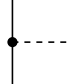



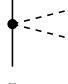
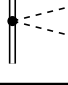
$$\tilde{\mathcal{B}}_N = \mathcal{B}_N + \mathcal{C}_{N\Delta}\mathcal{C}_{\Delta}^{-1}\mathcal{B}_{N\Delta}, \quad (2.47)$$

$$\tilde{\mathcal{C}}_N = \mathcal{C}_N - \mathcal{C}_{N\Delta}\mathcal{C}_{\Delta}^{-1}\mathcal{C}_{N\Delta}^{\dagger}, \quad (2.48)$$

$$\tilde{\mathcal{D}}_{N\Delta} = \mathcal{D}_{N\Delta} + \mathcal{C}_{N\Delta}\mathcal{C}_{\Delta}^{-1}\mathcal{B}_{\Delta}. \quad (2.49)$$

The leading order is given by the first term for each of these Lagrangians.

TABLE 2.1: Propagators and vertices in the non-relativistic heavy baryon approach, π^a are outgoing pions, π^b are incoming pions. Here, τ^a and σ are the usual (isospin and spin) 2×2 Pauli matrices. The transition operators T^a and \mathbf{S} , as well as the 4×4 matrices Θ^a and Σ are explained in Appendix A.2.

N	\rightarrow	$\frac{i}{v \cdot l + i\epsilon}$
Δ	\Rightarrow	$\frac{i}{v \cdot l - \Delta + i\epsilon}$
$N \rightarrow \pi^a N$		$-\frac{g_A}{2f_\pi} \boldsymbol{\sigma} \cdot \mathbf{q} \tau^a$
$N \rightarrow \pi^a \Delta$		$-\frac{3g_A}{2\sqrt{2}f_\pi} \mathbf{S}^\dagger \cdot \mathbf{q} T^a$
$\Delta \rightarrow \pi^a N$		$-\frac{3g_A}{2\sqrt{2}f_\pi} \mathbf{S} \cdot \mathbf{q} T^a$
$\Delta \rightarrow \pi^a \Delta$		$-\frac{g_A}{10f_\pi} \Sigma \cdot \mathbf{q} \Theta^a$
$\pi^b N \rightarrow \pi^a N$		$\frac{1}{4f_\pi^2} \epsilon^{bac} \tau^c v \cdot (q_{\pi^a} + q_{\pi^b})$
$\pi^b \Delta \rightarrow \pi^a \Delta$		$\frac{1}{4f_\pi^2} \epsilon^{bac} \Theta^c v \cdot (q_{\pi^a} + q_{\pi^b})$

2.2.4 Propagators and vertices in non-relativistic limit

In order to take the extreme non-relativistic limit, the Lagrangians in Section 2.2.3 have to be expanded in the inverse baryon mass M_N^{-1} . The expansion of the baryon bilinears in M_N^{-1} is summarized in Appendix A.4. This yields the baryon propagators and baryon-pion vertices collected in Table 2.1.

We use the large N_C -values for the $\pi N \Delta$ and $\pi \Delta \Delta$ coupling constants,

$$g_{\pi N \Delta} = \frac{3g_{\pi NN}}{\sqrt{2}}, \quad g_{\pi \Delta \Delta} = \frac{g_{\pi NN}}{5}. \quad (2.50)$$

2.2.5 Power counting in chiral effective field theory

Due to the infinite number of terms in the chiral effective Lagrangian the resulting diagrams have to be ordered according to their importance to obtain a calculable and predictive theory. In ChEFT, the diagrams are ordered in terms of powers of the small momentum

scale Q over the chiral symmetry breaking scale Λ_χ : $(Q/\Lambda_\chi)^\nu$. The dimensional analysis from covariant perturbation theory counts a nucleon propagator as Q^{-1} , a pion propagator as Q^{-2} , a derivative in a vertex as Q , and a four-momentum integration as Q^4 . Following Weinberg's works [7, 8, 42], one obtains for the power of an irreducible diagram [34]

$$\nu = -2 + 2A - 2C + 2L + \sum_i \Delta_i, \quad (2.51)$$

with A the number of nucleons, C the number of separately connected pieces, L the number of loops, and Δ_i the so called index of interaction defined as

$$\Delta_i = d_i + \frac{n_i}{2} - 2. \quad (2.52)$$

Here, d_i denotes the number of derivatives or pion mass insertions and n_i is the number of nucleon fields involved in the vertex i . For an irreducible NN diagram ($A = 2$, $C = 1$) the formula simplifies to

$$\nu = 2L + \sum_i \Delta_i. \quad (2.53)$$

The contributions at leading order (LO), next-to-leading order (NLO) and next-to-next-to-leading order (N2LO) are shown in Fig. 2.1 for the two- and three-nucleon interaction. In this work, we perform calculations up to next-to-leading order.

3

NUCLEON NUCLEON POTENTIAL

The nucleon-nucleon (NN) potential is defined as the sum of all (two-particle) irreducible diagrams arising from the chiral interaction vertices. The reducible components of the diagrammatic amplitudes are accounted for by iterating the NN potential in a scattering equation which determines the T-matrix as it is explained in Section 3.1. The NN potential can be obtained from the Lagrangian by applying the Feynman rules in Table 2.1 to the diagrams listed in Fig. 2.2. The general decomposition of the NN potential reads (e. g. [12])

$$\begin{aligned}
 V_{NN} = & V_C + \boldsymbol{\tau}_1 \cdot \boldsymbol{\tau}_2 W_C + (V_S + \boldsymbol{\tau}_1 \cdot \boldsymbol{\tau}_2 W_S) \boldsymbol{\sigma}_1 \cdot \boldsymbol{\sigma}_2 \\
 & + (V_T + \boldsymbol{\tau}_1 \cdot \boldsymbol{\tau}_2 W_T) \boldsymbol{\sigma}_1 \cdot \mathbf{q} \boldsymbol{\sigma}_2 \cdot \mathbf{q} \\
 & + (V_{LS} + \boldsymbol{\tau}_1 \cdot \boldsymbol{\tau}_2 W_{LS}) i (\boldsymbol{\sigma}_1 + \boldsymbol{\sigma}_2) \cdot (\mathbf{q} \times \mathbf{p}) \\
 & + (V_Q + \boldsymbol{\tau}_1 \cdot \boldsymbol{\tau}_2 W_Q) i \boldsymbol{\sigma}_1 \cdot (\mathbf{q} \times \mathbf{p}) \boldsymbol{\sigma}_2 \cdot (\mathbf{q} \times \mathbf{p}) ,
 \end{aligned} \tag{3.1}$$

where \mathbf{p} is the ingoing momentum of one nucleon in the center of mass frame and \mathbf{q} is the momentum transfer between the two nucleons. The superscripts denote the central, spin-spin, tensor, spin-orbit and quadratic spin-orbit components of the NN potential. For each component there exists an isoscalar (V) and an isovector (W) part.

To compare the potential obtained in the theoretical framework with experimental results one needs to calculate the phase shifts and mixing angles. They parameterize the NN S-matrix $S_{\ell\ell'}^{sj}$ via the relations for uncoupled ($\ell = \ell' = j$) spin-singlet ($s = 0$) and spin-triplet ($s = 1$) states

$$S_{jj}^{sj} = \exp(2i\delta_j^{sj}) \tag{3.2}$$

and for coupled ($\ell, \ell' = j \pm 1$) spin-triplet partial wave channels

$$\begin{pmatrix} S_{j-1j-1}^{sj} & S_{j-1j+1}^{sj} \\ S_{j+1j-1}^{sj} & S_{j+1j+1}^{sj} \end{pmatrix} = \begin{pmatrix} \cos(2\epsilon_j) \exp(2i\delta_{j-1}^{sj}) & -i \sin(2\epsilon_j) \exp(i\delta_{j-1}^{sj} + i\delta_{j+1}^{sj}) \\ -i \sin(2\epsilon_j) \exp(i\delta_{j-1}^{sj} + i\delta_{j+1}^{sj}) & \cos(2\epsilon_j) \exp(2i\delta_{j+1}^{sj}) \end{pmatrix} \tag{3.3}$$

in the so called Stapp convention [43]. The total isospin $I = 0$ or 1 is determined in each partial wave by the condition that $I + s + \ell$ is odd. Note that the S-matrix is unitary and symmetric, due to time-reversal invariance. The minus sign in the off diagonal matrix elements is due to our convention in the relation between the S-matrix and the (one-pion exchange) potential.

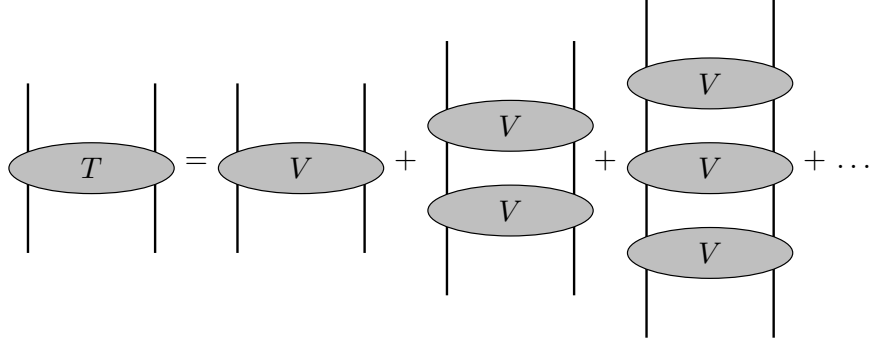
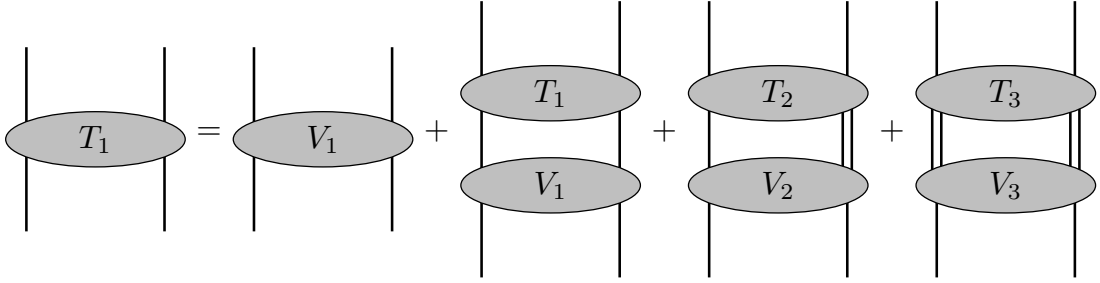


FIGURE 3.1: Scheme of a NN scattering equation


 FIGURE 3.2: Scheme of a $(N\Delta, \Delta\Delta)$ -coupled channel scattering equation

3.1 SCATTERING EQUATIONS

The NN S-matrix is calculated from the T-matrix by

$$S = 1 + i \frac{p M_N^2}{8\pi^2 \sqrt{p^2 + M_N^2}} T \quad (3.4)$$

where the latter follows from a scattering equation of the form

$$T = V + VGT \quad (3.5)$$

written in operator notation. This resummation of the iterated diagrams is shown schematically in Fig. 3.1. In practice, the Lippmann-Schwinger equation is further more projected onto states with total spin $s = 0, 1$, total angular momentum j and allowed orbital angular momenta l . After that projection, it reads

$$T_{l'l}^{sj}(p', p) = V_{l'l}^{sj}(p', p) + \sum_{l''} \int_0^\infty \frac{dp'' p''^2}{(2\pi)^3} \frac{V_{l'l''}^{sj}(p', p'') T_{l''l}^{sj}(p'', p)}{2\sqrt{p^2 + M_N^2} - 2\sqrt{p''^2 + M_N^2} + i\eta}, \quad (3.6)$$

and in the non-relativistic approximation this simplifies to [44]

$$\tilde{T}_{\nu l}^{sj}(p', p) = \tilde{V}_{\nu l}^{sj}(p', p) + \sum_{l''} \int_0^\infty \frac{dp'' p''^2}{(2\pi)^3} \tilde{V}_{l''}^{sj}(p', p'') \frac{M_N}{p^2 - p''^2 + i\eta} \tilde{T}_{\nu l}^{sj}(p'', p). \quad (3.7)$$

This equation contains a sum over all coupled partial waves. It can be extended by the inclusion of other intermediate states, namely the channels $N\Delta$ and $\Delta\Delta$ with total isospin $I = 0, 1$ which couple to NN .

$$T_{\nu'\nu}^{\rho'\rho,j}(p', p, W) = V_{\nu'\nu}^{\rho'\rho,j}(p', p) + \sum_{\rho'', \nu''} \int_0^\infty \frac{dp'' p''^2}{(2\pi)^3} V_{\nu'\nu''}^{\rho'\rho'',j}(p', p'') \frac{2\mu_{\nu''}}{p_{\nu''}^2 - p''^2 + i\eta} T_{\nu''\nu}^{\rho''\rho,j}(p'', p) \quad (3.8)$$

where j stands for the total angular momentum, ν denotes the two-particle channels, and $\rho = (s, \ell)$ labels the partial waves. W is the center of mass energy and μ_ν the appropriate reduced baryon mass. The masses of the baryons contributing to the two-particle channels ν are denoted as $M_{B_{1,\nu}}$ and $M_{B_{2,\nu}}$. The on-shell momentum p_ν is given by $W = \sqrt{M_{B_{1,\nu}}^2 + p_\nu^2} + \sqrt{M_{B_{2,\nu}}^2 + p_\nu^2}$ [45, 46]. The coupled particle channel equation is shown schematically in Fig. 3.2. Another possibility is the Kadyshevsky equation [47, 48] formulated for coupled channels,

$$T_{\nu'\nu}^{\rho'\rho,j}(p', p) = V_{\nu'\nu}^{\rho'\rho,j}(p', p) - \sum_{\rho'', \nu''} M_{B_{1,\nu''}} M_{B_{2,\nu''}} \int_0^\infty \frac{dp'' p''^2}{(2\pi)^3} \frac{V_{\nu'\nu''}^{\rho'\rho'',j}(p', p'') T_{\nu''\nu}^{\rho''\rho,j}(p'', p)}{E_1 E_2 (2p_0 - E_1 - E_2 + i\eta)}, \quad (3.9)$$

with energy variables $p_0 = \sqrt{p^2 + M_N^2}$, and $E_{1,2} = \sqrt{p''^2 + M_{B_{1,2,\nu''}}^2}$. This equation is a modification of the non-relativistic Lippmann-Schwinger equation which includes relativistically improved kinematics.

The Kadyshevsky equation is expected to have a milder UV behavior in the limit of large integration momenta than the corresponding Lippmann-Schwinger equation [49]. A comparison of results from these two equations will be given in Section 6.4.

Following Ref. [50], one can modify the integral equation by replacing the T-matrix with the K-matrix. The T-matrix is complex because of the Cauchy-type singularity in the denominator of the scattering equation. The corresponding K-matrix is defined through the principal value of the integral and is thus real by definition. The S-matrix is related to the K-matrix via

$$S = \left(1 + i \frac{p M_N^2}{16\pi^2 \sqrt{p^2 + M_N^2}} K \right) \left(1 - i \frac{p M_N^2}{16\pi^2 \sqrt{p^2 + M_N^2}} K \right)^{-1}. \quad (3.10)$$

Note that S is unitary if K is hermitian. This is the case if the potential V is hermitian.

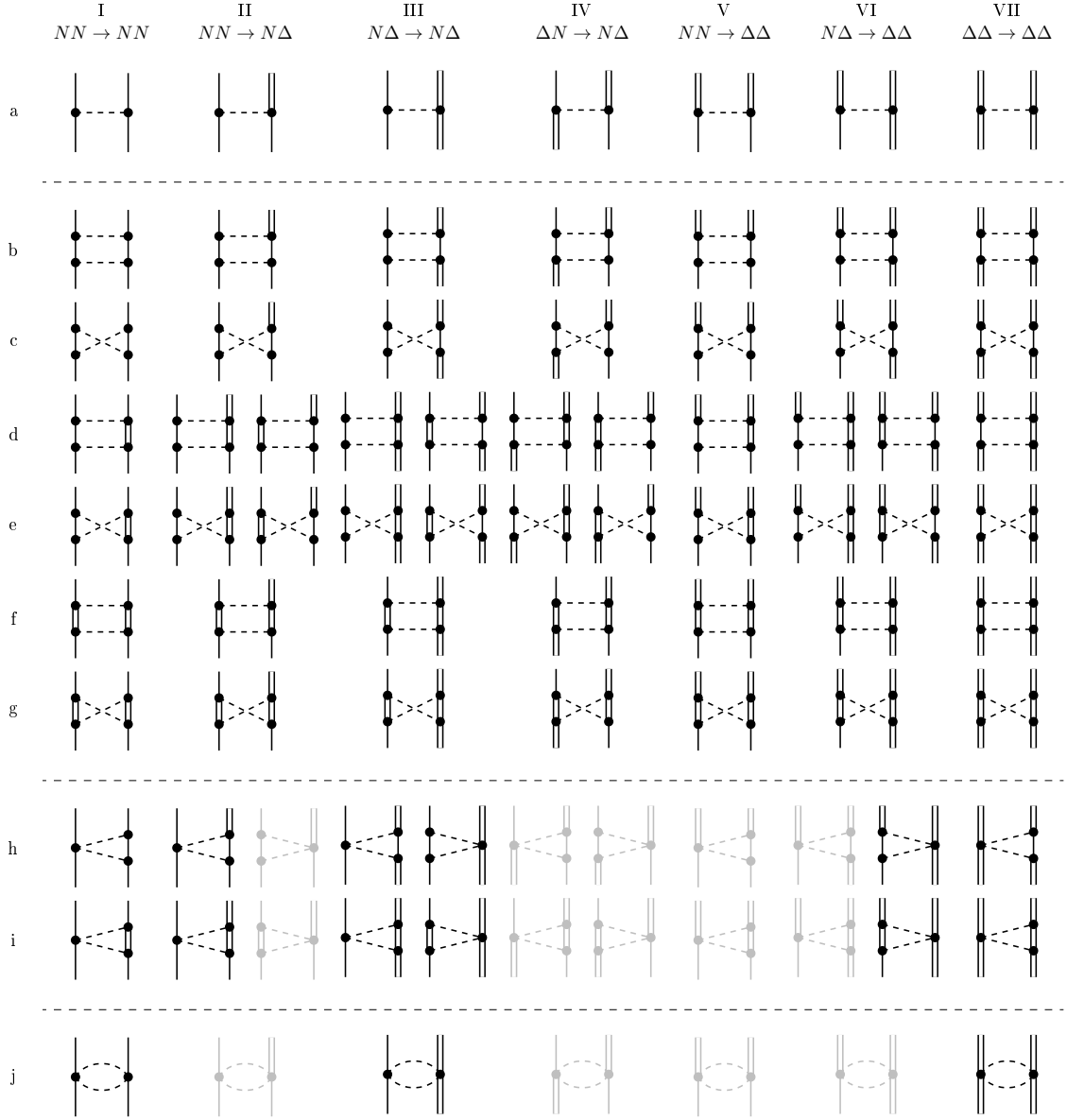


FIGURE 3.3: One- and two-pion exchange diagrams contributing to the coupled channel equation. The $\pi\pi N\Delta$ -vertex in the shaded diagrams appears at higher order in the chiral Lagrangian. Solid, double and dashed lines denote nucleons, deltas and pions, respectively.

The Kadyshevsky equation (3.9) gives also rise to a real equation of the form $K = V + VGK$, It can be written in matrix form for the different particle channels ν [49], which emphasizes the coupling between these channels,

$$K = \begin{pmatrix} K_{NNNN} & K_{NNN\Delta} & K_{NN\Delta\Delta} \\ K_{N\Delta NN} & K_{N\Delta N\Delta} & K_{N\Delta\Delta\Delta} \\ K_{\Delta\Delta NN} & K_{\Delta\Delta N\Delta} & K_{\Delta\Delta\Delta\Delta} \end{pmatrix}, \quad (3.11)$$

$$V = \begin{pmatrix} V_{NNNN} & V_{NNN\Delta} & V_{NN\Delta\Delta} \\ V_{N\Delta NN} & V_{N\Delta N\Delta} & V_{N\Delta\Delta\Delta} \\ V_{\Delta\Delta NN} & V_{\Delta\Delta N\Delta} & V_{\Delta\Delta\Delta\Delta} \end{pmatrix}, \quad (3.12)$$

$$G = \begin{pmatrix} G_{NN} & 0 & 0 \\ 0 & G_{N\Delta} & 0 \\ 0 & 0 & G_{\Delta\Delta} \end{pmatrix}, \quad (3.13)$$

with the two-baryon propagator

$$G_{IJ}(E) = \frac{1}{E_1 E_2} \frac{M_{B_1, \nu} M_{B_2, \nu}}{E_1 + E_2 - 2p'_0}. \quad (3.14)$$

To solve these coupled channel equations we need in addition to the usual NN potential also the potentials containing one or two Δ -isobars in the final and/or initial state. Up to next-to-leading order in the usual power counting scheme, see e.g. [34, 35], we have to calculate the pion exchange contributions listed in Fig. 3.3. In Chapter 4 we will present the potentials arising from all these diagrams. The contact interactions depicted in Fig. 2.1 are treated later in Chapter 5. Note that the delta introduces a rich coupling between different partial waves and two-particle channels. This is caused by the maximum spin of the two delta state, a spin of 3, that couples with the angular momentum ℓ to j . The angular momentum and spin quantum numbers, and the number of Δ -isobars for the coupled channels contributing to the NN partial waves for given total angular momentum j , total isospin I and parity π are listed in Appendix B.

3.2 TREATMENT OF PRINCIPLE VALUE INTEGRALS

There is a pole appearing in the integral in the Kadyshevsky and also in the Lippmann-Schwinger equation for the term with the two-nucleon intermediate state. The corresponding integral has to be treated by the principle value prescription. Following Ref. [50] it can be treated by adding “zero” to the integrand and utilizing the weighted sum of the numerical integration. For the principal value integral involving the NN intermediate state in the Kadyshevsky equation (3.9), this prescription reads

$$\begin{aligned} & \int_0^\infty dk k^2 \frac{V(p', k)K(k, p)}{(k^2 + m_N^2)(p_0 - \sqrt{k^2 + M_N^2})} = \\ & = \int_0^\infty dk \frac{k^2 V(p', k)K(k, p) \frac{\sqrt{p^2 + M_N^2} + \sqrt{k^2 + M_N^2}}{k^2 + m_N^2} - p^2 V(p', p)K(p, p) \frac{2\sqrt{p^2 + M_N^2}}{p^2 + m_N^2}}{(p^2 - k^2)} \\ & + \int_0^\infty dk \frac{p^2 V(p', p)K(p, p) \left(2\sqrt{p^2 + M_N^2}\right)}{(p^2 + m_N^2)(p^2 - k^2)} \\ & = \sum_i w_i k_i^2 \frac{V(p', k_i)K(k_i, p)}{(k_i^2 + m_N^2)(p_0 - \sqrt{k_i^2 + M_N^2})} \end{aligned}$$

$$+ p^2 V(p', p) K(p, p) \frac{2\sqrt{p^2 + M_N^2}}{p^2 + m_N^2} \left(-\sum_i \frac{w_i}{p^2 - k_i^2} + \int_0^\Lambda dk \frac{1}{p^2 - k^2} \right), \quad (3.15)$$

where the last two lines refer to the numerical treatment and the remaining principal value integral can be solved analytically by introducing the cutoff parameter Λ ,

$$\int_0^\Lambda \frac{1}{(p^2 - k^2)} = \frac{1}{2p} \ln \frac{\Lambda + p}{\Lambda - p}.$$

For the Lippmann-Schwinger equation (3.8) one arrives at

$$\begin{aligned} \mu_{NN} \int_0^\infty dk \frac{k^2 V(p', k) K(k, p)}{p^2 - k^2} &= \\ &= \mu_{NN} \int_0^\infty dk \frac{k^2 V(p', k) K(k, p) - p^2 V(p', p) K(p, p)}{p^2 - k^2} + \mu_{NN} \int_0^\infty dk \frac{p^2 V(p', p) K(p, p)}{p^2 - k^2} \\ &= \mu_{NN} \sum_i w_i k_i^2 \frac{V(p', k_i) K(k_i, p)}{p^2 - k_i^2} \\ &\quad + \mu_{NN} p^2 V(p', p) K(p, p) \left(-\sum_i w_i \frac{1}{p^2 - k_i^2} + \frac{1}{2p} \ln \frac{\Lambda + p}{\Lambda - p} \right). \end{aligned} \quad (3.16)$$

This method avoids unstable results from the numerical principal value integration close to the pole and replaces the singular part by an analytical known value, leading to a numerically stable evaluation of the integral.

3.3 REGULARIZATION

The potentials derived from chiral effective field theory need to be regularized to cut off unphysical high energy components: $V(p, p') \rightarrow f_R(p) V(p, p') f_R(p')$. Two common approaches are a sharp regulator, $f_R(p) = \Theta(\Lambda^2 - p^2)$, or an exponential regulator, $f_R(p) = \exp(-p^{2n}/\Lambda^{2n})$. We employ the local regulator of Ref. [24] following an approach in Ref. [51]. There, the regularization is implemented by replacing the Feynman propagators for pions by spectral integrals,

$$\frac{1}{\mathbf{q}^2 + m_\pi^2} \rightarrow \int_0^\infty d\mu^2 \frac{\rho(\mu^2)}{\mathbf{q}^2 + \mu^2} \rightarrow \frac{f_{\Lambda, 1\pi}(q)}{\mathbf{q}^2 + m_\pi^2}. \quad (3.17)$$

It is required, that the residue of the static pion propagator is not modified at the pion pole and consequently the long range part of the pion exchange remains unchanged by this regularization. A good choice for the regulator of the one-pion-exchange is

$$f_{\Lambda, 1\pi}(q) = \exp \left[-(q^2 + m_\pi^2)/\Lambda^2 \right]. \quad (3.18)$$

In a $1/\Lambda^2$ -expansion the regularization has the same effect as adding some short-range contact interactions to the unregularized pion exchange.

A generic three-momentum loop integral appearing in two-pion exchange calculations can be rewritten such that it resembles the product of two pion propagators with the energies $\omega_{1,2} = \sqrt{\mathbf{l}_{1,2}^2 + m_\pi^2}$ of the two pions [51].

$$I(\mathbf{q}) = \int_{-\infty}^{\infty} d\lambda \frac{d^3 l_1}{(2\pi)^3} \frac{d^3 l_2}{(2\pi)^3} (2\pi)^3 \delta(\mathbf{q} - \mathbf{l}_1 - \mathbf{l}_2) \frac{1}{(\omega_1^2 + \lambda^2)(\omega_2 + \lambda^2)} \times (\dots), \quad (3.19)$$

where \mathbf{q} is the nucleon momentum transfer. With the definitions $\mathbf{l} = \mathbf{l}_1 - \mathbf{l}_2$ and $\omega_\pm = \sqrt{(\mathbf{q} \pm \mathbf{l})^2 + 4M_\pi^2}$ and the transition to regularized pion propagators Eq. (3.18), one arrives according to Ref. [24] at

$$I_\Lambda(\mathbf{q}) = 2 \int_{-\infty}^{\infty} d\lambda \frac{d^3 l}{(2\pi)^3} \frac{e^{-(q^2 + l^2 + 4m_\pi^2 + 4\lambda^2)/(2\Lambda^2)}}{(\omega_+^2 + 4\lambda^2)(\omega_-^2 + 4\lambda^2)} \times (\dots), \quad (3.20)$$

As the two-pion-exchange is given in terms of spectral functions and dispersion integrals, this method leads to a regularization already at the level of the spectral integral by replacing $V(q)$ with $V_\Lambda(q)$

$$V(q) \rightarrow V_\Lambda(q) = e^{-\frac{q^2}{2\Lambda^2}} \frac{2}{\pi} \int_{2m_\pi}^{\infty} d\mu \frac{\mu \operatorname{Im} V(i\mu)}{\mu^2 + q^2} e^{-\frac{\mu^2}{2\Lambda^2}}, \quad (3.21)$$

where subtraction can be omitted. We choose the cutoff parameter Λ in the range 350...800 MeV.

3.4 PARTIAL WAVE PROJECTION

For the partial wave decomposition, we follow Ref. [52]. Since isospin mixing is excluded in our calculation, the potential is first projected onto the isospin states $|Im_I\rangle$ with $I = 0, 1$,

$$\langle I' m'_I | V | Im_I \rangle = \delta_{I'I} \delta_{m'_I m_I} V^I. \quad (3.22)$$

The matrix element in spin-space is given by the four-fold integral

$$\begin{aligned} \langle p'(l' s') j m_j | V^I | p(ls) j m_j \rangle &= \int d\Omega' \int d\Omega \sum_{m'_l} C(l', s', j; m'_l, m_j - m'_l, m_j) \\ &\quad \times \sum_{m_l} C(l, s, j; m_l, m_j - m_l, m_j) Y_{l' m'_l}^*(\theta', \phi') Y_{l m_l}(\theta, \phi) \\ &\quad \times \langle s' m_j - m'_l | V^I(\mathbf{p}', \mathbf{p}) | s m_j - m_l \rangle, \end{aligned} \quad (3.23)$$

where the $C(l, s, j; m_l, m_j - m_l, m_j)$ are the standard Clebsch-Gordan coefficients, and $Y_{lm_l}(\theta, \phi)$ the spherical harmonics. The angles θ, ϕ and θ', ϕ' correspond to the directions

of the momenta \mathbf{p}' and \mathbf{p} , respectively. The transition matrix element does actually not depend on m_j , so instead one can calculate the average

$$H(l', s', l, s, j) = \frac{1}{2j+1} \sum_{m_j=-j}^j \langle p'(l' s') j m_j | V | p(l s) j m_j \rangle , \quad (3.24)$$

where the isospin index $I = 0, 1$ is now dropped. For the momenta \mathbf{p} and \mathbf{p}' we choose the directions

$$\begin{aligned} \mathbf{p} &= (0, 0, p) , \\ \mathbf{p}' &= (p' \sqrt{1-z^2}, 0, p' z) \end{aligned}$$

with

$$z = \cos \theta$$

and

$$\mathbf{q} = \mathbf{p}' - \mathbf{p} .$$

As the integrand is a scalar now, the number of integrals can be reduced to one,

$$\begin{aligned} H(l', s', l, s, j) &= 8\pi^2 \int_{-1}^1 dz \frac{1}{2j+1} \sum_{m_j=-j}^j \sum_{m'_l=-l'}^{l'} C(l', s', j; m'_l, m_j - m'_l, m_j) \\ &\times \sum_{m_l=-l}^l C(l, s, j; m_l, m_j - m_l, m_j) Y_{l' m'_l}(\arccos z, 0) Y_{l m_l}^*(0, 0) \\ &\times \langle s' m_j - m'_l | V(\mathbf{q}) | s m_j - m_l \rangle . \end{aligned} \quad (3.25)$$

The integrand of

$$H(l', s', l, s, j) := \int_{-1}^1 dz h(l', s', l, s, j, z) , \quad (3.26)$$

can be further simplified to

$$\begin{aligned} h(l', s', l, s, j, z) &= \frac{2\pi \sqrt{(2l+1)(2l'+1)}}{2j+1} \sum_{m_j=-j}^j \sum_{m'_l=-l'}^{l'} C(l', s', j; m'_l, m_j - m'_l, m_j) \\ &\times C(l, s, j; 0, m_j, m_j) \sqrt{\frac{(l' - m'_l)!}{(l' + m'_l)!}} P_{l'}^{m'_l}(z) \langle s' m_j - m'_l | V(\mathbf{q}) | s m_j \rangle . \end{aligned} \quad (3.27)$$

The remaining transition matrix elements in spin-space $\langle s', m_j - m'_l | V(\mathbf{q}) | s, m_j - m_l \rangle$ can be calculated directly with the help of the well-known coupled spin-multiplet states $|0, 0\rangle$, $|1, m_s\rangle$, $|2, m_s\rangle$ and $|3, m_s\rangle$ represented by products of one-body spin states.

 ONE- AND TWO-PION EXCHANGE

The one- and two-pion exchange potentials at leading and next-to-leading order for $NN \rightarrow NN$ are well known. We extend this description by calculating the additional diagrams in Fig. 3.3 and expressing the NN two-pion exchange diagrams in our new notation.

4.1 ONE-PION EXCHANGE POTENTIALS

The one-pion exchange potentials for the diagrams involving up to four Δ -isobars, shown in line (a) of Fig. 3.3, follow straightforwardly from the $NN \rightarrow NN$ potential in Eq. (4.1) by replacing the coupling constants and the spin and isospin matrices. This way we arrive at

$$V_{NN \rightarrow NN}^{OPE} = \frac{g_A^2 (\boldsymbol{\sigma}_1 \cdot \mathbf{q})(\boldsymbol{\sigma}_2 \cdot \mathbf{q})}{4f_\pi^2 (q^2 + m_\pi^2)} \boldsymbol{\tau}_1 \cdot \boldsymbol{\tau}_2, \quad (4.1)$$

$$V_{NN \rightarrow N\Delta}^{OPE} = \frac{3g_A^2 (\boldsymbol{\sigma}_1 \cdot \mathbf{q})(\mathbf{S}_2^\dagger \cdot \mathbf{q})}{4\sqrt{2}f_\pi^2 (q^2 + m_\pi^2)} \boldsymbol{\tau}_1 \cdot \mathbf{T}_2^\dagger, \quad (4.2)$$

$$V_{N\Delta \rightarrow N\Delta}^{OPE} = \frac{g_A^2 (\boldsymbol{\sigma}_1 \cdot \mathbf{q})(\boldsymbol{\Sigma}_2 \cdot \mathbf{q})}{20f_\pi^2 (q^2 + m_\pi^2)} \boldsymbol{\tau}_1 \cdot \boldsymbol{\Theta}_2, \quad (4.3)$$

$$V_{\Delta N \rightarrow N\Delta}^{OPE} = \frac{9g_A^2 (\mathbf{S}_1 \cdot \mathbf{q})(\mathbf{S}_2^\dagger \cdot \mathbf{q})}{8f_\pi^2 (q^2 + m_\pi^2)} \mathbf{T}_1 \cdot \mathbf{T}_2^\dagger, \quad (4.4)$$

$$V_{NN \rightarrow \Delta\Delta}^{OPE} = \frac{9g_A^2 (\mathbf{S}_1^\dagger \cdot \mathbf{q})(\mathbf{S}_2^\dagger \cdot \mathbf{q})}{8f_\pi^2 (q^2 + m_\pi^2)} \mathbf{T}_1^\dagger \cdot \mathbf{T}_2^\dagger, \quad (4.5)$$

$$V_{N\Delta \rightarrow \Delta\Delta}^{OPE} = \frac{3g_A^2 (\mathbf{S}_1^\dagger \cdot \mathbf{q})(\boldsymbol{\Sigma}_2 \cdot \mathbf{q})}{20\sqrt{2}f_\pi^2 (q^2 + m_\pi^2)} \mathbf{T}_1^\dagger \cdot \boldsymbol{\Theta}_2, \quad (4.6)$$

$$V_{\Delta\Delta \rightarrow \Delta\Delta}^{OPE} = \frac{g_A^2 (\boldsymbol{\Sigma}_1 \cdot \mathbf{q})(\boldsymbol{\Sigma}_2 \cdot \mathbf{q})}{100f_\pi^2 (q^2 + m_\pi^2)} \boldsymbol{\Theta}_1 \cdot \boldsymbol{\Theta}_2. \quad (4.7)$$

The (iso)spin-(transition-)matrices are listed in Appendix A.2. We have used the coupling constants defined in Eq. (2.50).

4.2 TWO-PION EXCHANGE POTENTIALS

The amplitudes of Feynman diagrams in ChEFT possess the analytic structure required to be rewritten as dispersion integrals, see Refs. [53, 54]. By means of dispersion relations one

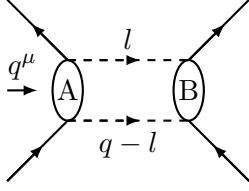


FIGURE 4.1: Schematic figure of a two-pion exchange process with momentum transfer q and loop momentum l

can calculate the full scattering amplitude (or just its real part) from the corresponding imaginary part. By unitarity, this imaginary part arises from the propagation of on-shell intermediate states. In the general form the dispersion relation reads

$$f(s) = \frac{1}{\pi} \int_{s_{thr}}^{\infty} ds' \frac{\text{Im} f(s')}{s' - s - i\epsilon}, \quad (4.8)$$

where s and s' are energy parameters and s_{thr} is the threshold for the occurrence of the lowest hadronic intermediate state. In order to determine the interesting part of $f(s)$ corresponding to small s , the imaginary part has to be known for all s' . Subtractions at $s = 0$ reduce the influence of high energy part and increase the weight of the low energy part of $\text{Im} f(s')$.

The non-polynomial or finite-range terms are determined by the imaginary parts of the NN -amplitudes. The dispersion relation and its once or twice subtracted version read for the 2π -exchange (setting $s = -q^2$ and $s' = \mu^2$)

$$F(q) = \frac{2}{\pi} \int_{2m_\pi}^{\infty} d\mu \frac{\mu \text{Im} F(i\mu)}{\mu^2 + q^2}, \quad (4.9)$$

$$F(q) = c_1 - \frac{2q^2}{\pi} \int_{2m_\pi}^{\infty} d\mu \frac{\text{Im} F(i\mu)}{\mu(\mu^2 + q^2)}, \quad (4.10)$$

$$F(q) = c_1 + c_2 q^2 + \frac{2q^4}{\pi} \int_{2m_\pi}^{\infty} d\mu \frac{\text{Im} F(i\mu)}{\mu^3(\mu^2 + q^2)}. \quad (4.11)$$

We will use the unsubtracted dispersion relation Eq. (4.9) since the local regulator Eq. (3.21) that enters at the level of the 2π -spectral functions $F(i\mu)$, has a similar effect on the high energy part as a subtraction.

For the calculation of the imaginary parts of the two-pion exchange we follow the approach in Ref. [16] by using the Cutkosky cutting rules [55] (see also Ref. [56]). These imaginary parts refer to an analytical continuation of the loop-amplitude to timelike momentum transfers $q \cdot q = \mu^2 > 4m_\pi^2$, corresponding formally to $|\mathbf{q}| = i\mu + 0^+$. The 2π -exchange contribution is worked out as integrals of $\bar{N}N \rightarrow 2\pi \rightarrow \bar{N}N$ transition amplitudes over the Lorentz-invariant 2π -phase space, which reduces to an angular integral $\int_{-1}^1 dx$ in the 2π center-of-mass frame. The imaginary parts or spectral functions of the 2π -exchange

diagrams are then given via the integral over the two S-matrices A and B for the left and right 2π -baryon interaction, shown schematically in Fig. 4.1. With the following definitions in the 2π center-of-mass frame

$$\begin{aligned}
 q^\mu &= (\mu, \mathbf{0}), \quad \mu \ll M_N, \\
 l_0 &= \frac{\mu}{2}, \\
 |\mathbf{l}| &= \frac{1}{2} \sqrt{\mu^2 - 4m_\pi^2}, \\
 v^\mu &= (0, \mathbf{i}\mathbf{v}), \\
 |\mathbf{v}| &= 1, \\
 v \cdot l &= -ix|\mathbf{l}|, \\
 v \cdot q &= 0,
 \end{aligned} \tag{4.12}$$

one arrives at

$$\text{Im } V = -\frac{|\mathbf{l}|}{16\pi\mu} \int_{-1}^1 dx A \cdot B. \tag{4.13}$$

In a representation of the NN-interaction by local coordinate-space potentials,

$$\begin{aligned}
 V(\mathbf{r}) &= \tilde{V}_C(r) + \boldsymbol{\tau}_1 \cdot \boldsymbol{\tau}_2 \tilde{W}_C(r) + \left[\tilde{V}_S(r) + \boldsymbol{\tau}_1 \cdot \boldsymbol{\tau}_2 \tilde{W}_S(r) \right] \boldsymbol{\sigma}_1 \cdot \boldsymbol{\sigma}_2 \\
 &\quad + \left[\tilde{V}_T(r) + \boldsymbol{\tau}_1 \cdot \boldsymbol{\tau}_2 \tilde{W}_T(r) \right] (3 \boldsymbol{\sigma}_1 \cdot \hat{r} \boldsymbol{\sigma}_2 \cdot \hat{r} - \boldsymbol{\sigma}_1 \cdot \boldsymbol{\sigma}_2),
 \end{aligned} \tag{4.14}$$

these imaginary parts play the role of mass spectra in a continuous superposition of Yukawa potentials

$$\tilde{V}_C(r) = -\frac{1}{2\pi^2 r} \int_{2m_\pi}^{\infty} d\mu \mu e^{-\mu r} \text{Im } V_C(i\mu), \tag{4.15}$$

$$\tilde{V}_S(r) = \frac{1}{6\pi^2 r} \int_{2m_\pi}^{\infty} d\mu \mu e^{-\mu r} \left[\mu^2 \text{Im } V_T(i\mu) - 3 \text{Im } V_S(i\mu) \right], \tag{4.16}$$

$$\tilde{V}_T(r) = \frac{1}{6\pi^2 r^3} \int_{2m_\pi}^{\infty} d\mu \mu e^{-\mu r} (3 + 3\mu r + \mu^2 r^2) \text{Im } V_T(i\mu). \tag{4.17}$$

Analogous representations hold for the isovector potentials $\tilde{W}_{C,S,T}(r)$.

The planar box diagrams (lines (b) to (g) in Fig. 3.3) include reducible parts which are also generated by the iteration of the Lippmann-Schwinger equation, therefore these parts have to be excluded from the potential. We come back to this issue in Section 4.2.3.

The diagrams in Fig. 3.3 include many combinations of spin and isospin (transition) matrices. With the isospin and spin matrices and their relations defined in Appendix A.2 we obtain the isospin and spin factors for each diagram as listed in Tables 4.1 and 4.2.

TABLE 4.1: Isospin matrices of the relevant Feynman diagrams. An asterisk indicates, that this diagram does not exist at leading or next-to-leading order.

	$NN \rightarrow NN$	$NN \rightarrow N\Delta$	$N\Delta \rightarrow N\Delta$	$\Delta N \rightarrow N\Delta$	$NN \rightarrow \Delta\Delta$	$N\Delta \rightarrow \Delta\Delta$	$\Delta\Delta \rightarrow \Delta\Delta$
	$\tau_1^a \tau_2^a$	$\tau_1^a T_2^{a\dagger}$	$\tau_1^a \Theta_2^a$	$T_1^a T_2^{a\dagger}$	$T_1^{a\dagger} T_2^{a\dagger}$	$T_1^{a\dagger} \Theta_2^a$	$\Theta_1^a \Theta_2^a$
	$3 - 2\tau_1^a \tau_2^a$	$\tau_1^a T_2^{a\dagger}$	$1 - \frac{1}{3}\tau_1^a \Theta_2^a$	$\frac{3}{2}T_1^{ab}T_2^{ab\dagger} - \frac{1}{2}T_1^a T_2^{a\dagger}$	$\frac{3}{2}T_1^{ab\dagger}T_2^{ab\dagger} - \frac{1}{2}T_1^{a\dagger}T_2^{a\dagger}$	$\sqrt{\frac{1}{6}}T_1^{ab\dagger}\Theta_2^{ab} + \frac{1}{6}T_1^{a\dagger}\Theta_2^a$	$\frac{1}{3} + \frac{1}{9}\Theta_1^{ab}\Theta_2^{ab} - \frac{1}{18}\Theta_1^a\Theta_2^a$
	$3 + 2\tau_1^a \tau_2^a$	$-\tau_1^a T_2^{a\dagger}$	$1 + \frac{1}{3}\tau_1^a \Theta_2^a$	$\frac{3}{2}T_1^{ab}T_2^{ab\dagger} + \frac{1}{2}T_1^a T_2^{a\dagger}$	$\frac{3}{2}T_1^{ab\dagger}T_2^{ab\dagger} + \frac{1}{2}T_1^{a\dagger}T_2^{a\dagger}$	$\sqrt{\frac{1}{6}}T_1^{ab\dagger}\Theta_2^{ab} - \frac{1}{6}T_1^{a\dagger}\Theta_2^a$	$\frac{1}{3} + \frac{1}{9}\Theta_1^{ab}\Theta_2^{ab} + \frac{1}{18}\Theta_1^a\Theta_2^a$
	$2 + \frac{2}{3}\tau_1^a \tau_2^a$	$-5\tau_1^a T_2^{a\dagger}$	$15 - 2\tau_1^a \Theta_2^a$	$\frac{3}{2}T_1^{ab}T_2^{ab\dagger} + \frac{5}{2}T_1^a T_2^{a\dagger}$	$\frac{3}{2}T_1^{ab\dagger}T_2^{ab\dagger} + \frac{5}{2}T_1^{a\dagger}T_2^{a\dagger}$	$-2\sqrt{6}T_1^{ab\dagger}\Theta_2^{ab} + T_1^{a\dagger}\Theta_2^a$	$5 - \frac{4}{3}\Theta_1^{ab}\Theta_2^{ab} - \frac{1}{3}\Theta_1^a\Theta_2^a$
	$2 - \frac{2}{3}\tau_1^a \tau_2^a$	$5\tau_1^a T_2^{a\dagger}$	$15 + 2\tau_1^a \Theta_2^a$	$\frac{3}{2}T_1^{ab}T_2^{ab\dagger} - \frac{5}{2}T_1^a T_2^{a\dagger}$	$\frac{3}{2}T_1^{ab\dagger}T_2^{ab\dagger} - \frac{5}{2}T_1^{a\dagger}T_2^{a\dagger}$	$-2\sqrt{6}T_1^{ab\dagger}\Theta_2^{ab} - T_1^{a\dagger}\Theta_2^a$	$5 - \frac{4}{3}\Theta_1^{ab}\Theta_2^{ab} + \frac{1}{3}\Theta_1^a\Theta_2^a$
	$\frac{4}{3} - \frac{2}{9}\tau_1^a \tau_2^a$	$\frac{5}{3}\tau_1^a T_2^{a\dagger}$	$10 + \frac{2}{3}\tau_1^a \Theta_2^a$	$\frac{3}{2}T_1^{ab}T_2^{ab\dagger} - \frac{25}{2}T_1^a T_2^{a\dagger}$	$\frac{3}{2}T_1^{ab\dagger}T_2^{ab\dagger} - \frac{25}{2}T_1^{a\dagger}T_2^{a\dagger}$	$-2\sqrt{6}T_1^{ab\dagger}\Theta_2^{ab} - 5T_1^{a\dagger}\Theta_2^a$	$75 + 16\Theta_1^{ab}\Theta_2^{ab} - 2\Theta_1^a\Theta_2^a$
	$\frac{4}{3} + \frac{2}{9}\tau_1^a \tau_2^a$	$-\frac{5}{3}\tau_1^a T_2^{a\dagger}$	$10 - \frac{2}{3}\tau_1^a \Theta_2^a$	$\frac{3}{2}T_1^{ab}T_2^{ab\dagger} + \frac{25}{2}T_1^a T_2^{a\dagger}$	$\frac{3}{2}T_1^{ab\dagger}T_2^{ab\dagger} + \frac{25}{2}T_1^{a\dagger}T_2^{a\dagger}$	$-2\sqrt{6}T_1^{ab\dagger}\Theta_2^{ab} + 5T_1^{a\dagger}\Theta_2^a$	$75 + 16\Theta_1^{ab}\Theta_2^{ab} + 2\Theta_1^a\Theta_2^a$
	$2\tau_1^a \tau_2^a$	*	$2\tau_1^a \Theta_2^a$	*	*	*	$2\Theta_1^a \Theta_2^a$
	$-2i\tau_1^a \tau_2^a$	$i\tau_1^a T_2^{a\dagger}$	$-\frac{1}{3}i\tau_1^a \Theta_2^a$	*	*	*	$-\frac{1}{3}i\Theta_1^a \Theta_2^a$
	$\frac{2}{3}i\tau_1^a \tau_2^a$	$-5i\tau_1^a T_2^{a\dagger}$	$-2i\tau_1^a \Theta_2^a$	*	*	*	$-2i\Theta_1^a \Theta_2^a$
	$2 + \frac{2}{3}\tau_1^a \tau_2^a$	$-\frac{1}{3}\tau_1^a T_2^{a\dagger}$	$\frac{2}{3} + \frac{1}{9}\tau_1^a \Theta_2^a$	$\frac{3}{2}T_1^{ab}T_2^{ab\dagger} + \frac{5}{2}T_1^a T_2^{a\dagger}$	$\frac{3}{2}T_1^{ab\dagger}T_2^{ab\dagger} + \frac{5}{2}T_1^{a\dagger}T_2^{a\dagger}$	$\sqrt{\frac{1}{6}}T_1^{ab\dagger}\Theta_2^{ab} - \frac{5}{6}T_1^{a\dagger}\Theta_2^a$	$5 - \frac{4}{3}\Theta_1^{ab}\Theta_2^{ab} - \frac{1}{3}\Theta_1^a\Theta_2^a$
	$2 - \frac{2}{3}\tau_1^a \tau_2^a$	$\frac{1}{3}\tau_1^a T_2^{a\dagger}$	$\frac{2}{3} - \frac{1}{9}\tau_1^a \Theta_2^a$	$\frac{3}{2}T_1^{ab}T_2^{ab\dagger} - \frac{5}{2}T_1^a T_2^{a\dagger}$	$\frac{3}{2}T_1^{ab\dagger}T_2^{ab\dagger} - \frac{5}{2}T_1^{a\dagger}T_2^{a\dagger}$	$\sqrt{\frac{1}{6}}T_1^{ab\dagger}\Theta_2^{ab} + \frac{5}{6}T_1^{a\dagger}\Theta_2^a$	$5 - \frac{4}{3}\Theta_1^{ab}\Theta_2^{ab} + \frac{1}{3}\Theta_1^a\Theta_2^a$
	$-2i\tau_1^a \tau_2^a$	*	$-2i\tau_1^a \Theta_2^a$	*	*	$iT_1^{a\dagger}\Theta_2^a$	$-\frac{1}{3}i\Theta_1^a \Theta_2^a$
	$\frac{2}{3}i\tau_1^a \tau_2^a$	*	$\frac{2}{3}i\tau_1^a \Theta_2^a$	*	*	$-5iT_1^{a\dagger}\Theta_2^a$	$-2i\Theta_1^a \Theta_2^a$

4.2.1 Lorentz tensors and pertinent projectors

The phase space integral for two-pion exchange can be split into terms containing up to four powers of the loop momentum l^μ . For each term we find the resulting Lorentz structure and give the integrals for the coefficients together with the corresponding projectors. With the definitions of the four-momenta q , v and l (in the 2π center-of-mass frame) given in the previous section, one can derive simplified expressions for these integrals.

Integrals involving l^μ

The first case concerns one power of the loop momentum l^μ . The corresponding 2π phase space integral $\int d\Phi$ has the form

$$\int d\Phi(\dots) l^\mu = q^\mu \tilde{A}_1 + v^\mu \tilde{B}_1, \quad (4.18)$$

where the ellipsis stands for further factors coming from baryon propagators. The second Lorentz structure on the right hand side vanishes when contracted with spin-operators. Moreover, since $v \cdot q = 0$ the projector on \tilde{A}_1 is given by

$$Pr_1 = \frac{q_\mu}{\mu^2}. \quad (4.19)$$

Applying this projector on Eq. (4.18) yields the following expression to calculate the coefficient \tilde{A}_1 ,

$$\tilde{A}_1 = \int d\Phi(\dots) \left(\frac{l \cdot q}{\mu^2} \right) = \int d\Phi(\dots) \cdot \frac{1}{2}, \quad (4.20)$$

where we used the definitions in Eq. (4.12) in the last step.

Integrals involving $l^\mu l^\nu$

For two powers of the loop momentum l^μ we decompose the second rank Lorentz tensor resulting from the phase space integration

$$\int d\Phi(\dots) l^\mu l^\nu = -g^{\mu\nu} \tilde{A}_2 + q^\mu q^\nu \tilde{B}_2 + \dots, \quad (4.21)$$

where the dots on the right hand side include terms with v^μ , that are not needed. The ansatz for the projectors on \tilde{A}_2 (and \tilde{B}_2) reads

$$Pr_2 = a q_\mu q_\nu + b v_\mu v_\nu + c g^{\mu\nu} + d (q_\nu v_\mu + q_\mu v_\nu). \quad (4.22)$$

The detailed derivation of these projectors and those for all subsequent coefficients are given in Appendix A.5. After solving the four linear equations for a , b , c and d , one finds for the two coefficients of interest the following expressions

$$\begin{aligned} \tilde{A}_2 &= \int d\Phi(\dots) \left(-\frac{l^2}{2} + \frac{(l \cdot q)^2}{2\mu^2} + \frac{1}{2}(l \cdot v)^2 \right) \\ &= \int d\Phi(\dots) \cdot \frac{1}{8} (x^2 - 1) (4m_\pi^2 - \mu^2), \end{aligned} \quad (4.23)$$

and

$$\begin{aligned}\tilde{B}_2 &= \int d\Phi(\dots) \left(-\frac{l^2}{2\mu^2} + \frac{3(l \cdot q)^2}{2\mu^4} + \frac{(l \cdot v)^2}{2\mu^2} \right) \\ &= \int d\Phi(\dots) \cdot \frac{4m_\pi^2(x^2 - 1) - \mu^2(x^2 - 3)}{8\mu^2},\end{aligned}\quad (4.24)$$

using $l^2 = m_\pi^2$ and $l \cdot q = \mu^2/2$.

Integrals involving $l^\mu l^\nu l^\rho$

The phase space integral including three powers of the loop momentum is decomposed as

$$\int d\Phi(\dots) l^\mu l^\nu l^\rho = (-q^\rho g^{\mu\nu} - q^\nu g^{\mu\rho} - q^\mu g^{\nu\rho}) \tilde{A}_3 + q^\mu q^\nu q^\rho \tilde{B}_3 + \dots \quad (4.25)$$

and we take

$$\begin{aligned}Pr_3 &= a(-q_\rho g_{\mu\nu} - q_\nu g_{\mu\rho} - q_\mu g_{\nu\rho}) + b q_\mu q_\nu q_\rho + c v_\mu v_\nu v_\rho, \\ &+ d(-v_\rho g_{\mu\nu} - v_\nu g_{\mu\rho} - v_\mu g_{\nu\rho}) + e(q_\nu q_\rho v_\mu + q_\mu q_\rho v_\nu + q_\mu q_\nu v_\rho) \\ &+ f(q_\rho v_\mu v_\nu + q_\nu v_\mu v_\rho + q_\mu v_\nu v_\rho)\end{aligned}\quad (4.26)$$

as an ansatz for the projector on \tilde{A}_3 or \tilde{B}_3 .

The coefficients of interest are calculated as follows

$$\begin{aligned}\tilde{A}_3 &= \int d\Phi(\dots) \left(-\frac{l^2 l \cdot q}{2\mu^2} + \frac{(l \cdot q)^3}{2\mu^4} + \frac{l \cdot q (l \cdot v)^2}{2\mu^2} \right) \\ &= \int d\Phi(\dots) \cdot \frac{1}{16} (x^2 - 1) (4m_\pi^2 - \mu^2),\end{aligned}\quad (4.27)$$

$$\begin{aligned}\tilde{B}_3 &= \int d\Phi(\dots) \left(-\frac{3l^2 l \cdot q}{2\mu^4} + \frac{5(l \cdot q)^3}{2\mu^6} + \frac{3l \cdot q (l \cdot v)^2}{2\mu^4} \right) \\ &= \int d\Phi(\dots) \cdot \frac{12m_\pi^2(x^2 - 1) + \mu^2(5 - 3x^2)}{16\mu^2}.\end{aligned}\quad (4.28)$$

Integrals involving $l^\mu l^\nu l^\rho l^\sigma$

The phase space integral with four loop momenta has the following Lorentz structure,

$$\begin{aligned}\int d\Phi(\dots) l^\mu l^\nu l^\rho l^\sigma &= (g^{\mu\nu} g^{\rho\sigma} + g^{\mu\rho} g^{\nu\sigma} + g^{\mu\sigma} g^{\nu\rho}) \tilde{A}_4 \\ &+ (-q^\rho q^\sigma g^{\mu\nu} - q^\nu q^\sigma g^{\mu\rho} - q^\mu q^\sigma g^{\nu\rho} - q^\nu q^\rho g^{\mu\sigma} - q^\mu q^\rho g^{\nu\sigma} - q^\mu q^\nu g^{\rho\sigma}) \tilde{B}_4 \\ &+ q^\mu q^\nu q^\rho q^\sigma \tilde{C}_4 + \dots.\end{aligned}\quad (4.29)$$

The ansatz for the projector reads now

$$\begin{aligned}
 Pr_4 = & a (g_{\mu\nu}g_{\rho\sigma} + g_{\mu\rho}g_{\nu\sigma} + g_{\mu\sigma}g_{\nu\rho}) \\
 & + b (-q_\rho q_\sigma g_{\mu\nu} - q_\nu q_\sigma g_{\mu\rho} - q_\mu q_\sigma g_{\nu\rho} - q_\nu q_\rho g_{\mu\sigma} - q_\mu q_\rho g_{\nu\sigma} - q_\mu q_\nu g_{\rho\sigma}) \\
 & + c q_\mu q_\nu q_\rho q_\sigma + d v_\mu v_\nu v_\rho v_\sigma \\
 & + e (-v_\rho v_\sigma g_{\mu\nu} - v_\nu v_\sigma g_{\mu\rho} - v_\mu v_\sigma g_{\nu\rho} - v_\nu v_\rho g_{\mu\sigma} - v_\mu v_\rho g_{\nu\sigma} - v_\mu v_\nu g_{\rho\sigma}) \\
 & + f (q_\rho q_\sigma v_\mu v_\nu + q_\nu q_\sigma v_\mu v_\rho + q_\mu q_\sigma v_\nu v_\rho + q_\nu q_\rho v_\mu v_\sigma + q_\mu q_\rho v_\nu v_\sigma + q_\mu q_\nu v_\rho v_\sigma) \\
 & + g (-g_{\mu\nu} (q_\sigma v_\rho + q_\rho v_\sigma) - g_{\mu\rho} (q_\sigma v_\nu + q_\nu v_\sigma) - g_{\nu\rho} (q_\sigma v_\mu + q_\mu v_\sigma) \\
 & \quad - g_{\mu\sigma} (q_\rho v_\nu + q_\nu v_\rho) - g_{\nu\sigma} (q_\rho v_\mu + q_\mu v_\rho) - g_{\rho\sigma} (q_\nu v_\mu + q_\mu v_\nu)) \\
 & + h (q_\nu q_\rho q_\sigma v_\mu + q_\mu q_\rho q_\sigma v_\nu + q_\mu q_\nu q_\sigma v_\rho + q_\mu q_\nu q_\rho v_\sigma) \\
 & + j (q_\sigma v_\mu v_\nu v_\rho + q_\rho v_\mu v_\nu v_\sigma + q_\nu v_\mu v_\rho v_\sigma + q_\mu v_\nu v_\rho v_\sigma) .
 \end{aligned} \tag{4.30}$$

We find for the coefficients of interest the following expressions

$$\begin{aligned}
 \tilde{A}_4 = & \int d\Phi(\dots) \left(-\frac{l^2(l \cdot q)^2}{4\mu^2} - \frac{1}{4}l^2(l \cdot v)^2 + \frac{(l^2)^2}{8} + \frac{(l \cdot q)^4}{8\mu^4} + \frac{(l \cdot q)^2(l \cdot v)^2}{4\mu^2} + \frac{1}{8}(l \cdot v)^4 \right) \\
 = & \int d\Phi(\dots) \cdot \frac{1}{128} (x^2 - 1)^2 (\mu^2 - 4m_\pi^2)^2 ,
 \end{aligned} \tag{4.31}$$

$$\begin{aligned}
 \tilde{B}_4 = & \int d\Phi(\dots) \left(\frac{(l^2)^2}{8\mu^2} - \frac{3l^2(l \cdot q)^2}{4\mu^4} - \frac{l^2(l \cdot v)^2}{4\mu^2} + \frac{5(l \cdot q)^4}{8\mu^6} + \frac{3(l \cdot q)^2(l \cdot v)^2}{4\mu^4} + \frac{(l \cdot v)^4}{8\mu^2} \right) \\
 = & \int d\Phi(\dots) \cdot \frac{(x^2 - 1) (\mu^2 - 4m_\pi^2) (\mu^2 (x^2 - 5) - 4m_\pi^2 (x^2 - 1))}{128\mu^2} ,
 \end{aligned} \tag{4.32}$$

and

$$\begin{aligned}
 \tilde{C}_4 = & \int d\Phi(\dots) \left(\frac{3(l^2)^2}{8\mu^4} - \frac{15l^2(l \cdot q)^2}{4\mu^6} - \frac{3l^2(l \cdot v)^2}{4\mu^4} + \frac{35(l \cdot q)^4}{8\mu^8} \right. \\
 & \left. + \frac{15(l \cdot q)^2(l \cdot v)^2}{4\mu^6} + \frac{3(l \cdot v)^4}{8\mu^4} \right) \\
 = & \int d\Phi(\dots) \cdot \frac{48m_\pi^4 (x^2 - 1)^2 - 24\mu^2 m_\pi^2 (x^4 - 6x^2 + 5) + \mu^4 (3x^4 - 30x^2 + 35)}{128\mu^4} .
 \end{aligned} \tag{4.33}$$

TABLE 4.2: Spin matrices of the relevant Feynman diagrams. An asterisk indicates, that this diagram does not exist at leading or next-to-leading order. For the crossed box diagrams the matrices are the same as for the planar box diagrams only with the indices k and l interchanged as indicated in these rows

	$NN \rightarrow NN$	$NN \rightarrow N\Delta$	$N\Delta \rightarrow N\Delta$	$\Delta N \rightarrow N\Delta$	$NN \rightarrow \Delta\Delta$	$N\Delta \rightarrow \Delta\Delta$	$\Delta\Delta \rightarrow \Delta\Delta$
	$\sigma_1^i \sigma_2^j$	$\sigma_1^i S_2^{j\dagger}$	$\sigma_1^i \Sigma_2^j$	$S_1^i S_2^{j\dagger}$	$S_1^{i\dagger} S_2^{j\dagger}$	$S_1^{i\dagger} \Sigma_2^j$	$\Sigma_1^i \Sigma_2^j$
	$\sigma_1^i \sigma_1^j \sigma_2^k \sigma_2^l$	$\sigma_1^i \sigma_1^j S_2^{k\dagger} \sigma_2^l$	$\sigma_1^i \sigma_1^j S_2^{k\dagger} S_2^l$	$\sigma_1^i S_1^j S_2^{k\dagger} \sigma_2^l$	$S_1^{i\dagger} \sigma_1^j S_2^{k\dagger} \sigma_2^l$	$S_1^{i\dagger} \sigma_1^j S_2^{k\dagger} S_2^l$	$S_1^{i\dagger} S_1^j S_2^{k\dagger} S_2^l$
	$\sigma_1^i \sigma_1^j \sigma_2^l \sigma_2^k$	$k \leftrightarrow l$					
	$\sigma_1^i \sigma_1^j S_2^k S_2^{l\dagger}$	$\sigma_1^i \sigma_1^j \Sigma_2^k S_2^{l\dagger}$	$\sigma_1^i \sigma_1^j \Sigma_2^k \Sigma_2^l$	$\sigma_1^i S_1^j \Sigma_2^k S_2^{l\dagger}$	$S_1^{i\dagger} \sigma_1^j \Sigma_2^k S_2^{l\dagger}$	$S_1^{i\dagger} \sigma_1^j \Sigma_2^k \Sigma_2^l$	$S_1^{i\dagger} S_1^j \Sigma_2^k \Sigma_2^l$
	$k \leftrightarrow l$						
	$S_1^i S_1^{j\dagger} S_2^k S_2^{l\dagger}$	$S_1^i S_1^{j\dagger} \Sigma_2^k S_2^{l\dagger}$	$S_1^i S_1^{j\dagger} \Sigma_2^k \Sigma_2^l$	$S_1^i \Sigma_1^j \Sigma_2^k S_2^{l\dagger}$	$\Sigma_1^{i\dagger} S_1^{j\dagger} \Sigma_2^k S_2^{l\dagger}$	$\Sigma_1^{i\dagger} S_1^{j\dagger} \Sigma_2^k \Sigma_2^l$	$\Sigma_1^{i\dagger} \Sigma_1^j \Sigma_2^k \Sigma_2^l$
	$k \leftrightarrow l$						
	$\mathbb{1} \otimes \mathbb{1}$	*	$\mathbb{1} \otimes \mathbb{1}$	*	*	*	$\mathbb{1} \otimes \mathbb{1}$
	$\mathbb{1} \otimes \sigma_2^k \sigma_2^l$	$\mathbb{1} \otimes S_2^{k\dagger} \sigma_2^l$	$\mathbb{1} \otimes S_2^{k\dagger} S_2^l$	*	*	*	$\mathbb{1} \otimes S_2^{k\dagger} S_2^l$
	$\mathbb{1} \otimes S_2^k S_2^{l\dagger}$	$\mathbb{1} \otimes \Sigma_2^k S_2^{l\dagger}$	$\mathbb{1} \otimes \Sigma_2^k \Sigma_2^l$	*	*	*	$\mathbb{1} \otimes \Sigma_2^k \Sigma_2^l$
	$S_1^i S_1^{j\dagger} \sigma_2^k \sigma_2^l$	$S_1^i S_1^{j\dagger} S_2^{k\dagger} \sigma_2^l$	$S_1^i S_1^{j\dagger} S_2^{k\dagger} S_2^l$	$S_1^i \Sigma_1^j S_2^{k\dagger} \sigma_2^l$	$\Sigma_1^{i\dagger} S_1^{j\dagger} S_2^{k\dagger} \sigma_2^l$	$\Sigma_1^{i\dagger} S_1^{j\dagger} S_2^{k\dagger} S_2^l$	$\Sigma_1^{i\dagger} \Sigma_1^j S_2^{k\dagger} S_2^l$
	$k \leftrightarrow l$						
	$\sigma_1^i \sigma_1^j \otimes \mathbb{1}$	*	$\sigma_1^i \sigma_1^j \otimes \mathbb{1}$	*	*	$S_1^{i\dagger} \sigma_1^j \otimes \mathbb{1}$	$S_1^{i\dagger} S_1^j \otimes \mathbb{1}$
	$S_1^i S_1^{j\dagger} \otimes \mathbb{1}$	*	$S_1^i S_1^{j\dagger} \otimes \mathbb{1}$	*	*	$\Sigma_1^{i\dagger} S_1^{j\dagger} \otimes \mathbb{1}$	$\Sigma_1^{i\dagger} \Sigma_1^j \otimes \mathbb{1}$

4.2.2 Phase space integral including spin matrices

We apply the procedure described above to the two-pion exchange box diagrams. For a planar TPE box diagram the phase space integral with inclusion of the spin-operators reads

$$\begin{aligned}
 \int d\Phi(\dots) \mathcal{S}_1^{ij} \mathcal{S}_2^{kl} l^i (q-l)^j l^k (q-l)^l &= \int d\Phi(\dots) \mathcal{S}_1^{ij} \mathcal{S}_2^{kl} \left[\delta^{ik} q^j q^l \tilde{A}_2 + q^i q^j q^k q^l \tilde{B}_2 \right. \\
 &\quad - \left(\delta^{ij} q^k q^l + \delta^{ik} q^j q^l + \delta^{jk} q^i q^l \right) \tilde{A}_3 - q^i q^j q^k q^l \tilde{B}_3 \\
 &\quad - \left(\delta^{ik} q^j q^l + \delta^{il} q^j q^k + \delta^{kl} q^i q^j \right) \tilde{A}_3 - q^i q^j q^k q^l \tilde{B}_3 \\
 &\quad + \left(\delta^{ij} \delta^{kl} + \delta^{ik} \delta^{jl} + \delta^{il} \delta^{jk} \right) \tilde{A}_4 \\
 &\quad + \left(\delta^{ij} q^k q^l + \delta^{ik} q^j q^l + \delta^{jk} q^i q^l + \delta^{il} q^j q^k + \delta^{jl} q^i q^k + \delta^{kl} q^i q^j \right) \tilde{B}_4 \\
 &\quad \left. + q^i q^j q^k q^l \tilde{C}_4 \right], \tag{4.34}
 \end{aligned}$$

where the respective spin operator

$$\mathcal{S}^{ij} \in \{ \sigma^i \sigma^j, S^{i\dagger} \sigma^j, \sigma^i S^j, S^{i\dagger} S^j, S^i S^{j\dagger}, \Sigma^i S^{j\dagger}, S^i \Sigma^j, \Sigma^i \Sigma^j, S^{ij\dagger}, S^{ij}, \Sigma^{ij} \}. \tag{4.35}$$

depends on the type of planar box diagram. The corresponding crossed diagram has the structure $\mathcal{S}_1^{ij} \mathcal{S}_2^{lk} l^i (q-l)^j (q-l)^l l^k$, so we can combine the calculation of the planar and crossed box diagrams.

As the spin structure gets more complicated when the Δ -isobar enters the calculation, we cannot carry over the common decomposition of the NN potential in Eq. (3.1) to the Δ -sector. For the box diagrams split for the box diagrams the product of spin matrices \mathcal{S}_2^{lk} and the product of isospin matrices \mathcal{T}_2^{ji} belonging to the second baryon into a symmetric and an antisymmetric part (under the exchange of the upper indices). In combination with the spin and isospin operators of the first baryon one can construct the even and odd operators

$$\mathcal{S}^+ = \mathcal{S}_1^{ij} \left(\frac{1}{2} \mathcal{S}_2^{kl} + \frac{1}{2} \mathcal{S}_2^{lk} \right), \tag{4.36}$$

$$\mathcal{S}^- = \mathcal{S}_1^{ij} \left(\frac{1}{2} \mathcal{S}_2^{kl} - \frac{1}{2} \mathcal{S}_2^{lk} \right), \tag{4.37}$$

$$\mathcal{T}^+ = \mathcal{T}_1^{ij} \left(\frac{1}{2} \mathcal{T}_2^{ij} + \frac{1}{2} \mathcal{T}_2^{ji} \right), \tag{4.38}$$

$$\mathcal{T}^- = \mathcal{T}_1^{ij} \left(\frac{1}{2} \mathcal{T}_2^{ij} - \frac{1}{2} \mathcal{T}_2^{ji} \right). \tag{4.39}$$

By applying these definitions and merging planar and crossed box diagrams, the imaginary part of the two-pion exchange potential from box diagrams can be split into four different parts

$$\text{Im } V^{++} = \mathcal{T}^+ \mathcal{S}^+ \text{Im} \left(\text{planar box} + \text{crossed box} \right), \quad (4.40)$$

$$\text{Im } V^{+-} = \mathcal{T}^+ \mathcal{S}^- \text{Im} \left(\text{planar box} - \text{crossed box} \right), \quad (4.41)$$

$$\text{Im } V^{-+} = \mathcal{T}^- \mathcal{S}^+ \text{Im} \left(\text{planar box} - \text{crossed box} \right), \quad (4.42)$$

$$\text{Im } V^{--} = \mathcal{T}^- \mathcal{S}^- \text{Im} \left(\text{planar box} + \text{crossed box} \right), \quad (4.43)$$

where the symbolic diagrams in parenthesis represent the irreducible part of the planar box and the crossed box without their spin and isospin operators. The sign combination on $V^{\pm\pm}$ tells whether these diagrams are added or subtracted. V^{++} and V^{--} equal to zero for purely nucleonic intermediate states, because such combinations of diagrams vanish in this case. In the case of the $\text{NN} \rightarrow \text{NN}$ 2π -exchange potential this corresponds to the conventional notation in Eq. (3.1) as follows

$$\begin{aligned} \text{Im } V^{++}(i\mu) &\propto \text{Im } V_C(i\mu), \\ \text{Im } V^{+-}(i\mu) &\propto \text{Im } V_T(i\mu), \\ \text{Im } V^{-+}(i\mu) &\propto \text{Im } W_C(i\mu), \\ \text{Im } V^{--}(i\mu) &\propto \text{Im } W_T(i\mu). \end{aligned} \quad (4.44)$$

For a two-pion exchange triangle diagram the 2π phase space integrals read

$$\text{triangle} \rightarrow \text{Im } V = -\frac{|\mathbf{l}|}{16\pi\mu} \cdot g \cdot T \cdot (\mathbb{1} \otimes \mathcal{S}_2^{ij}) \left[q^i q^j \tilde{A}'_1 - \delta^{ij} \tilde{A}'_2 - q^i q^j \tilde{B}'_2 \right], \quad (4.45)$$

$$\text{triangle} \rightarrow \text{Im } V = -\frac{|\mathbf{l}|}{16\pi\mu} \cdot g \cdot T \cdot (\mathcal{S}_1^{ij} \otimes \mathbb{1}) \left[q^i q^j \tilde{A}'_1 - \delta^{ij} \tilde{A}'_2 - q^i q^j \tilde{B}'_2 \right]. \quad (4.46)$$

where g denotes the product of coupling constants and T stands for the isospin factor. The diagram containing two Tomozawa-Weinberg vertices is most easily evaluated

$$\text{bubble} \rightarrow \text{Im } V = -\frac{|\mathbf{l}|}{16\pi\mu} \cdot g \cdot T \cdot \frac{1}{2} \int_{-1}^1 dx \, 4x^2 |\mathbf{l}|^2 = -\frac{w^3}{96\pi\mu} \cdot g \cdot T, \quad (4.47)$$

where $|\mathbf{l}| = w/2$. The resulting contributions for the triangle and bubble diagrams are listed in Section 4.4.

4.2.3 Irreducible 2π -exchange from planar box diagrams

The set of planar and crossed box diagrams is shown in lines (b) to (g) of Fig. 3.3. Reducible parts of planar box diagrams will be generated by iteration of the 1π -exchange potentials in the coupled channel scattering equation, and therefore they have to be excluded from

the 2π -exchange potentials. To identify the irreducible parts of the planar box diagrams we calculate the l_0 -integral over the baryon and pion propagators. Here, ω_1 and ω_2 denote the on-shell energies of the two exchanged pions for the three types of planar box diagrams and their crossed partners. By applying residue calculus as outlined in Refs. [12, 13], we find the following results for the three different intermediate states NN, N Δ , $\Delta\Delta$:

$$\begin{aligned}
 \begin{array}{c} \bullet \text{---} \bullet \\ \bullet \text{---} \bullet \end{array} &\longrightarrow \int \frac{dl_0}{2\pi i} \frac{1}{(l_0 + i\epsilon)(-l_0 + i\epsilon)(l_0^2 - \omega_1^2 + i\epsilon)(l_0^2 - \omega_2^2 + i\epsilon)} \\
 &= \frac{1}{2\epsilon\omega_1^2\omega_2^2} - \frac{\omega_1^2 + \omega_1\omega_2 + \omega_2^2}{2\omega_1^3\omega_2^3(\omega_1 + \omega_2)}, \quad (4.48)
 \end{aligned}$$

$$\begin{aligned}
 \begin{array}{c} \bullet \text{---} \bullet \\ \bullet \text{---} \bullet \end{array} &\longrightarrow \int \frac{dl_0}{2\pi i} \frac{1}{(l_0 + i\epsilon)(-l_0 + i\epsilon)(l_0^2 - \omega_1^2 + i\epsilon)(l_0^2 - \omega_2^2 + i\epsilon)} \\
 &= \frac{\omega_1^2 + \omega_1\omega_2 + \omega_2^2}{2\omega_1^3\omega_2^3(\omega_1 + \omega_2)}, \quad (4.49)
 \end{aligned}$$

$$\begin{aligned}
 \begin{array}{c} \bullet \text{---} \bullet \\ \bullet \text{---} \bullet \end{array} &\longrightarrow \int \frac{dl_0}{2\pi i} \frac{1}{(l_0 - \Delta + i\epsilon)(-l_0 + i\epsilon)(l_0^2 - \omega_1^2 + i\epsilon)(l_0^2 - \omega_2^2 + i\epsilon)} \\
 &= \frac{1}{\Delta\omega_1^2\omega_2^2} - \frac{\omega_1^2 + \omega_1\omega_2 + \omega_2^2 + \Delta(\omega_1 + \omega_2)}{2\omega_1^2\omega_2^2(\omega_1 + \omega_2)(\omega_1 + \Delta)(\omega_2 + \Delta)}, \quad (4.50)
 \end{aligned}$$

$$\begin{aligned}
 \begin{array}{c} \bullet \text{---} \bullet \\ \bullet \text{---} \bullet \end{array} &\longrightarrow \int \frac{dl_0}{2\pi i} \frac{1}{(l_0 - \Delta + i\epsilon)(l_0 + i\epsilon)(l_0^2 - \omega_1^2 + i\epsilon)(l_0^2 - \omega_2^2 + i\epsilon)} \\
 &= \frac{\omega_1^2 + \omega_1\omega_2 + \omega_2^2 + \Delta(\omega_1 + \omega_2)}{2\omega_1^2\omega_2^2(\omega_1 + \omega_2)(\omega_1 + \Delta)(\omega_2 + \Delta)}, \quad (4.51)
 \end{aligned}$$

$$\begin{aligned}
 \begin{array}{c} \bullet \text{---} \bullet \\ \bullet \text{---} \bullet \end{array} &\longrightarrow \int \frac{dl_0}{2\pi i} \frac{1}{(l_0 - \Delta + i\epsilon)(-l_0 - \Delta + i\epsilon)(l_0^2 - \omega_1^2 + i\epsilon)(l_0^2 - \omega_2^2 + i\epsilon)} \\
 &= \frac{1}{2\Delta\omega_1^2\omega_2^2} - \frac{\omega_1^2 + \omega_1\omega_2 + \omega_2^2 + \Delta(\omega_1 + \omega_2)}{2\omega_1^2\omega_2^2(\omega_1 + \omega_2)(\omega_1 + \Delta)(\omega_2 + \Delta)}, \quad (4.52)
 \end{aligned}$$

$$\begin{aligned}
 \begin{array}{c} \bullet \text{---} \bullet \\ \bullet \text{---} \bullet \end{array} &\longrightarrow \int \frac{dl_0}{2\pi i} \frac{1}{(l_0 - \Delta + i\epsilon)^2(l_0^2 - \omega_1^2 + i\epsilon)(l_0^2 - \omega_2^2 + i\epsilon)} \\
 &= \frac{\omega_1^2 + \omega_1\omega_2 + \omega_2^2 + 2\Delta(\omega_1 + \omega_2) + \Delta^2}{2\omega_1\omega_2(\omega_1 + \omega_2)(\omega_1 + \Delta)^2(\omega_2 + \Delta)^2}. \quad (4.53)
 \end{aligned}$$

The reducible part is identified either by the inverse of the nucleon kinetic energy difference between intermediate and initial or final state (here just $1/\epsilon$) or by the $1/\Delta$ -dependence. The irreducible part of the planar NN-diagram is equal to the negative of the crossed NN-box, as it was also shown in Ref. [12]. By comparison with Eq. (4.51), one makes the interesting observation that the irreducible parts of the planar N Δ and $\Delta\Delta$ boxes are equal, and coincide with the negative of the crossed N Δ box. The crossed $\Delta\Delta$ box in Eq. (4.53), however, reveals a different structure. So we arrive at the following expressions for the baryon propagators of the combined planar and crossed box diagrams

$$\left(\begin{array}{c} \bullet \text{---} \bullet \\ \bullet \text{---} \bullet \end{array} + \begin{array}{c} \bullet \text{---} \bullet \\ \bullet \text{---} \bullet \end{array} \right) \longrightarrow \frac{i}{-ixl - \epsilon} \frac{i}{ixl + \epsilon} + \left(\frac{i}{-ixl - \epsilon} \right)^2 = 0,$$

$$\begin{aligned}
 \left(\begin{array}{c} \text{---} \\ \text{---} \\ \text{---} \\ \text{---} \end{array} \right) - \left(\begin{array}{c} \text{---} \\ \text{---} \\ \text{---} \\ \text{---} \end{array} \right) &\rightarrow \frac{i}{-ixl - \epsilon} \frac{i}{ixl + \epsilon} - \left(\frac{i}{-ixl - \epsilon} \right)^2 = \frac{2}{(-ixl - \epsilon)^2} \\
 \left(\begin{array}{c} \text{---} \\ \text{---} \\ \text{---} \\ \text{---} \end{array} \right) + \left(\begin{array}{c} \text{---} \\ \text{---} \\ \text{---} \\ \text{---} \end{array} \right) &\rightarrow \frac{i}{-ixl - \epsilon} \left(\frac{-i}{-ixl - \Delta} + \frac{i}{-ixl - \Delta} \right) = 0, \\
 \left(\begin{array}{c} \text{---} \\ \text{---} \\ \text{---} \\ \text{---} \end{array} \right) - \left(\begin{array}{c} \text{---} \\ \text{---} \\ \text{---} \\ \text{---} \end{array} \right) &\rightarrow \frac{i}{-ixl - \epsilon} \left(\frac{-i}{-ixl - \Delta} - \frac{i}{-ixl - \Delta} \right) = \left(\frac{1}{l} \mathcal{P} \frac{1}{x} + \frac{i\pi}{l} \delta(x) \right) \frac{-2}{xl - i\Delta} \\
 \left(\begin{array}{c} \text{---} \\ \text{---} \\ \text{---} \\ \text{---} \end{array} \right) + \left(\begin{array}{c} \text{---} \\ \text{---} \\ \text{---} \\ \text{---} \end{array} \right) &\rightarrow \frac{i}{-ixl - \epsilon} \frac{-i}{-ixl - \Delta} + \left(\frac{i}{-ixl - \Delta} \right)^2 \\
 &= \left(\frac{1}{l} \mathcal{P} \frac{1}{x} + \frac{i\pi}{l} \delta(x) \right) \frac{-1}{xl - i\Delta} + \frac{1}{(xl - i\Delta)^2}, \\
 \left(\begin{array}{c} \text{---} \\ \text{---} \\ \text{---} \\ \text{---} \end{array} \right) - \left(\begin{array}{c} \text{---} \\ \text{---} \\ \text{---} \\ \text{---} \end{array} \right) &\rightarrow \frac{i}{-ixl - \epsilon} \frac{-i}{-ixl - \Delta} - \left(\frac{i}{-ixl - \Delta} \right)^2 \\
 &= \left(\frac{1}{l} \mathcal{P} \frac{1}{x} + \frac{i\pi}{l} \delta(x) \right) \frac{-1}{xl - i\Delta} - \frac{1}{(xl - i\Delta)^2}. \tag{4.54}
 \end{aligned}$$

4.3 CONTRIBUTIONS OF TWO-PION EXCHANGE BOX DIAGRAMS

The phase space integrals for the coefficients (Eqs. (4.20), (4.24), (4.28) and (4.33)) taking into account the propagators of the two intermediate baryons (Eq. (4.54)) give rise to the following list of imaginary parts. The labels denote the intermediate state NN , $N\Delta$ or $\Delta\Delta$ and the relative sign between the planar and crossed box diagram.

$$\begin{aligned}
 \text{Im } A_2^{NN-} &= -\frac{w}{8\mu\pi} \\
 \text{Im } A_3^{NN-} &= -\frac{w}{16\mu\pi} \\
 \text{Im } A_4^{NN-} &= -\frac{w^3}{96\mu\pi} \\
 \text{Im } B_2^{NN-} &= -\frac{\mu^2 - 2m_\pi^2}{4\mu^3 w \pi} \\
 \text{Im } B_3^{NN-} &= -\frac{\mu^2 - 3m_\pi^2}{4\mu^3 w \pi} \\
 \text{Im } B_4^{NN-} &= -\frac{\mu^4 - 5\mu^2 m_\pi^2 + 4m_\pi^4}{24\mu^3 w \pi} \\
 \text{Im } C_4^{NN-} &= -\frac{\mu^4 - 4\mu^2 m_\pi^2 + 2m_\pi^4}{4\mu^5 w \pi} \tag{4.55}
 \end{aligned}$$

$$\begin{aligned}
 \text{Im } A_2^{N\Delta-} &= \frac{1}{32\Delta\mu\pi} \left[-2\Delta w - \frac{\pi}{2} w^2 + (4\Delta^2 + w^2) \arctan \frac{w}{2\Delta} \right] \\
 \text{Im } A_3^{N\Delta-} &= \frac{1}{64\Delta\mu\pi} \left[-2\Delta w - \frac{\pi}{2} w^2 + (4\Delta^2 + w^2) \arctan \frac{w}{2\Delta} \right]
 \end{aligned}$$

$$\begin{aligned}
 \text{Im } A_4^{N\Delta-} &= \frac{1}{512\Delta\mu\pi} \left[-8\Delta^3 w - \frac{10}{3}\Delta w^3 - \frac{\pi}{2}w^4 + (4\Delta^2 + w^2)^2 \arctan \frac{w}{2\Delta} \right] \\
 \text{Im } B_2^{N\Delta-} &= \frac{1}{32\Delta\mu^3\pi} \left[-2\Delta w + \frac{\pi}{2}(4m_\pi^2 - 3\mu^2) + (4\Delta^2 - 4m_\pi^2 + 3\mu^2) \arctan \frac{w}{2\Delta} \right] \\
 \text{Im } B_3^{N\Delta-} &= \frac{1}{64\Delta\mu^3\pi} \left[-6\Delta w + \frac{\pi}{2}(12m_\pi^2 - 5\mu^2) + (12\Delta^2 - 12m_\pi^2 + 5\mu^2) \arctan \frac{w}{2\Delta} \right] \\
 \text{Im } B_4^{N\Delta-} &= \frac{1}{512\Delta\mu^3\pi} \left[-\frac{2}{3}\Delta w(12\Delta^2 - 20m_\pi^2 + 17\mu^2) - \frac{\pi}{2}(16m_\pi^4 - 24m_\pi\mu + 5\mu^4) \right. \\
 &\quad \left. + (4\Delta^2 - 4m_\pi^2 + \mu^2)(4\Delta^2 - 4m_\pi^2 + 5\mu^2) \arctan \frac{w}{2\Delta} \right] \\
 \text{Im } C_4^{N\Delta-} &= \frac{1}{512\Delta\mu^5\pi} \left[-2\Delta w(12\Delta^2 - 20m_\pi^2 + 29\mu^2) - \frac{\pi}{2}(48m_\pi^4 - 120m_\pi^2\mu^2 + 35\mu^2) \right. \\
 &\quad \left. + (48(\Delta^2 - m_\pi^2)^2 + 120(\Delta^2 - m_\pi^2)\mu^2 + 35\mu^2) \arctan \frac{w}{2\Delta} \right] \tag{4.56}
 \end{aligned}$$

$$\begin{aligned}
 \text{Im } A_2^{\Delta\Delta-} &= \frac{1}{64\Delta\mu\pi} \left[-6\Delta w - \frac{\pi}{2}w^2 + (12\Delta^2 + w^2) \arctan \frac{w}{2\Delta} \right] \\
 \text{Im } A_3^{\Delta\Delta-} &= \frac{1}{128\Delta\mu\pi} \left[-6\Delta w - \frac{\pi}{2}w^2 + (12\Delta^2 + w^2) \arctan \frac{w}{2\Delta} \right] \\
 \text{Im } A_4^{\Delta\Delta-} &= \frac{1}{1024\Delta\mu\pi} \left[-\frac{2}{3}\Delta w(60\Delta^2 - 52m_\pi^2 + 13\mu^2) - \frac{\pi}{2}w^4 \right. \\
 &\quad \left. + (4\Delta^2 + w^2)(20\Delta^2 + w^2) \arctan \frac{w}{2\Delta} \right] \\
 \text{Im } B_2^{\Delta\Delta-} &= \frac{1}{64\Delta\mu^3\pi} \left[-2\Delta w \frac{12\Delta^2 - 12m_\pi^2 + 5\mu^2}{w^2 + 4\Delta^2} + \frac{\pi}{2}(4m_\pi^2 - 3\mu^2) \right. \\
 &\quad \left. + (12\Delta^2 - 4m_\pi^2 + 3\mu^2) \arctan \frac{w}{2\Delta} \right] \\
 \text{Im } B_3^{\Delta\Delta-} &= \frac{1}{128\Delta\mu^3\pi} \left[-2\Delta w \frac{36\Delta^2 - 36m_\pi^2 + 11\mu^2}{w^2 + 4\Delta^2} + \frac{\pi}{2}(12m_\pi^2 - 5\mu^2) \right. \\
 &\quad \left. + (36\Delta^2 - 12m_\pi^2 + 5\mu^2) \arctan \frac{w}{2\Delta} \right] \\
 \text{Im } B_4^{\Delta\Delta-} &= \frac{1}{1024\Delta\mu^3\pi} \left[-\frac{2}{3}\Delta w(60\Delta^2 - 52m_\pi^2 + 49\mu^2) - \frac{\pi}{2}(16m_\pi^4 - 24m_\pi^2 + 5\mu^2) \right. \\
 &\quad \left. + (80\Delta^4 - 96\Delta^2 m_\pi^2 + 72\Delta^2 \mu^2 + 16m_\pi^4 - 24m_\pi^2 \mu^2 + 5\mu^4) \arctan \frac{w}{2\Delta} \right] \\
 \text{Im } C_4^{\Delta\Delta-} &= \frac{1}{1024\Delta\mu^5\pi} \left[-2\Delta w \left(60\Delta^2 - 52m_\pi^2 + 85\mu^2 + \frac{8\mu^2}{w^2 + 4\Delta^2} \right) \right. \\
 &\quad - \frac{\pi}{2}(48m_\pi^4 - 120m_\pi^2\mu^2 + 35\mu^2) + (240\Delta^4 - 288\Delta^2 m_\pi^2 + 360\Delta^2 \mu^2) \\
 &\quad \left. + 48m_\pi^4 - 120m_\pi^2\mu^2 + 35\mu^4) \arctan \frac{w}{2\Delta} \right] \tag{4.57}
 \end{aligned}$$

$$\begin{aligned}
 \text{Im } A_2^{\Delta\Delta^+} &= \frac{1}{64\Delta\mu\pi} \left[2\Delta w - \frac{\pi}{2}w^2 + (-4\Delta^2 + w^2) \arctan \frac{w}{2\Delta} \right] \\
 \text{Im } A_3^{\Delta\Delta^+} &= \frac{1}{128\Delta\mu\pi} \left[2\Delta w - \frac{\pi}{2}w^2 + (-4\Delta^2 + w^2) \arctan \frac{w}{2\Delta} \right] \\
 \text{Im } A_4^{\Delta\Delta^+} &= -\frac{1}{2048\Delta\mu\pi} \left[4\Delta w(12\Delta^2 + w^2) - w^4\pi - 2(12\Delta^2 - w^2)(4\Delta^2 + w^2) \arctan \frac{w}{2\Delta} \right] \\
 \text{Im } B_2^{\Delta\Delta^+} &= \frac{1}{128\Delta\mu^3\pi} \left[4\Delta w \frac{4\Delta^2 - 4m_\pi^2 + 3\mu^2}{w^2 + 4\Delta^2} + (4m_\pi^2 - 3\mu^2)\pi \right. \\
 &\quad \left. - 2(4\Delta^2 + 4m_\pi^2 - 3\mu^2) \arctan \frac{w}{2\Delta} \right] \\
 \text{Im } B_3^{\Delta\Delta^+} &= \frac{1}{256\Delta\mu^3\pi} \left[4\Delta w \frac{12\Delta^2 - 12m_\pi^2 + 5\mu^2}{w^2 + 4\Delta^2} + (12m_\pi^2 - 5\mu^2)\pi \right. \\
 &\quad \left. - 2(12\Delta^2 + 12m_\pi^2 - 5\mu^2) \arctan \frac{w}{2\Delta} \right] \\
 \text{Im } B_4^{\Delta\Delta^+} &= \frac{1}{1024\Delta\mu^3\pi} \left[2\Delta w(12\Delta^2 - 4m_\pi^2 + 5\mu^2) + \frac{\pi}{2}(-16m_\pi^4 + 24m_\pi^2\mu^2 - 5\mu^4) \right. \\
 &\quad \left. + (-48\Delta^4 + 32\Delta^2m_\pi^2 - 24\Delta^2\mu^2 + 16m_\pi^4 - 24m_\pi^2\mu^2 + 5\mu^4) \arctan \frac{w}{2\Delta} \right] \\
 \text{Im } C_4^{\Delta\Delta^+} &= \frac{1}{2048\Delta\mu^5\pi} \left[4\Delta w \left(4\Delta^2 + 20m_\pi^2 + 35\mu^2 + \frac{128(\Delta^2 - m_\pi^2)^2}{w^2 + 4\Delta^2} \right) \right. \\
 &\quad \left. - (48m_\pi^4 - 120m_\pi^2\mu^2 + 35\mu^4)\pi - 2(144\Delta^4 - 96\Delta^2m_\pi^2 + 120\Delta^2\mu^2 \right. \\
 &\quad \left. - 48m_\pi^4 + 120m_\pi^2\mu^2 - 35\mu^4) \arctan \frac{w}{2\Delta} \right] \tag{4.58}
 \end{aligned}$$

with the abbreviation $w = \sqrt{\mu^2 - 4m_\pi^2}$.

These basic results feed into the calculation of two-pion exchange potentials. The potentials are labeled as follows: $V_{in\ out}^{\pm\pm\ int\pm}$, where both \pm refer to the sign of the decomposition from Eqs. (4.40) to (4.43). The subscripts *in* and *out* denote the two ingoing and outgoing baryons, respectively, and *int* refers to the intermediate baryon pair. The q -dependent functions A_i , B_i and C_i have to be calculated numerically as (regularized) dispersion integrals from their imaginary parts. The isospin factors $\mathcal{T}_{in\ out}^{\pm\int int}$ in front of the potentials can be calculated with little effort for total isospin $I = 0, 1$ and are collected in Table 4.3. It is worth mentioning, that nonvanishing potentials V^{++} and V^{--} exist only for the $\Delta\Delta$ intermediate state. This is a consequence of the negative sign of the irreducible part from planar NN and $N\Delta$ boxes.

I) $NN \rightarrow NN$:

$$V_{NNNN}^{+-NN} = \mathcal{T}_{NNNN}^{+NN} \frac{g_A^4}{16f_\pi^4} A_2^{NN-} (q^i q^j \sigma_1^i \sigma_2^j - q^2 \sigma_1^i \sigma_2^i)$$

$$\begin{aligned}
 V_{NNNN}^{-+NN} &= \mathcal{T}_{NNNN}^{-NN} \frac{9g_A^4}{16f_\pi^4} \left[q^2 \left[A_2^{NN-} + 10(B_4^{NN-} - A_3^{NN-}) \right. \right. \\
 &\quad \left. \left. + q^2(B_2^{NN-} - 2B_3^{NN-} + C_4^{NN-}) \right] + 15A_4^{NN-} \right] \\
 V_{NNNN}^{+-N\Delta} &= \mathcal{T}_{NNNN}^{+N\Delta} \frac{3g_A^4}{32f_\pi^4} A_2^{N\Delta-} (q^2 \sigma_1^i \sigma_2^i - q^i q^j \sigma_1^i \sigma_2^j) \\
 V_{NNNN}^{-+N\Delta} &= \mathcal{T}_{NNNN}^{-N\Delta} \frac{9g_A^4}{32f_\pi^4} \left[\frac{2}{3} q^2 \left[A_2^{N\Delta-} + 10(B_4^{N\Delta-} - A_3^{N\Delta-}) \right. \right. \\
 &\quad \left. \left. + q^2(B_2^{N\Delta-} - 2B_3^{N\Delta-} + C_4^{N\Delta-}) \right] + 10A_4^{N\Delta-} \right] \\
 V_{NNNN}^{\pm-\Delta\Delta} &= \mathcal{T}_{NNNN}^{\pm\Delta\Delta} \frac{9g_A^4}{64f_\pi^4} A_2^{\Delta\Delta\mp} (q^i q^j \sigma_1^i \sigma_2^j - q^2 \sigma_1^i \sigma_2^i) \\
 V_{NNNN}^{\pm+\Delta\Delta} &= \mathcal{T}_{NNNN}^{\pm\Delta\Delta} \frac{9g_A^4}{16f_\pi^4} \left[q^2 \left[A_2^{\Delta\Delta\pm} + 10(B_4^{\Delta\Delta\pm} - A_3^{\Delta\Delta\pm}) \right. \right. \\
 &\quad \left. \left. + q^2(B_2^{\Delta\Delta\pm} - 2B_3^{\Delta\Delta\pm} + C_4^{\Delta\Delta\pm}) \right] + 15A_4^{\Delta\Delta\pm} \right] \tag{4.59}
 \end{aligned}$$

 II) $NN \rightarrow N\Delta$:

$$\begin{aligned}
 V_{NNN\Delta}^{+-NN} &= \mathcal{T}_{NNN\Delta}^{+NN} \frac{3g_A^4}{32\sqrt{2}f_\pi^4} A_2^{NN-} (q^2 \sigma_1^i S_2^{i\dagger} - q^i q^j \sigma_1^i S_2^{j\dagger}) \\
 V_{NNN\Delta}^{-+NN} &= \mathcal{T}_{NNN\Delta}^{-NN} \frac{-3\sqrt{3}g_A^4}{32f_\pi^4} (q^i q^j S_2^{ij\dagger}) \left[A_2^{NN-} - 7A_3^{NN-} + 7B_4^{NN-} \right. \\
 &\quad \left. + q^2(B_2^{NN-} - 2B_3^{NN-} + C_4^{NN-}) \right] \\
 V_{NNN\Delta}^{+-N\Delta} &= \mathcal{T}_{NNN\Delta}^{+N\Delta} \frac{3g_A^4}{32\sqrt{2}f_\pi^4} A_2^{N\Delta-} (q^i q^j \sigma_1^i S_2^{j\dagger} - q^2 \sigma_1^i S_2^{i\dagger}) \\
 V_{NNN\Delta}^{-+N\Delta} &= \mathcal{T}_{NNN\Delta}^{-N\Delta} \frac{-\sqrt{3}g_A^4}{80f_\pi^4} (q^i q^j S_2^{ij\dagger}) \left[A_2^{N\Delta-} - 7A_3^{N\Delta-} + 7B_4^{N\Delta-} \right. \\
 &\quad \left. + q^2(B_2^{N\Delta-} - 2B_3^{N\Delta-} + C_4^{N\Delta-}) \right] \\
 V_{NNN\Delta}^{+-\Delta N} &= \mathcal{T}_{NNN\Delta}^{+\Delta N} \frac{9g_A^4}{64\sqrt{2}f_\pi^4} A_2^{N\Delta-} (q^i q^j \sigma_1^i S_2^{j\dagger} - q^2 \sigma_1^i S_2^{i\dagger})
 \end{aligned}$$

$$\begin{aligned}
 V_{NNN\Delta}^{-+\Delta N} &= \mathcal{T}_{NNN\Delta}^{-\Delta N} \frac{-27\sqrt{3}g_A^4}{64f_\pi^4} (q^i q^j S_2^{ij\dagger}) \left[A_2^{N\Delta-} - 7A_3^{N\Delta-} + 7B_4^{N\Delta-} \right. \\
 &\quad \left. + q^2 (B_2^{N\Delta-} - 2B_3^{N\Delta-} + C_4^{N\Delta-}) \right] \\
 V_{NNN\Delta}^{\pm-\Delta\Delta} &= \mathcal{T}_{NNN\Delta}^{\pm\Delta\Delta} \frac{9g_A^4}{64\sqrt{2}f_\pi^4} A_2^{\Delta\Delta\mp} (q^2 \sigma_1^i S_2^{i\dagger} - q^i q^j \sigma_1^i S_2^{j\dagger}) \\
 V_{NNN\Delta}^{\pm+\Delta\Delta} &= \mathcal{T}_{NNN\Delta}^{\pm\Delta\Delta} \frac{-9\sqrt{3}g_A^4}{160f_\pi^4} (q^i q^j S_2^{ij\dagger}) \left[A_2^{\Delta\Delta\pm} - 7A_3^{\Delta\Delta\pm} + 7B_4^{\Delta\Delta\pm} \right. \\
 &\quad \left. + q^2 (B_2^{\Delta\Delta\pm} - 2B_3^{\Delta\Delta\pm} + C_4^{\Delta\Delta\pm}) \right]
 \end{aligned} \tag{4.60}$$

III) $N\Delta \rightarrow N\Delta$:

$$\begin{aligned}
 V_{N\Delta N\Delta}^{+-NN} &= \mathcal{T}_{N\Delta N\Delta}^{+NN} \frac{3g_A^4}{64f_\pi^4} A_2^{NN-} (q^i q^j \sigma_1^i \Sigma_2^j - q^2 \sigma_1^i \Sigma_2^i) \\
 V_{N\Delta N\Delta}^{-+NN} &= \mathcal{T}_{N\Delta N\Delta}^{-NN} \frac{3g_A^4}{32f_\pi^4} \left[-(q^i q^j \Sigma_2^{ij}) \left[A_2^{NN-} - 7A_3^{NN-} + 7B_4^{NN-} \right. \right. \\
 &\quad \left. \left. + q^2 (B_2^{NN-} - 2B_3^{NN-} + C_4^{NN-}) \right] + q^2 \left[A_2^{NN-} - 10A_3^{NN-} + 10B_4^{NN-} \right. \right. \\
 &\quad \left. \left. + q^2 (B_2^{NN-} - 2B_3^{NN-} + C_4^{NN-}) \right] + 15A_4^{NN-} \right] \\
 V_{N\Delta N\Delta}^{+-N\Delta} &= \mathcal{T}_{N\Delta N\Delta}^{+N\Delta} \frac{g_A^4}{400f_\pi^4} A_2^{N\Delta-} (q^i q^j \sigma_1^i \Sigma_2^j - q^2 \sigma_1^i \Sigma_2^i) \\
 V_{N\Delta N\Delta}^{-+N\Delta} &= \mathcal{T}_{N\Delta N\Delta}^{-N\Delta} \frac{g_A^4}{400f_\pi^4} \left[4q^i q^j \Sigma_2^{ij} \left[A_2^{N\Delta-} - 7A_3^{N\Delta-} + 7B_4^{N\Delta-} \right. \right. \\
 &\quad \left. \left. + q^2 (B_2^{N\Delta-} - 2B_3^{N\Delta-} + C_4^{N\Delta-}) \right] + 5q^2 \left[A_2^{N\Delta-} - 10A_3^{N\Delta-} + 10B_4^{N\Delta-} \right. \right. \\
 &\quad \left. \left. + q^2 (B_2^{N\Delta-} - 2B_3^{N\Delta-} + C_4^{N\Delta-}) \right] + 75A_4^{N\Delta-} \right] \\
 V_{N\Delta N\Delta}^{+-\Delta N} &= \mathcal{T}_{N\Delta N\Delta}^{+\Delta N} \frac{9g_A^4}{128f_\pi^4} A_2^{N\Delta-} (q^2 \sigma_1^i \Sigma_2^i - q^i q^j \sigma_1^i \Sigma_2^j) \\
 V_{N\Delta N\Delta}^{-+\Delta N} &= \mathcal{T}_{N\Delta N\Delta}^{-\Delta N} \frac{9g_A^4}{32f_\pi^4} \left[-(q^i q^j \Sigma_2^{ij}) \left[A_2^{N\Delta-} - 7A_3^{N\Delta-} + 7B_4^{N\Delta-} \right. \right. \\
 &\quad \left. \left. + q^2 (B_2^{N\Delta-} - 2B_3^{N\Delta-} + C_4^{N\Delta-}) \right] + q^2 \left[A_2^{N\Delta-} - 10A_3^{N\Delta-} + 10B_4^{N\Delta-} \right. \right. \\
 &\quad \left. \left. + q^2 (B_2^{N\Delta-} - 2B_3^{N\Delta-} + C_4^{N\Delta-}) \right] + 15A_4^{N\Delta-} \right]
 \end{aligned}$$

$$\begin{aligned}
 V_{N\Delta N\Delta}^{\pm-\Delta\Delta} &= \mathcal{T}_{N\Delta N\Delta}^{\pm\Delta\Delta} \frac{3g_A^4}{800f_\pi^4} A_2^{\Delta\Delta\mp} (q^2 \sigma_1^i \Sigma_2^i - q^i q^j \sigma_1^i \Sigma_2^j) \\
 V_{N\Delta N\Delta}^{\pm+\Delta\Delta} &= \mathcal{T}_{N\Delta N\Delta}^{\pm\Delta\Delta} \frac{3g_A^4}{400f_\pi^4} \left[4q^i q^j \Sigma_2^{ij} \left[A_2^{\Delta\Delta\pm} - 7A_3^{\Delta\Delta\pm} + 7B_4^{\Delta\Delta\pm} \right. \right. \\
 &\quad \left. \left. + q^2 (B_2^{\Delta\Delta\pm} - 2B_3^{\Delta\Delta\pm} + C_4^{\Delta\Delta\pm}) \right] + 5q^2 \left[A_2^{\Delta\Delta\pm} - 10A_3^{\Delta\Delta\pm} + 10B_4^{\Delta\Delta\pm} \right. \right. \\
 &\quad \left. \left. + q^2 (B_2^{\Delta\Delta\pm} - 2B_3^{\Delta\Delta\pm} + C_4^{\Delta\Delta\pm}) \right] + 75A_4^{\Delta\Delta\pm} \right] \quad (4.61)
 \end{aligned}$$

IV) $\Delta N \rightarrow N\Delta$:

$$\begin{aligned}
 V_{\Delta N N\Delta}^{+-NN} &= \mathcal{T}_{\Delta N N\Delta}^{+NN} \frac{9g_A^4}{128f_\pi^4} A_2^{NN-} (q^i q^j S_1^i S_2^{j\dagger} - q^2 S_1^i S_2^{i\dagger}) \\
 V_{\Delta N N\Delta}^{-+NN} &= \mathcal{T}_{\Delta N N\Delta}^{-NN} \frac{27g_A^4}{64f_\pi^4} \left[(A_2^{NN-} - 4A_3^{NN-} + 4B_4^{NN-}) (q^i q^j S_1^{ik} S_2^{jk\dagger}) \right. \\
 &\quad \left. + 2A_4^{NN-} (S_1^{ij} S_2^{ij\dagger}) + (B_2^{NN-} - 2B_3^{NN-} + C_4^{NN-}) (q^i q^j q^k q^l S_1^{ij} S_2^{kl\dagger}) \right] \\
 V_{\Delta N N\Delta}^{+-N\Delta} &= \mathcal{T}_{\Delta N N\Delta}^{+N\Delta} \frac{9g_A^4}{128f_\pi^4} A_2^{N\Delta-} (q^2 S_1^i S_2^{i\dagger} - q^i q^j S_1^i S_2^{j\dagger}) \\
 V_{\Delta N N\Delta}^{-+N\Delta} &= \mathcal{T}_{\Delta N N\Delta}^{-N\Delta} \frac{27g_A^4}{320f_\pi^4} \left[(A_2^{N\Delta-} - 4A_3^{N\Delta-} + 4B_4^{N\Delta-}) (q^i q^j S_1^{ik} S_2^{jk\dagger}) \right. \\
 &\quad \left. + 2A_4^{N\Delta-} (S_1^{ij} S_2^{ij\dagger}) + (B_2^{N\Delta-} - 2B_3^{N\Delta-} + C_4^{N\Delta-}) (q^i q^j q^k q^l S_1^{ij} S_2^{kl\dagger}) \right] \\
 V_{\Delta N N\Delta}^{+-\Delta N} &= \mathcal{T}_{\Delta N N\Delta}^{+\Delta N} \frac{9g_A^4}{128f_\pi^4} A_2^{N\Delta-} (q^2 S_1^i S_2^{i\dagger} - q^i q^j S_1^i S_2^{j\dagger}) \\
 V_{\Delta N N\Delta}^{-+\Delta N} &= \mathcal{T}_{\Delta N N\Delta}^{-\Delta N} \frac{27g_A^4}{320f_\pi^4} \left[(A_2^{N\Delta-} - 4A_3^{N\Delta-} + 4B_4^{N\Delta-}) (q^i q^j S_1^{ik} S_2^{jk\dagger}) \right. \\
 &\quad \left. + 2A_4^{N\Delta-} (S_1^{ij} S_2^{ij\dagger}) + (B_2^{N\Delta-} - 2B_3^{N\Delta-} + C_4^{N\Delta-}) (q^i q^j q^k q^l S_1^{ij} S_2^{kl\dagger}) \right] \\
 V_{\Delta N N\Delta}^{\pm-\Delta\Delta} &= \mathcal{T}_{\Delta N N\Delta}^{\pm\Delta\Delta} \frac{9g_A^4}{128f_\pi^4} A_2^{\Delta\Delta\mp} (q^i q^j S_1^i S_2^{j\dagger} - q^2 S_1^i S_2^{i\dagger}) \\
 V_{\Delta N N\Delta}^{\pm+\Delta\Delta} &= \mathcal{T}_{\Delta N N\Delta}^{\pm\Delta\Delta} \frac{27g_A^4}{1600f_\pi^4} \left[(A_2^{\Delta\Delta\pm} - 4A_3^{\Delta\Delta\pm} + 4B_4^{\Delta\Delta\pm}) (q^i q^j S_1^{ik} S_2^{jk\dagger}) \right. \\
 &\quad \left. + 2A_4^{\Delta\Delta\pm} (S_1^{ij} S_2^{ij\dagger}) + (B_2^{\Delta\Delta\pm} - 2B_3^{\Delta\Delta\pm} + C_4^{\Delta\Delta\pm}) (q^i q^j q^k q^l S_1^{ij} S_2^{kl\dagger}) \right] \quad (4.62)
 \end{aligned}$$

V) $NN \rightarrow \Delta\Delta$:

$$\begin{aligned}
 V_{NN\Delta\Delta}^{+-NN} &= \mathcal{T}_{NN\Delta\Delta}^{+NN} \frac{9g_A^4}{128f_\pi^4} A_2^{NN-} (q^i q^j S_1^{i\dagger} S_2^{j\dagger} - q^2 S_1^{i\dagger} S_2^{j\dagger}) \\
 V_{NN\Delta\Delta}^{-+NN} &= \mathcal{T}_{NN\Delta\Delta}^{-NN} \frac{27g_A^4}{64f_\pi^4} \left[(A_2^{NN-} - 4A_3^{NN-} + 4B_4^{NN-}) (q^i q^j S_1^{ik\dagger} S_2^{jk\dagger}) \right. \\
 &\quad \left. + 2A_4^{NN-} (S_1^{ij\dagger} S_2^{ij\dagger}) + (B_2^{NN-} - 2B_3^{NN-} + C_4^{NN-}) (q^i q^j q^k q^l S_1^{ij\dagger} S_2^{kl\dagger}) \right] \\
 V_{NN\Delta\Delta}^{+-N\Delta} &= \mathcal{T}_{NN\Delta\Delta}^{+N\Delta} \frac{9g_A^4}{128f_\pi^4} A_2^{N\Delta-} (q^2 S_1^{i\dagger} S_2^{i\dagger} - q^i q^j S_1^{i\dagger} S_2^{j\dagger}) \\
 V_{NN\Delta\Delta}^{-+N\Delta} &= \mathcal{T}_{NN\Delta\Delta}^{-N\Delta} \frac{27g_A^4}{320f_\pi^4} \left[(A_2^{N\Delta-} - 4A_3^{N\Delta-} + 4B_4^{N\Delta-}) (q^i q^j S_1^{ik\dagger} S_2^{jk\dagger}) \right. \\
 &\quad \left. + 2A_4^{N\Delta-} (S_1^{ij\dagger} S_2^{ij\dagger}) + (B_2^{N\Delta-} - 2B_3^{N\Delta-} + C_4^{N\Delta-}) (q^i q^j q^k q^l S_1^{ij\dagger} S_2^{kl\dagger}) \right] \\
 V_{NN\Delta\Delta}^{\pm-\Delta\Delta} &= \mathcal{T}_{NN\Delta\Delta}^{\pm\Delta\Delta} \frac{9g_A^4}{128f_\pi^4} A_2^{\Delta\Delta-} (q^i q^j S_1^{i\dagger} S_2^{j\dagger} - q^2 S_1^{i\dagger} S_2^{j\dagger}) \\
 V_{NN\Delta\Delta}^{\pm+\Delta\Delta} &= \mathcal{T}_{NN\Delta\Delta}^{\pm\Delta\Delta} \frac{27g_A^4}{1600f_\pi^4} \left[(A_2^{\Delta\Delta\pm} - 4A_3^{\Delta\Delta\pm} + 4B_4^{\Delta\Delta\pm}) (q^i q^j S_1^{ik\dagger} S_2^{jk\dagger}) \right. \\
 &\quad \left. + 2A_4^{\Delta\Delta\pm} (S_1^{ij\dagger} S_2^{ij\dagger}) + (B_2^{\Delta\Delta\pm} - 2B_3^{\Delta\Delta\pm} + C_4^{\Delta\Delta\pm}) (q^i q^j q^k q^l S_1^{ij\dagger} S_2^{kl\dagger}) \right] \quad (4.63)
 \end{aligned}$$

VI) $N\Delta \rightarrow \Delta\Delta$:

$$\begin{aligned}
 V_{N\Delta\Delta\Delta}^{+-NN} &= \mathcal{T}_{N\Delta\Delta\Delta}^{+NN} \frac{9g_A^4}{128\sqrt{2}f_\pi^4} A_2^{NN-} (q^2 S_1^{i\dagger} \Sigma_2^i - q^i q^j S_1^{i\dagger} \Sigma_2^j) \\
 V_{N\Delta\Delta\Delta}^{-+NN} &= \mathcal{T}_{N\Delta\Delta\Delta}^{-NN} \frac{9\sqrt{3}g_A^4}{64f_\pi^4} \left[- \left[A_2^{NN-} - 7A_3^{NN-} + 7B_4^{NN-} \right. \right. \\
 &\quad \left. \left. + q^2 (B_2^{NN-} - 2B_3^{NN-} + C_4^{NN-}) \right] (q^i q^j S_1^{ij\dagger}) \right. \\
 &\quad \left. + (A_2^{NN-} - 4A_3^{NN-} + 4B_4^{NN-}) (q^i q^j S_1^{ik\dagger} \Sigma_2^{jk}) + 2A_4^{NN-} (S_1^{ij\dagger} \Sigma_2^{ij}) \right. \\
 &\quad \left. + (B_2^{NN-} - 2B_3^{NN-} + C_4^{NN-}) (q^i q^j q^k q^l S_1^{ij\dagger} \Sigma_2^{kl}) \right] \\
 V_{N\Delta\Delta\Delta}^{+-N\Delta} &= \mathcal{T}_{N\Delta\Delta\Delta}^{+N\Delta} \frac{3g_A^4}{800\sqrt{2}f_\pi^4} A_2^{N\Delta-} (q^2 S_1^{i\dagger} \Sigma_2^i - q^i q^j S_1^{i\dagger} \Sigma_2^j)
 \end{aligned}$$

$$\begin{aligned}
 V_{N\Delta\Delta\Delta}^{-+N\Delta} &= \mathcal{T}_{N\Delta\Delta\Delta}^{-N\Delta} \frac{-3\sqrt{3}g_A^4}{800f_\pi^4} \left[5 \left[A_2^{N\Delta-} - 7A_3^{N\Delta-} + 7B_4^{N\Delta-} \right. \right. \\
 &\quad \left. \left. + q^2(B_2^{N\Delta-} - 2B_3^{N\Delta-} + C_4^{N\Delta-}) \right] (q^i q^j S_1^{ij\dagger}) \right. \\
 &\quad \left. + 4(A_2^{N\Delta-} - 4A_3^{N\Delta-} + 4B_4^{N\Delta-}) (q^i q^j S_1^{ik\dagger} \Sigma_2^{jk}) + 8A_4^{N\Delta-} (S_1^{ij\dagger} \Sigma_2^{ij}) \right. \\
 &\quad \left. + 4(B_2^{N\Delta-} - 2B_3^{N\Delta-} + C_4^{N\Delta-}) (q^i q^j q^k q^l S_1^{ij\dagger} \Sigma_2^{kl}) \right] \\
 V_{N\Delta\Delta\Delta}^{+-\Delta N} &= \mathcal{T}_{N\Delta\Delta\Delta}^{+\Delta N} \frac{9g_A^4}{128\sqrt{2}f_\pi^4} A_2^{N\Delta-} (q^i q^j S_1^{i\dagger} \Sigma_2^j - q^2 S_1^{i\dagger} \Sigma_2^i) \\
 V_{N\Delta\Delta\Delta}^{-+\Delta N} &= \mathcal{T}_{N\Delta\Delta\Delta}^{-\Delta N} \frac{9\sqrt{3}g_A^4}{320f_\pi^4} \left[- \left[A_2^{N\Delta-} - 7A_3^{N\Delta-} + 7B_4^{N\Delta-} \right. \right. \\
 &\quad \left. \left. + q^2(B_2^{N\Delta-} - 2B_3^{N\Delta-} + C_4^{N\Delta-}) \right] (q^i q^j S_1^{ij\dagger}) \right. \\
 &\quad \left. + (A_2^{N\Delta-} - 4A_3^{N\Delta-} + 4B_4^{N\Delta-}) (q^i q^j S_1^{ik\dagger} \Sigma_2^{jk}) + 2A_4^{N\Delta-} (S_1^{ij\dagger} \Sigma_2^{ij}) \right. \\
 &\quad \left. + (B_2^{N\Delta-} - 2B_3^{N\Delta-} + C_4^{N\Delta-}) (q^i q^j q^k q^l S_1^{ij\dagger} \Sigma_2^{kl}) \right] \\
 V_{N\Delta\Delta\Delta}^{\pm-\Delta\Delta} &= \mathcal{T}_{N\Delta\Delta\Delta}^{\pm\Delta\Delta} \frac{3g_A^4}{800\sqrt{2}f_\pi^4} A_2^{\Delta\Delta\mp} (q^i q^j S_1^{i\dagger} \Sigma_2^j - q^2 S_1^{i\dagger} \Sigma_2^i) \\
 V_{N\Delta\Delta\Delta}^{\pm+\Delta\Delta} &= \mathcal{T}_{N\Delta\Delta\Delta}^{\pm\Delta\Delta} \frac{-3\sqrt{3}g_A^4}{4000f_\pi^4} \left[5 \left[A_2^{\Delta\Delta\pm} - 7A_3^{\Delta\Delta\pm} + 7B_4^{\Delta\Delta\pm} \right. \right. \\
 &\quad \left. \left. + q^2(B_2^{\Delta\Delta\pm} - 2B_3^{\Delta\Delta\pm} + C_4^{\Delta\Delta\pm}) \right] (q^i q^j S_1^{ij\dagger}) \right. \\
 &\quad \left. + 4(A_2^{\Delta\Delta\pm} - 4A_3^{\Delta\Delta\pm} + 4B_4^{\Delta\Delta\pm}) (q^i q^j S_1^{ik\dagger} \Sigma_2^{jk}) + 8A_4^{\Delta\Delta\pm} (S_1^{ij\dagger} \Sigma_2^{ij}) \right. \\
 &\quad \left. + 4(B_2^{\Delta\Delta\pm} - 2B_3^{\Delta\Delta\pm} + C_4^{\Delta\Delta\pm}) (q^i q^j q^k q^l S_1^{ij\dagger} \Sigma_2^{kl}) \right] \tag{4.64}
 \end{aligned}$$

 VII) $\Delta\Delta \rightarrow \Delta\Delta$:

$$\begin{aligned}
 V_{\Delta\Delta\Delta\Delta}^{+ - NN} &= \mathcal{T}_{\Delta\Delta\Delta\Delta}^{+ NN} \frac{9g_A^4}{256f_\pi^4} A_2^{NN-} (q^i q^j \Sigma_1^i \Sigma_2^j - q^2 \Sigma_1^i \Sigma_2^i) \\
 V_{\Delta\Delta\Delta\Delta}^{-+ NN} &= \mathcal{T}_{\Delta\Delta\Delta\Delta}^{- NN} \frac{9g_A^4}{64f_\pi^4} \left[q^i q^j q^k q^l \Sigma_1^{ij} \Sigma_2^{kl} (B_2 - 2B_3 + C_4) \right. \\
 &\quad \left. + q^i q^j \Sigma_1^{ik} \Sigma_2^{jk} (A_2^{NN-} - 4A_3^{NN-} + 4B_4^{NN-}) + 2\Sigma_1^{ij} \Sigma_2^{ij} A_4^{NN-} \right. \\
 &\quad \left. - q^i q^j (\Sigma_1^{ij} + \Sigma_2^{ij}) \left[A_2^{NN-} - 7A_3^{NN-} + 7B_4^{NN-} \right. \right. \\
 &\quad \left. \left. + q^2(B_2^{NN-} - 2B_3^{NN-} + C_4^{NN-}) \right] + \left[15A_4^{NN-} \right. \right. \\
 &\quad \left. \left. + q^2(A_2^{NN-} - 10A_3^{NN-} + 10B_4^{NN-}) + q^4(B_2^{NN-} - 2B_3^{NN-} + C_4^{NN-}) \right] \right]
 \end{aligned}$$

TABLE 4.3: Isospin factors evaluated for the total isospin $I = 0, 1$ as described in the text.

	$NN \rightarrow NN$	$NN \rightarrow N\Delta$	$N\Delta \rightarrow N\Delta$	$\Delta N \rightarrow N\Delta$	$NN \rightarrow \Delta\Delta$	$N\Delta \rightarrow \Delta\Delta$	$\Delta\Delta \rightarrow \Delta\Delta$
\mathcal{T}^{+NN}	3	0	1	$-\frac{5}{2}I$	$\frac{1}{\sqrt{2}}(5(1-I) - \sqrt{5}I)$	$-\sqrt{\frac{5}{3}}I$	$\frac{1}{6}(7 - 4I)$
\mathcal{T}^{-NN}	$6 - 8I$	$2\sqrt{\frac{2}{3}}I$	$\frac{5}{3}I$	$\frac{1}{6}I$	$\frac{1}{3\sqrt{2}}(3(1-I) + \sqrt{5}I)$	$-\frac{1}{3}\sqrt{\frac{5}{3}}I$	$\frac{5}{6} - \frac{2}{9}I$
$\mathcal{T}^{+N\Delta}$	2	0	15	$-\frac{5}{2}I$	$\frac{1}{\sqrt{2}}(5(1-I) - \sqrt{5}I)$	$2\sqrt{10}I$	$-5 + 8I$
$\mathcal{T}^{-N\Delta}$	$-2 + \frac{8}{3}I$	$-10\sqrt{\frac{2}{3}}I$	$10I$	$-\frac{5}{6}I$	$-\frac{5}{3\sqrt{2}}(3(1-I) + \sqrt{5}I)$	$-2\sqrt{\frac{5}{3}}I$	$5 - \frac{4}{3}I$
$\mathcal{T}^{+\Delta N}$	2	0	$\frac{2}{3}$	$-\frac{5}{2}I$	$\frac{1}{\sqrt{2}}(5(1-I) - \sqrt{5}I)$	$-\sqrt{\frac{5}{3}}I$	$-5 + 8I$
$\mathcal{T}^{-\Delta N}$	$-2 + \frac{8}{3}I$	$-\frac{2}{3}\sqrt{\frac{2}{3}}I$	$-\frac{5}{9}I$	$-\frac{5}{6}I$	$-\frac{5}{3\sqrt{2}}(3(1-I) + \sqrt{5}I)$	$\frac{5}{3}\sqrt{\frac{5}{3}}I$	$5 - \frac{4}{3}I$
$\mathcal{T}^{+\Delta\Delta}$	$\frac{4}{3}$	0	10	$-\frac{5}{2}I$	$\frac{1}{\sqrt{2}}(5(1-I) - \sqrt{5}I)$	$2\sqrt{10}I$	$195 - 96I$
$\mathcal{T}^{-\Delta\Delta}$	$\frac{2}{3} - \frac{8}{9}I$	$\frac{10}{3}\sqrt{\frac{2}{3}}I$	$-\frac{10}{3}I$	$\frac{25}{6}I$	$-\frac{25}{3\sqrt{2}}(3(1-I) + \sqrt{5}I)$	$10\sqrt{\frac{5}{3}}I$	$30 - 8I$

$$\begin{aligned}
 V_{\Delta\Delta\Delta\Delta}^{+-N\Delta} &= \mathcal{T}_{\Delta\Delta\Delta\Delta}^{+N\Delta} \frac{3g_A^4}{1600f_\pi^4} A_2^{N\Delta-} (q^i q^j \Sigma_1^i \Sigma_2^j - q^2 \Sigma_1^i \Sigma_2^i) \\
 V_{\Delta\Delta\Delta\Delta}^{-+N\Delta} &= \mathcal{T}_{\Delta\Delta\Delta\Delta}^{-N\Delta} \frac{3g_A^4}{800f_\pi^4} \left[-4q^i q^j q^k q^l \Sigma_1^{ij} \Sigma_2^{kl} (B_2^{N\Delta-} - 2B_3^{N\Delta-} + C_4^{N\Delta-}) \right. \\
 &\quad + 4q^i q^j \Sigma_1^{ik} \Sigma_2^{jk} (A_2^{N\Delta-} - 4A_3^{N\Delta-} + 4B_4^{N\Delta-}) - 8\Sigma_1^{ij} \Sigma_2^{ij} A_4^{N\Delta-} \\
 &\quad - q^i q^j (5\Sigma_1^{ij} - 4\Sigma_2^{ij}) [A_2^{N\Delta-} - 7A_3^{N\Delta-} + 7B_4^{N\Delta-} \\
 &\quad + q^2 (B_2^{N\Delta-} - 2B_3^{N\Delta-} + C_4^{N\Delta-})] + 5[15A_4^{N\Delta-} \\
 &\quad \left. + q^2 (A_2^{N\Delta-} - 10A_3^{N\Delta-} + 10B_4^{N\Delta-}) + q^4 (B_2^{N\Delta-} - 2B_3^{N\Delta-} + C_4^{N\Delta-}) \right] \\
 V_{\Delta\Delta\Delta\Delta}^{\pm-\Delta\Delta} &= \mathcal{T}_{\Delta\Delta\Delta\Delta}^{\pm\Delta\Delta} \frac{g_A^4}{10000f_\pi^4} A_2^{\Delta\Delta\mp} (q^i q^j \Sigma_1^i \Sigma_2^j - q^2 \Sigma_1^i \Sigma_2^i) \\
 V_{\Delta\Delta\Delta\Delta}^{\pm+\Delta\Delta} &= \mathcal{T}_{\Delta\Delta\Delta\Delta}^{\pm\Delta\Delta} \frac{g_A^4}{10000f_\pi^4} \left[16q^i q^j q^k q^l \Sigma_1^{ij} \Sigma_2^{kl} (B_2^{\Delta\Delta\pm} - 2B_3^{\Delta\Delta\pm} + C_4^{\Delta\Delta\pm}) \right. \\
 &\quad + 16q^i q^j \Sigma_1^{ik} \Sigma_2^{jk} (A_2^{\Delta\Delta\pm} - 4A_3^{\Delta\Delta\pm} + 4B_4^{\Delta\Delta\pm} + 32\Sigma_1^{ij} \Sigma_2^{ij} A_4^{\Delta\Delta\pm} \\
 &\quad + 20q^i q^j (\Sigma_1^{ij} + \Sigma_2^{ij}) [A_2^{\Delta\Delta\pm} - 7A_3^{\Delta\Delta\pm} + 7B_4^{\Delta\Delta\pm} \\
 &\quad + q^2 (B_2^{\Delta\Delta\pm} - 2B_3^{\Delta\Delta\pm} + C_4^{\Delta\Delta\pm})] + 25[15A_4^{\Delta\Delta\pm} \\
 &\quad \left. + q^2 (A_2^{\Delta\Delta\pm} - 10A_3^{\Delta\Delta\pm} + 10B_4^{\Delta\Delta\pm}) + q^4 (B_2^{\Delta\Delta\pm} - 2B_3^{\Delta\Delta\pm} + C_4^{\Delta\Delta\pm}) \right] \quad (4.65)
 \end{aligned}$$

4.4 TRIANGLE AND BUBBLE DIAGRAMS

The set of contributing 2π -exchange triangle diagrams is shown in lines (h) and (i) of Fig. 3.3. The triangle diagrams have a single baryon (N or Δ) in the intermediate state and the corresponding imaginary parts arising from the phase space integrals in Eqs. (4.20) and (4.24) are given by the following expressions

$$\begin{aligned}
 \text{Im } A_1^N &= \frac{w}{16\pi\mu} , \\
 \text{Im } A_2^N &= \frac{w^3}{96\pi\mu} , \\
 \text{Im } B_2^N &= \frac{w}{24\pi\mu^3} (\mu^2 - m_\pi^2) , \quad (4.66)
 \end{aligned}$$

$$\begin{aligned}
 \text{Im } A_1^\Delta &= \frac{1}{48\pi\mu} \left[\frac{w}{2} - \Delta \arctan \frac{w}{2\Delta} \right], \\
 \text{Im } A_2^\Delta &= \frac{1}{192\pi\mu} \left[12\Delta^2 w + 2w^3 - 6\Delta(4\Delta^2 + w^2) \arctan \frac{w}{2\Delta} \right], \\
 \text{Im } B_2^\Delta &= \frac{1}{96\pi\mu^3} \left[6\Delta^2 w + 4w^3 - 3\Delta(4\Delta^2 - 4m_\pi^2 + 3\mu^2) \arctan \frac{w}{2\Delta} \right]. \tag{4.67}
 \end{aligned}$$

with $w = \sqrt{\mu^2 - 4m_\pi^2}$. Using the general forms of the 2π phase space integrals in Eqs. (4.45) and (4.46), the 2π -exchange potentials from the triangle diagrams with a nucleon intermediate state read

$$\begin{aligned}
 V_{NNNN}^{\bullet\leftarrow\leftarrow\leftarrow\leftarrow} &= \frac{g_A^2}{8f_\pi^4} (4I - 3) \left[q^2 A_1^N - 3A_2^N - q^2 B_2^N \right], \\
 V_{NNNN}^{\leftarrow\leftarrow\leftarrow\bullet} &= \frac{g_A^2}{8f_\pi^4} (4I - 3) \left[q^2 A_1^N - 3A_2^N - q^2 B_2^N \right], \\
 V_{NNN\Delta}^{\bullet\leftarrow\leftarrow\leftarrow} &= \frac{3g_A^2}{8\sqrt{2}f_\pi^4} IS_2^{ij\uparrow} \left[q^i q^j A_1^N - \delta^{ij} A_2^N - q^i q^j B_2^N \right], \\
 V_{N\Delta N\Delta}^{\bullet\leftarrow\leftarrow\leftarrow} &= \frac{-15\sqrt{3}g_A^2}{32\sqrt{2}f_\pi^4} IS_2^{ij\uparrow} \left[q^i q^j A_1^N - \delta^{ij} A_2^N - q^i q^j B_2^N \right], \\
 V_{N\Delta N\Delta}^{\leftarrow\leftarrow\leftarrow\bullet} &= \frac{5g_A^2}{8f_\pi^4} I \left[q^2 A_1^N - 3A_2^N - q^2 B_2^N \right], \\
 V_{N\Delta\Delta\Delta}^{\leftarrow\leftarrow\leftarrow\bullet} &= \frac{-3\sqrt{5}g_A^2}{16f_\pi^4} IS_1^{ij\uparrow} \left[q^i q^j A_1^N - \delta^{ij} A_2^N - q^i q^j B_2^N \right], \\
 V_{\Delta\Delta\Delta\Delta}^{\bullet\leftarrow\leftarrow\leftarrow\leftarrow} &= \frac{3\sqrt{3}g_A^2}{32\sqrt{2}f_\pi^4} (15 - 4I) S_2^{ij\uparrow} \left[q^i q^j A_1^N - \delta^{ij} A_2^N - q^i q^j B_2^N \right], \\
 V_{\Delta\Delta\Delta\Delta}^{\leftarrow\leftarrow\leftarrow\leftarrow\bullet} &= \frac{3\sqrt{3}g_A^2}{32\sqrt{2}f_\pi^4} (15 - 4I) S_1^{ij\uparrow} \left[q^i q^j A_1^N - \delta^{ij} A_2^N - q^i q^j B_2^N \right], \tag{4.68}
 \end{aligned}$$

and those from triangle diagrams with a Δ intermediate state take the form

$$\begin{aligned}
 V_{NNNN}^{\bullet\leftarrow\leftarrow\leftarrow\leftarrow} &= \frac{3\sqrt{3}g_A^2}{16\sqrt{2}f_\pi^4} (4I - 3) S_2^{ij\uparrow} \left[q^i q^j A_1^\Delta - \delta^{ij} A_2^\Delta - q^i q^j B_2^\Delta \right], \\
 V_{NNNN}^{\leftarrow\leftarrow\leftarrow\bullet} &= \frac{3\sqrt{3}g_A^2}{16\sqrt{2}f_\pi^4} (4I - 3) S_1^{ij\uparrow} \left[q^i q^j A_1^\Delta - \delta^{ij} A_2^\Delta - q^i q^j B_2^\Delta \right], \\
 V_{NNN\Delta}^{\bullet\leftarrow\leftarrow\leftarrow} &= \frac{-3g_A^2}{8\sqrt{2}f_\pi^4} IS_2^{ij\uparrow} \left[q^i q^j A_1^\Delta - \delta^{ij} A_2^\Delta - q^i q^j B_2^\Delta \right], \\
 V_{N\Delta N\Delta}^{\bullet\leftarrow\leftarrow\leftarrow} &= \frac{-g_A^2}{40f_\pi^4} I (5\delta_2^{ij} + 4\Sigma_2^{ij}) \left[q^i q^j A_1^\Delta - \delta^{ij} A_2^\Delta - q^i q^j B_2^\Delta \right], \\
 V_{N\Delta N\Delta}^{\leftarrow\leftarrow\leftarrow\bullet} &= \frac{-15\sqrt{3}g_A^2}{16\sqrt{2}f_\pi^4} IS_1^{ij\uparrow} \left[q^i q^j A_1^\Delta - \delta^{ij} A_2^\Delta - q^i q^j B_2^\Delta \right], \\
 V_{N\Delta\Delta\Delta}^{\leftarrow\leftarrow\leftarrow\bullet} &= \frac{3\sqrt{5}g_A^2}{16f_\pi^4} IS_1^{ij\uparrow} \left[q^i q^j A_1^\Delta - \delta^{ij} A_2^\Delta - q^i q^j B_2^\Delta \right],
 \end{aligned}$$

$$\begin{aligned}
 V_{\Delta\Delta\Delta\Delta}^{\bullet\downarrow} &= \frac{g_A^2}{200f_\pi^4} (4I - 15) (5\delta_2^{ij} + 4\Sigma_2^{ij}) \left[q^i q^j A_1^\Delta - \delta^{ij} A_2^\Delta - q^i q^j B_2^\Delta \right], \\
 V_{\Delta\Delta\Delta\Delta}^{\downarrow\bullet} &= \frac{g_A^2}{200f_\pi^4} (4I - 15) (5\delta_1^{ij} + 4\Sigma_1^{ij}) \left[q^i q^j A_1^\Delta - \delta^{ij} A_2^\Delta - q^i q^j B_2^\Delta \right], \quad (4.69)
 \end{aligned}$$

where $I = 0, 1$ is the total isospin. The left and right triangle diagram have been carefully distinguished, although they give in some cases identical results.

The 2π -exchange bubble diagrams with identical initial and final states are shown in line (j) of Fig. 3.3 and the general form of the 2π phase space integral is given in Eq. (4.47). The imaginary parts for the three non-vanishing potentials read

$$\begin{aligned}
 \text{Im } V_{NNNN}^{\bullet\circ} &= \frac{w^3}{768f_\pi^4\pi\mu} (3 - 4I), \\
 \text{Im } V_{N\Delta N\Delta}^{\bullet\circ} &= \frac{5w^3}{768f_\pi^4\pi\mu} I, \\
 \text{Im } V_{\Delta\Delta\Delta\Delta}^{\bullet\circ} &= \frac{w^3}{768f_\pi^4\pi\mu} (15 - 4I). \quad (4.70)
 \end{aligned}$$

The numerical results for NN phase shifts based on these potentials which have been given in Sections 4.3 and 4.4 will be presented in Chapter 6. Before that the contact interactions for the coupled NN, N Δ , Δ N, $\Delta\Delta$ system are derived in Chapter 5.

5

CONTACT POTENTIAL

The NN contact interactions are built from four nucleon legs and no pion fields. These contact terms describe the short-range part of the nuclear potential as mentioned in Chapter 1. Due to parity conservation, only vertices with even powers of momenta are allowed. In this chapter, we give the LO and NLO contact potentials for all relevant N- Δ combinations and evaluate their matrix elements in those partial waves where they contribute. We present the results of the fits and investigate the influence of contact potentials which include deltas.

5.1 DEFINITION OF CONTACT POTENTIAL AND LOW-ENERGY CONSTANTS

The contact term of the two-nucleon potential up to next-to-leading order takes for initial and final momenta \mathbf{p} and \mathbf{p}' the form

$$V_{ct}(\mathbf{p}, \mathbf{p}') = V_{ct}^{(0)} + V_{ct}^{(2)}(\mathbf{p}, \mathbf{p}') \quad (5.1)$$

The leading order contributions for the different combinations of particles were first given in Ref. [57] by

$$\begin{aligned} V_{ct,NNNN}^{(0)} &= C_S + C_T \boldsymbol{\sigma}_1 \cdot \boldsymbol{\sigma}_2 \\ V_{ct,NNN\Delta}^{(0)} &= C_{2,NNN\Delta}^{(0)} \boldsymbol{\sigma}_1 \cdot \mathbf{S}_2^\dagger \\ V_{ct,N\Delta N\Delta}^{(0)} &= C_{1,N\Delta N\Delta}^{(0)} + C_{2,N\Delta N\Delta}^{(0)} \boldsymbol{\sigma}_1 \cdot \boldsymbol{\Sigma}_2 \\ V_{ct,NN\Delta\Delta}^{(0)} &= C_{2,NN\Delta\Delta}^{(0)} \mathbf{S}_1^\dagger \cdot \mathbf{S}_2^\dagger + C_{3,NN\Delta\Delta}^{(0)} S_1^{ij\dagger} S_2^{ij\dagger} \\ V_{ct,N\Delta\Delta\Delta}^{(0)} &= C_{2,N\Delta\Delta\Delta}^{(0)} \mathbf{S}_1^\dagger \cdot \boldsymbol{\Sigma}_2 + C_{3,N\Delta\Delta\Delta}^{(0)} S_1^{ij\dagger} \Sigma_2^{ij} \\ V_{ct,\Delta\Delta\Delta\Delta}^{(0)} &= C_{1,\Delta\Delta\Delta\Delta}^{(0)} + C_{2,\Delta\Delta\Delta\Delta}^{(0)} \boldsymbol{\Sigma}_1 \cdot \boldsymbol{\Sigma}_2 \\ &\quad + C_{3,\Delta\Delta\Delta\Delta}^{(0)} \Sigma_1^{ij} \Sigma_2^{ij} + C_{4,\Delta\Delta\Delta\Delta}^{(0)} \Sigma_1^{ijk} \Sigma_2^{ijk} \end{aligned} \quad (5.2)$$

The spin (transition) matrices $\boldsymbol{\sigma}$, \mathbf{S} , $\boldsymbol{\Sigma}$ and their combinations with multiple indices are defined in Appendix A.2. The LO contact potential is momentum independent. Finally, the potential $V_{ct,NNN\Delta}^{(0)}$ does not contribute due to the limitations imposed by the Pauli exclusion principle, which requires the initial NN state to be either ($s = 0$, $I = 1$) or ($s = 1$, $I = 0$) for $l = 0$, whereas the final N Δ state has spin $s = 1, 2$ and isospin $I = 1, 2$. We use

the definitions $\mathbf{q} = \mathbf{p}' - \mathbf{p}$ and $\mathbf{k} = \frac{1}{2}(\mathbf{p}' + \mathbf{p})$. Following the notation for the LO terms, we obtain the NLO contact potentials as:

$$\begin{aligned}
V_{ct,NNNN}^{(2)} &= C_{1,NNNN}^{(2)} q^2 + C_{2,NNNN}^{(2)} k^2 + \left(C_{3,NNNN}^{(2)} q^2 + C_{4,NNNN}^{(2)} k^2 \right) \boldsymbol{\sigma}_1 \cdot \boldsymbol{\sigma}_2 \\
&\quad - iC_{5,NNNN}^{(2)} (\mathbf{q} \times \mathbf{k}) \cdot (\boldsymbol{\sigma}_1 + \boldsymbol{\sigma}_2) \\
&\quad + C_{6,NNNN}^{(2)} (\boldsymbol{\sigma}_1 \cdot \mathbf{q}) (\boldsymbol{\sigma}_2 \cdot \mathbf{q}) + C_{7,NNNN}^{(2)} (\boldsymbol{\sigma}_1 \cdot \mathbf{k}) (\boldsymbol{\sigma}_2 \cdot \mathbf{k}) \\
V_{ct,NNN\Delta}^{(2)} &= \left(C_{3,NNN\Delta}^{(2)} q^2 + C_{4,NNN\Delta}^{(2)} k^2 \right) \boldsymbol{\sigma}_1 \cdot \mathbf{S}_2^\dagger - iC_{5,NNN\Delta}^{(2)} (\mathbf{q} \times \mathbf{k}) \cdot \mathbf{S}_2^\dagger \\
&\quad + C_{6,NNN\Delta}^{(2)} (\boldsymbol{\sigma}_1 \cdot \mathbf{q}) (\mathbf{S}_2^\dagger \cdot \mathbf{q}) + C_{7,NNN\Delta}^{(2)} (\boldsymbol{\sigma}_1 \cdot \mathbf{k}) (\mathbf{S}_2^\dagger \cdot \mathbf{k}) \\
V_{ct,N\Delta N\Delta}^{(2)} &= C_{1,N\Delta N\Delta}^{(2)} q^2 + C_{2,N\Delta N\Delta}^{(2)} k^2 + \left(C_{3,N\Delta N\Delta}^{(2)} q^2 + C_{4,N\Delta N\Delta}^{(2)} k^2 \right) \boldsymbol{\sigma}_1 \cdot \boldsymbol{\Sigma}_2 \\
&\quad - iC_{5,N\Delta N\Delta}^{(2)} (\mathbf{q} \times \mathbf{k}) \cdot (\boldsymbol{\sigma}_1 + \boldsymbol{\Sigma}_2) - iC_{5-,N\Delta N\Delta}^{(2)} (\mathbf{q} \times \mathbf{k}) \cdot (\boldsymbol{\sigma}_1 - \boldsymbol{\Sigma}_2) \\
&\quad + C_{6,N\Delta N\Delta}^{(2)} (\boldsymbol{\sigma}_1 \cdot \mathbf{q}) (\boldsymbol{\Sigma}_2 \cdot \mathbf{q}) + C_{7,N\Delta N\Delta}^{(2)} (\boldsymbol{\sigma}_1 \cdot \mathbf{k}) (\boldsymbol{\Sigma}_2 \cdot \mathbf{k}) \\
V_{ct,NN\Delta\Delta}^{(2)} &= \left(C_{3,NN\Delta\Delta}^{(2)} q^2 + C_{4,NN\Delta\Delta}^{(2)} k^2 \right) \mathbf{S}_1^\dagger \cdot \mathbf{S}_2^\dagger \\
&\quad + C_{6,NN\Delta\Delta}^{(2)} (\mathbf{S}_1^\dagger \cdot \mathbf{q}) (\mathbf{S}_2^\dagger \cdot \mathbf{q}) + C_{7,NN\Delta\Delta}^{(2)} (\mathbf{S}_1^\dagger \cdot \mathbf{k}) (\mathbf{S}_2^\dagger \cdot \mathbf{k}) \\
&\quad + \left(C_{8,NN\Delta\Delta}^{(2)} q^2 + C_{9,NN\Delta\Delta}^{(2)} k^2 \right) S_1^{ij\dagger} S_2^{ij\dagger} \\
&\quad + \left(C_{10,NN\Delta\Delta}^{(2)} q^i q^k + C_{11,NN\Delta\Delta}^{(2)} k^i k^k \right) S_1^{ij\dagger} S_2^{kj\dagger} \\
V_{ct,N\Delta\Delta\Delta}^{(2)} &= \left(C_{3,N\Delta\Delta\Delta}^{(2)} q^2 + C_{4,N\Delta\Delta\Delta}^{(2)} k^2 \right) \mathbf{S}_1^\dagger \cdot \boldsymbol{\Sigma}_2 - iC_{5,N\Delta\Delta\Delta}^{(2)} (\mathbf{q} \times \mathbf{k}) \cdot \mathbf{S}_1^\dagger \\
&\quad + C_{6,N\Delta\Delta\Delta}^{(2)} (\mathbf{S}_1^\dagger \cdot \mathbf{q}) (\boldsymbol{\Sigma}_2 \cdot \mathbf{q}) + C_{7,N\Delta\Delta\Delta}^{(2)} (\mathbf{S}_1^\dagger \cdot \mathbf{k}) (\boldsymbol{\Sigma}_2 \cdot \mathbf{k}) \\
&\quad + \left(C_{8,N\Delta\Delta\Delta}^{(2)} q^2 + C_{9,N\Delta\Delta\Delta}^{(2)} k^2 \right) S_1^{ij\dagger} \Sigma_2^{ij} \\
&\quad + \left(C_{10,N\Delta\Delta\Delta}^{(2)} q^i q^k + C_{11,N\Delta\Delta\Delta}^{(2)} k^i k^k \right) S_1^{ij\dagger} \Sigma_2^{kj} \\
V_{ct,\Delta\Delta\Delta\Delta}^{(2)} &= C_{1,\Delta\Delta\Delta\Delta}^{(2)} q^2 + C_{2,\Delta\Delta\Delta\Delta}^{(2)} k^2 + \left(C_{3,\Delta\Delta\Delta\Delta}^{(2)} q^2 + C_{4,\Delta\Delta\Delta\Delta}^{(2)} k^2 \right) \boldsymbol{\Sigma}_1 \cdot \boldsymbol{\Sigma}_2 \\
&\quad - iC_{5,\Delta\Delta\Delta\Delta}^{(2)} (\mathbf{q} \times \mathbf{k}) \cdot (\boldsymbol{\Sigma}_1 + \boldsymbol{\Sigma}_2) \\
&\quad + C_{6,\Delta\Delta\Delta\Delta}^{(2)} (\boldsymbol{\Sigma}_1 \cdot \mathbf{q}) (\boldsymbol{\Sigma}_2 \cdot \mathbf{q}) + C_{7,\Delta\Delta\Delta\Delta}^{(2)} (\boldsymbol{\Sigma}_1 \cdot \mathbf{k}) (\boldsymbol{\Sigma}_2 \cdot \mathbf{k}) \\
&\quad + \left(C_{8,\Delta\Delta\Delta\Delta}^{(2)} q^2 + C_{9,\Delta\Delta\Delta\Delta}^{(2)} k^2 \right) \Sigma_1^{ij} \Sigma_2^{ij} \\
&\quad + \left(C_{10,\Delta\Delta\Delta\Delta}^{(2)} q^i q^k + C_{11,\Delta\Delta\Delta\Delta}^{(2)} k^i k^k \right) \Sigma_1^{ij} \Sigma_2^{kj} \\
&\quad + \left(C_{12,\Delta\Delta\Delta\Delta}^{(2)} q^2 + C_{13,\Delta\Delta\Delta\Delta}^{(2)} k^2 \right) \Sigma_1^{ijk} \Sigma_2^{ijk} \\
&\quad + \left(C_{14,\Delta\Delta\Delta\Delta}^{(2)} q^i q^l + C_{15,\Delta\Delta\Delta\Delta}^{(2)} k^i k^l \right) \Sigma_1^{ijk} \Sigma_2^{ljk}
\end{aligned} \tag{5.3}$$

The potential $V_{ct,N\Delta N\Delta}^{(2)}$ is the only one to which a term of the form $(\mathbf{q} \times \mathbf{k}) \cdot (\mathbf{S}_1 - \mathbf{S}_2)$ contributes, where \mathbf{S}_i are the appropriate spin operators. The standard spin-orbit term $(\mathbf{q} \times \mathbf{k}) \cdot (\mathbf{S}_1 + \mathbf{S}_2)$ appears in $\text{NN} \rightarrow \text{NN}$, $\text{N}\Delta \rightarrow \text{N}\Delta$, and $\Delta\Delta \rightarrow \Delta\Delta$, whereas in $\text{NN} \rightarrow \text{N}\Delta$ and $\text{N}\Delta \rightarrow \Delta\Delta$ only the part $(\mathbf{q} \times \mathbf{k}) \cdot \mathbf{S}^\dagger$ exists.

The contact potentials in Eqs. (5.2) and (5.3) contribute to certain (low) partial waves as verified in the following equations. The constants in each partial wave carry also the index related to the particular two-baryon channel which we have dropped for better readability:

NN → NN:

$$\begin{aligned}
 \langle {}^1S_0 | V_{ct,NNNN} | {}^1S_0 \rangle &= \tilde{C}^{1S_0} + C^{1S_0}(p^2 + p'^2) & \langle {}^3P_0 | V_{ct,NNNN} | {}^3P_0 \rangle &= C^{3P_0} pp' \\
 \langle {}^3S_1 | V_{ct,NNNN} | {}^3S_1 \rangle &= \tilde{C}^{3S_1} + C^{3S_1}(p^2 + p'^2) & \langle {}^3P_2 | V_{ct,NNNN} | {}^3P_2 \rangle &= C^{3P_2} pp' \\
 \langle {}^1P_1 | V_{ct,NNNN} | {}^1P_1 \rangle &= C^{1P_1} pp' & \langle {}^3S_1 | V_{ct,NNNN} | {}^3D_1 \rangle &= C^{3D_1-3S_1} p^2 \\
 \langle {}^3P_1 | V_{ct,NNNN} | {}^3P_1 \rangle &= C^{3P_1} pp' & \langle {}^3D_1 | V_{ct,NNNN} | {}^3S_1 \rangle &= C^{3D_1-3S_1} p'^2
 \end{aligned} \tag{5.4}$$

NN → NΔ:

$$\begin{aligned}
 \langle {}^3P_0 | V_{ct,NNN\Delta} | {}^3P_0 \rangle &= C^{3P_0} pp' & \langle {}^5P_2 | V_{ct,NNN\Delta} | {}^3P_2 \rangle &= C^{5P_2-3P_2} pp' \\
 \langle {}^3P_1 | V_{ct,NNN\Delta} | {}^3P_1 \rangle &= C^{3P_1} pp' & \langle {}^5D_0 | V_{ct,NNN\Delta} | {}^1S_0 \rangle &= C^{5D_0-1S_0} p'^2 \\
 \langle {}^3P_2 | V_{ct,NNN\Delta} | {}^3P_2 \rangle &= C^{3P_2} pp' & \langle {}^5S_2 | V_{ct,NNN\Delta} | {}^1D_2 \rangle &= C^{5S_2-1D_2} p^2 \\
 \langle {}^5P_1 | V_{ct,NNN\Delta} | {}^3P_1 \rangle &= C^{5P_1-3P_1} pp'
 \end{aligned} \tag{5.5}$$

NΔ → NΔ:

$$\begin{aligned}
 \langle {}^5S_2 | V_{ct,N\Delta N\Delta} | {}^5S_2 \rangle &= \tilde{C}^{5S_2} + C^{5S_2}(p^2 + p'^2) & \langle {}^5P_2 | V_{ct,N\Delta N\Delta} | {}^3P_2 \rangle &= C^{3P_2-5P_2} pp' \\
 \langle {}^3P_0 | V_{ct,N\Delta N\Delta} | {}^3P_0 \rangle &= C^{3P_0} pp' & \langle {}^5P_2 | V_{ct,N\Delta N\Delta} | {}^5P_2 \rangle &= C^{5P_2} pp' \\
 \langle {}^3P_1 | V_{ct,N\Delta N\Delta} | {}^3P_1 \rangle &= C^{3P_1} pp' & \langle {}^5P_3 | V_{ct,N\Delta N\Delta} | {}^5P_3 \rangle &= C^{5P_3} pp' \\
 \langle {}^3P_1 | V_{ct,N\Delta N\Delta} | {}^5P_1 \rangle &= C^{3P_1-5P_1} pp' & \langle {}^5S_2 | V_{ct,N\Delta N\Delta} | {}^3D_2 \rangle &= C^{5S_2-3D_2} p^2 \\
 \langle {}^5P_1 | V_{ct,N\Delta N\Delta} | {}^3P_1 \rangle &= C^{3P_1-5P_1} pp' & \langle {}^5S_2 | V_{ct,N\Delta N\Delta} | {}^5D_2 \rangle &= C^{5S_2-5D_2} p^2 \\
 \langle {}^5P_1 | V_{ct,N\Delta N\Delta} | {}^5P_1 \rangle &= C^{5P_1} pp' & \langle {}^3D_2 | V_{ct,N\Delta N\Delta} | {}^5S_2 \rangle &= C^{5S_2-3D_2} p'^2 \\
 \langle {}^3P_2 | V_{ct,N\Delta N\Delta} | {}^3P_2 \rangle &= C^{3P_2} pp' & \langle {}^5D_2 | V_{ct,N\Delta N\Delta} | {}^5S_2 \rangle &= C^{5S_2-5D_2} p'^2 \\
 \langle {}^3P_2 | V_{ct,N\Delta N\Delta} | {}^5P_2 \rangle &= C^{3P_2-5P_2} pp'
 \end{aligned} \tag{5.6}$$

NN → ΔΔ:

$$\begin{aligned}
\langle {}^1S_0 | V_{ct, NN\Delta\Delta} | {}^1S_0 \rangle &= \tilde{C}^1S_0 + C^1S_0(p^2 + p'^2) & \langle {}^7P_2 | V_{ct, NN\Delta\Delta} | {}^3P_2 \rangle &= C^3P_2 - {}^7P_2 pp' \\
\langle {}^3S_1 | V_{ct, NN\Delta\Delta} | {}^3S_1 \rangle &= \tilde{C}^3S_1 + C^3S_1(p^2 + p'^2) & \langle {}^3S_1 | V_{ct, NN\Delta\Delta} | {}^3D_1 \rangle &= C^3S_1 - {}^3D_1 p^2 \\
\langle {}^3P_0 | V_{ct, NN\Delta\Delta} | {}^3P_0 \rangle &= C^3P_0 pp' & \langle {}^5S_2 | V_{ct, NN\Delta\Delta} | {}^1D_2 \rangle &= C^5S_2 - {}^1D_2 p^2 \\
\langle {}^1P_1 | V_{ct, NN\Delta\Delta} | {}^1P_1 \rangle &= C^1P_1 pp' & \langle {}^7S_3 | V_{ct, NN\Delta\Delta} | {}^3D_3 \rangle &= C^7S_3 - {}^3D_3 p^2 \\
\langle {}^3P_1 | V_{ct, NN\Delta\Delta} | {}^3P_1 \rangle &= C^3P_1 pp' & \langle {}^5D_0 | V_{ct, NN\Delta\Delta} | {}^1S_0 \rangle &= C^1S_0 - {}^5D_0 p'^2 \\
\langle {}^3P_2 | V_{ct, NN\Delta\Delta} | {}^3P_2 \rangle &= C^3P_2 pp' & \langle {}^3D_1 | V_{ct, NN\Delta\Delta} | {}^3S_1 \rangle &= C^3S_1 - {}^3D_1 p'^2 \\
\langle {}^5P_1 | V_{ct, NN\Delta\Delta} | {}^1P_1 \rangle &= C^3P_1 - {}^5P_1 pp' & \langle {}^7D_1 | V_{ct, NN\Delta\Delta} | {}^3S_1 \rangle &= C^3S_1 - {}^7D_1 p'^2
\end{aligned} \tag{5.7}$$

NΔ → ΔΔ:

$$\begin{aligned}
\langle {}^5S_2 | V_{ct, N\Delta\Delta\Delta} | {}^5S_2 \rangle &= \tilde{C}^5S_2 + C^5S_2(p^2 + p'^2) & \langle {}^7P_2 | V_{ct, N\Delta\Delta\Delta} | {}^5P_2 \rangle &= C^5P_2 - {}^7P_2 pp' \\
\langle {}^3P_0 | V_{ct, N\Delta\Delta\Delta} | {}^3P_0 \rangle &= C^3P_0 pp' & \langle {}^7P_3 | V_{ct, N\Delta\Delta\Delta} | {}^5P_3 \rangle &= C^5P_3 - {}^7P_3 pp' \\
\langle {}^3P_1 | V_{ct, N\Delta\Delta\Delta} | {}^3P_1 \rangle &= C^3P_1 pp' & \langle {}^1S_0 | V_{ct, N\Delta\Delta\Delta} | {}^5D_0 \rangle &= C^1S_0 - {}^5D_0 p^2 \\
\langle {}^3P_2 | V_{ct, N\Delta\Delta\Delta} | {}^3P_2 \rangle &= C^3P_2 pp' & \langle {}^5S_2 | V_{ct, N\Delta\Delta\Delta} | {}^3D_2 \rangle &= C^5S_2 - {}^3D_2 p^2 \\
\langle {}^3P_1 | V_{ct, N\Delta\Delta\Delta} | {}^5P_1 \rangle &= C^3P_1 - {}^5P_1 pp' & \langle {}^5S_2 | V_{ct, N\Delta\Delta\Delta} | {}^5D_2 \rangle &= C^5S_2 - {}^5D_2 p^2 \\
\langle {}^3P_2 | V_{ct, N\Delta\Delta\Delta} | {}^5P_2 \rangle &= C^3P_2 - {}^5P_2 pp' & \langle {}^1D_2 | V_{ct, N\Delta\Delta\Delta} | {}^5S_2 \rangle &= C^5S_2 - {}^1D_2 p'^2 \\
\langle {}^7P_2 | V_{ct, N\Delta\Delta\Delta} | {}^3P_2 \rangle &= C^3P_2 - {}^7P_2 pp' & \langle {}^5D_2 | V_{ct, N\Delta\Delta\Delta} | {}^5S_2 \rangle &= C^5S_2 - {}^5D_2 p'^2
\end{aligned} \tag{5.8}$$

$\Delta\Delta \rightarrow \Delta\Delta$:

$$\begin{aligned}
 \langle {}^1S_0 | V_{ct,\Delta\Delta\Delta\Delta} | {}^1S_0 \rangle &= \tilde{C}^{{}^1S_0} + C^{{}^1S_0}(p^2 + p'^2) & \langle {}^7P_4 | V_{ct,\Delta\Delta\Delta\Delta} | {}^7P_4 \rangle &= C^{{}^7P_4} pp' \\
 \langle {}^3S_1 | V_{ct,\Delta\Delta\Delta\Delta} | {}^3S_1 \rangle &= \tilde{C}^{{}^3S_1} + C^{{}^3S_1}(p^2 + p'^2) & \langle {}^1S_0 | V_{ct,\Delta\Delta\Delta\Delta} | {}^5D_0 \rangle &= C^{{}^1S_0-{}^5D_0} p^2 \\
 \langle {}^5S_2 | V_{ct,\Delta\Delta\Delta\Delta} | {}^5S_2 \rangle &= \tilde{C}^{{}^5S_2} + C^{{}^5S_2}(p^2 + p'^2) & \langle {}^3S_1 | V_{ct,\Delta\Delta\Delta\Delta} | {}^3D_1 \rangle &= C^{{}^3S_1-{}^3D_1} p^2 \\
 \langle {}^7S_3 | V_{ct,\Delta\Delta\Delta\Delta} | {}^7S_3 \rangle &= \tilde{C}^{{}^7S_3} + C^{{}^7S_3}(p^2 + p'^2) & \langle {}^3S_1 | V_{ct,\Delta\Delta\Delta\Delta} | {}^7D_1 \rangle &= C^{{}^3S_1-{}^7D_1} p^2 \\
 \langle {}^3P_0 | V_{ct,\Delta\Delta\Delta\Delta} | {}^3P_0 \rangle &= C^{{}^3P_0} pp' & \langle {}^5S_2 | V_{ct,\Delta\Delta\Delta\Delta} | {}^1D_2 \rangle &= C^{{}^5S_2-{}^1D_2} p^2 \\
 \langle {}^1P_1 | V_{ct,\Delta\Delta\Delta\Delta} | {}^1P_1 \rangle &= C^{{}^1P_1} pp' & \langle {}^5S_2 | V_{ct,\Delta\Delta\Delta\Delta} | {}^5D_2 \rangle &= C^{{}^5S_2-{}^5D_2} p^2 \\
 \langle {}^3P_1 | V_{ct,\Delta\Delta\Delta\Delta} | {}^3P_1 \rangle &= C^{{}^3P_1} pp' & \langle {}^7S_3 | V_{ct,\Delta\Delta\Delta\Delta} | {}^3D_3 \rangle &= C^{{}^7S_3-{}^3D_3} p^2 \\
 \langle {}^5P_1 | V_{ct,\Delta\Delta\Delta\Delta} | {}^5P_1 \rangle &= C^{{}^5P_1} pp' & \langle {}^7S_3 | V_{ct,\Delta\Delta\Delta\Delta} | {}^7D_3 \rangle &= C^{{}^7S_3-{}^7D_3} p^2 \\
 \langle {}^1P_1 | V_{ct,\Delta\Delta\Delta\Delta} | {}^5P_1 \rangle &= C^{{}^1P_1-{}^5P_1} pp' & \langle {}^5D_0 | V_{ct,\Delta\Delta\Delta\Delta} | {}^1S_0 \rangle &= C^{{}^1S_0-{}^5D_0} p'^2 \\
 \langle {}^5P_1 | V_{ct,\Delta\Delta\Delta\Delta} | {}^1P_1 \rangle &= C^{{}^1P_1-{}^5P_1} pp' & \langle {}^3D_1 | V_{ct,\Delta\Delta\Delta\Delta} | {}^3S_1 \rangle &= C^{{}^3S_1-{}^3D_1} p'^2 \\
 \langle {}^3P_2 | V_{ct,\Delta\Delta\Delta\Delta} | {}^3P_2 \rangle &= C^{{}^3P_2} pp' & \langle {}^7D_1 | V_{ct,\Delta\Delta\Delta\Delta} | {}^3S_1 \rangle &= C^{{}^3S_1-{}^7D_1} p'^2 \\
 \langle {}^7P_2 | V_{ct,\Delta\Delta\Delta\Delta} | {}^7P_2 \rangle &= C^{{}^7P_2} pp' & \langle {}^1D_2 | V_{ct,\Delta\Delta\Delta\Delta} | {}^5S_2 \rangle &= C^{{}^5S_2-{}^1D_2} p'^2 \\
 \langle {}^3P_2 | V_{ct,\Delta\Delta\Delta\Delta} | {}^7P_2 \rangle &= C^{{}^3P_2-{}^7P_2} pp' & \langle {}^5D_2 | V_{ct,\Delta\Delta\Delta\Delta} | {}^5S_2 \rangle &= C^{{}^5S_2-{}^5D_2} p'^2 \\
 \langle {}^7P_2 | V_{ct,\Delta\Delta\Delta\Delta} | {}^3P_2 \rangle &= C^{{}^3P_2-{}^7P_2} pp' & \langle {}^3D_3 | V_{ct,\Delta\Delta\Delta\Delta} | {}^7S_3 \rangle &= C^{{}^7S_3-{}^3D_3} p'^2 \\
 \langle {}^5P_3 | V_{ct,\Delta\Delta\Delta\Delta} | {}^5P_3 \rangle &= C^{{}^5P_3} pp' & \langle {}^7D_3 | V_{ct,\Delta\Delta\Delta\Delta} | {}^7S_3 \rangle &= C^{{}^7S_3-{}^7D_3} p'^2 \\
 \langle {}^7P_3 | V_{ct,\Delta\Delta\Delta\Delta} | {}^7P_3 \rangle &= C^{{}^7P_3} pp' & & \\
 \end{aligned}
 \tag{5.9}$$

The relations between the constants for the partial wave matrix elements and those in the underlying potentials are given in Appendix C.1.

One sees that the contact potential $V_{\Delta\Delta\Delta\Delta}^{(2)}$ contains fifteen low-energy constants which feed into 31 partial wave matrix elements. Thus there is no unique mapping between these two sets of constants. Consequently, the LECs in the spectroscopic notation are not independent from each other. This happens also in the other NLO contact potentials containing one, two or three deltas. We list the relations in Appendix C.2. If the delta LECs were to be fitted, this needs to be done simultaneously in all the partial waves in question, while respecting the relations between them.

The contributions of low-energy constants to the partial waves of the nucleon-nucleon potential with coupled ($N\Delta$, ΔN , $\Delta\Delta$)-channels are listed in Tables 5.1 and 5.2 at leading and next-to-leading order. At leading order there are at most three LECs per NN-partial wave channel. Only two of these four channels receive contributions from the delta-less potential $V_{NNNN}^{(2)}$. The inclusion of the deltas extends the outreach of the contact potential to higher partial waves. At NLO there are up to fifteen LECs per NN channel. The purely nucleonic potential reaches up to the 3F_2 -wave due to its coupling to the 3P_2 -wave. The

full contact potential reaches even the 3F_4 - 3H_4 -coupled NN channel because there is a $\Delta\Delta$ - 7P_4 -wave which couples to this NN channel due to the additional spin states of the Δ -isobar.

5.2 FITS OF LOW-ENERGY CONSTANTS

At next-to-leading order the short distance part of the NN potential is fitted to empirical phase shifts up to 100 MeV, see Ref. [20], this means to six data points per partial wave including mixing angles. Most of the NN-partial waves contain too many constants for a proper fit to the Nijmegen PWA [58]. Therefore, we decided to omit all contact potentials involving Δ -isobars and only fit the NN contact terms. The effects of the other contact terms are subleading compared to the NN potential as they enter only the iterated part in the coupled channel equation as it will be investigated in Sections 5.2.2 and 5.2.3.

5.2.1 Fits to Nijmegen phase shifts

In the fits, the values for the constants are obtained in the spectroscopic notation. From this the C_i in the NN-potential in Eqs. (5.2) and (5.3) can be determined via Eq. (C.1) as the mapping in the NN-sector is one-to-one. We find for the low-energy constants in the purely nucleonic case the values listed in Table 5.3, and with coupled channels the values listed in Table 5.4 for different choices of the cutoff parameter Λ .

TABLE 5.3: Low-energy constants from fits of the purely nucleonic chiral potential to the Nijmegen PWA. The leading order constants \tilde{C} are in units of 10^4 GeV^{-2} , while the next-to-leading order C are in units of 10^4 GeV^{-4} .

	350	400	450	500	550	600	650	700	750	800
$\tilde{C}_{NNNN}^{1S_0}$	0.153	0.147	0.138	0.123	0.110	0.079	0.067	0.007	-0.018	-0.324
$C_{NNNN}^{1S_0}$	-0.829	-0.820	-0.813	-0.823	-0.565	-0.656	-0.472	-0.547	-0.438	-0.723
$\tilde{C}_{NNNN}^{3S_1}$	0.152	0.166	0.173	0.129	0.170	0.113	0.048	-1.344	-1.252	-0.396
$C_{NNNN}^{3S_1}$	-0.110	-0.291	-0.769	-0.455	-0.801	-0.592	-0.599	-1.481	-1.511	-0.648
$C_{NNNN}^{3S_1-3D_1}$	-0.104	0.020	-0.214	-0.295	-0.026	-0.178	-0.245	-1.004	-0.598	-0.381
$C_{NNNN}^{3P_0}$	-0.094	-0.188	-0.253	-0.309	-0.367	-0.441	-0.551	-0.750	-1.221	-3.667
$C_{NNNN}^{1P_1}$	-0.788	-0.637	-0.528	-0.445	-0.379	-0.325	-0.280	-0.242	-0.210	-0.182
$C_{NNNN}^{3P_1}$	-0.341	-0.267	-0.220	-0.190	-0.170	-0.157	-0.150	-0.147	-0.147	-0.150
$C_{NNNN}^{3P_2}$	0.335	0.278	0.237	0.206	0.181	0.160	0.142	0.126	0.112	0.099

TABLE 5.4: Low-energy constants from fits including coupled $N\Delta$ -, ΔN - and $\Delta\Delta$ -channels in the chiral potential to the Nijmegen PWA. The leading order constants \tilde{C} are in units of 10^4 GeV^{-2} , while the next-to-leading order C are in units of 10^4 GeV^{-4} .

	350	400	450	500	550	600	650	700	750	800
$\tilde{C}_{NNNN}^{1S_0}$	0.151	0.144	0.134	0.119	0.095	0.046	-0.084	-1.234	-12.077	-16.096
$C_{NNNN}^{1S_0}$	-0.823	-0.804	-0.782	-0.773	-0.790	-0.855	-1.034	-2.064	-5.012	-4.786
$\tilde{C}_{NNNN}^{3S_1}$	0.171	0.156	0.139	0.122	0.103	0.081	0.055	0.017	-0.062	-0.77
$C_{NNNN}^{3S_1}$	-0.606	-0.638	-0.619	-0.588	-0.560	-0.542	-0.540	-0.566	-0.650	-1.272
$C_{NNNN}^{3S_1-3D_1}$	-0.502	-0.351	-0.246	-0.167	-0.101	-0.041	0.020	0.087	0.175	0.420
$C_{NNNN}^{3P_0}$	-0.148	-0.265	-0.362	-0.462	-0.588	-0.783	-1.173	-2.470	-2.844	1.654
$C_{NNNN}^{1P_1}$	-0.854	-0.732	-0.657	-0.614	-0.594	-0.597	-0.626	-0.693	-0.825	-1.111
$C_{NNNN}^{3P_1}$	-0.362	-0.302	-0.273	-0.262	-0.264	-0.278	-0.303	-0.341	-0.401	-0.498
$C_{NNNN}^{3P_2}$	0.307	0.239	0.187	0.146	0.111	0.083	0.059	0.039	0.021	0.006

The natural size of the LECs in the spectroscopic notation has been estimated in Refs. [20,24] as

$$\begin{aligned}
|\tilde{C}_i| &\sim \frac{4\pi}{f_\pi^2} \sim 0.15 \times 10^4 \text{ GeV}^{-2}, \\
|C_i| &\sim \frac{4\pi}{f_\pi^2 \Lambda_b^2} \sim 0.4 \times 10^4 \text{ GeV}^{-4}
\end{aligned} \tag{5.10}$$

where the breakdown scale of the chiral expansion is taken as $\Lambda_b \simeq 600 \text{ MeV}$. Then for cutoff parameters $\Lambda \gtrsim 700 \text{ MeV}$ some of the low energy constants would become unnaturally large.

5.2.2 Fits of leading order contact potentials in coupled channel approach

In the 1S_0 partial wave, there are two additional leading order contact terms contributing in the coupled particle channels: $\tilde{C}_{NN\Delta\Delta}^{1S_0}$ and $\tilde{C}_{\Delta\Delta\Delta\Delta}^{1S_0}$. In the fitting procedure they can cause an eigenvalue of close to 1 in the matrix VG introduced in Section 3.1. Then $(\mathbb{1} - VG)^{-1}$ becomes very large in such a way that one of the data points from the Nijmegen partial wave analysis is nearly hit which then leads to a minimum in χ^2 . This feature is shown in Fig. 5.1. Once $\tilde{C}_{NN\Delta\Delta}^{1S_0}$ and $\tilde{C}_{\Delta\Delta\Delta\Delta}^{1S_0}$ are treated as additional fit parameters, the phase shift shows spikes for most of the selected cutoff parameters. Which data point of the Nijmegen PWA is hit by the fitted phase shift depends on the maximum lab energy T_{max} chosen for the fit. For the 1S_0 , this is shown in Fig. 5.2. We choose the maximal lab energy of the fit in the range $T_{\text{max}} = 50 \text{ MeV} \dots 300 \text{ MeV}$. The obtained LECs are given in Table 5.5. This behavior is not only observed in the 1S_0 but also, for example, in the 1D_2 -wave (Fig. 5.3).

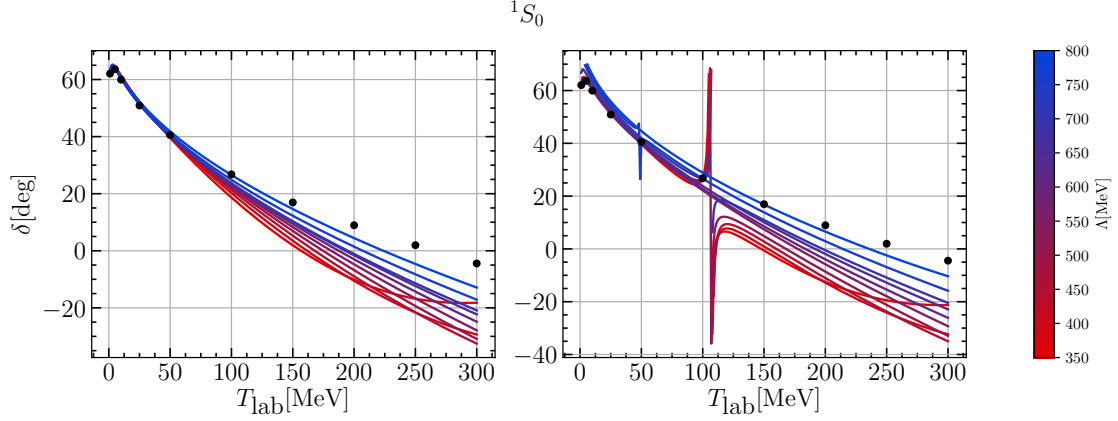


FIGURE 5.1: The 1S_0 phase shift with different sets of contact interactions fitted to the Nijmegen PWA [58] up to $T_{\max} = 100$ MeV is shown for different cutoff parameters Λ . Left: Adjustable constants $\tilde{C}_{NNN}^{1S_0}$ and $C_{NNNN}^{1S_0}$ only, Right: $\tilde{C}_{NN\Delta}^{1S_0}$ and $\tilde{C}_{\Delta\Delta\Delta}^{1S_0}$ are additionally adjusted.

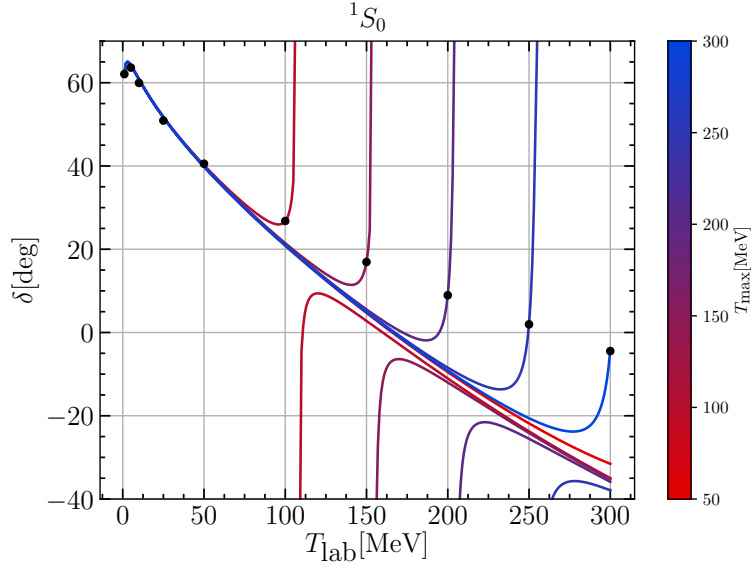


FIGURE 5.2: The 1S_0 phase shift with the LO contact potential in the coupled $N\Delta$ channels fitted to the Nijmegen PWA [58] is shown for different T_{\max} at a cutoff $\Lambda = 450$ GeV.

TABLE 5.5: Additional 1S_0 LECs for different T_{\max} at $\Lambda = 450$ GeV used in Fig. 5.2.

T_{\max}	50 MeV	100 MeV	150 MeV	200 MeV	250 MeV	300 MeV
$\tilde{C}_{NN\Delta}^{1S_0}$	-0.032	-0.047	-0.043	-0.040	-0.037	-0.034
$\tilde{C}_{\Delta\Delta\Delta}^{1S_0}$	0.714	0.922	0.884	0.845	0.805	0.765

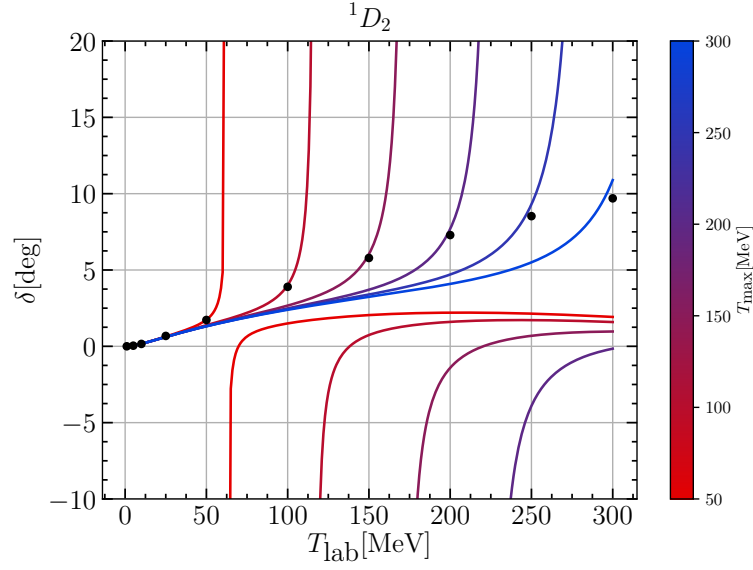


FIGURE 5.3: The 1D_2 phase shift with the LO contact interactions in the coupled $N\Delta$ channels fitted to the Nijmegen PWA is shown for different T_{max} at $\Lambda = 500$ GeV

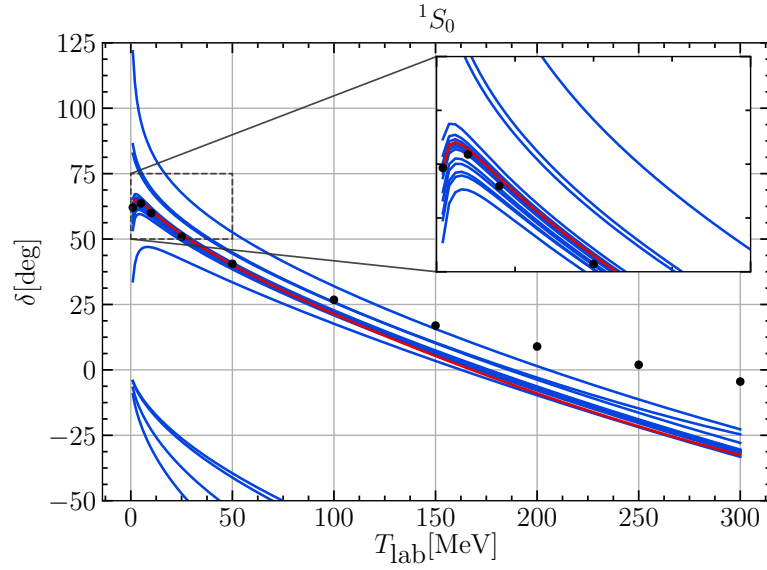


FIGURE 5.4: The 1S_0 phase shift for different sets of the LECs $\tilde{C}_{NN\Delta\Delta}^{1S_0}$ and $\tilde{C}_{\Delta\Delta\Delta\Delta}^{1S_0}$ at $\Lambda = 500$ GeV. The graph for both LECs equal zero is marked in red.

In addition, we have investigated, whether this behavior is a consequence of the fitting procedure. Fig. 5.4 shows the results for 20 different sets of $\tilde{C}_{NN\Delta\Delta}^{1S_0}$ and $\tilde{C}_{\Delta\Delta\Delta\Delta}^{1S_0}$. None of these choices yields the behavior of Figs. 5.1 and 5.2, even though the LECs in Table 5.5 are within the range of these sets. Finding the best values for these LECs is a tedious

work, since the condition that the phase shift needs to be a smooth curve, cannot be easily implemented into our fitting procedure. As we will point out in the next section in more detail, the contact potentials involving Δ -isobars have little impact on the resulting NN phase shift. We therefore refrain from determining these low-energy constants.

5.2.3 Influence of contact interactions involving deltas

The 1F_3 NN-channel and the coupled ($^3F_4, ^3H_4, \epsilon_4$) NN-channels receive contributions from one low-energy constant in the contact potential $V_{\Delta\Delta\Delta\Delta}^{(2)}$ only. The coupled ($^3G_3, ^3D_3, \epsilon_3$) NN-channels are affected by a contribution from the LO potential $V_{\Delta\Delta\Delta\Delta}^{(0)}$. For these waves the NLO contact potential $V_{\Delta\Delta\Delta\Delta}^{(2)}$ is non-vanishing in the matrix elements $\langle ^5P_3 | V_{ct, \Delta\Delta\Delta\Delta} | ^5P_3 \rangle = C_{^5P_3} pp'$ and $\langle ^7P_4 | V_{ct, \Delta\Delta\Delta\Delta} | ^7P_4 \rangle = C_{^7P_4} pp'$ and the LO contact potential $V_{\Delta\Delta\Delta\Delta}^{(0)}$ is non-vanishing in the matrix element $\langle ^7S_3 | V_{ct, \Delta\Delta\Delta\Delta} | ^7S_3 \rangle = \tilde{C}_{^7S_3}$. In the case of the 1F_3 wave there are five coupled equations for the T-matrix. We need to solve

$$\begin{aligned} T_{NNNN}^{^1F_3^1F_3} &= V_{NNNN}^{^1F_3^1F_3} + V_{NNNN}^{^1F_3^1F_3} G_{NN} T_{NNNN}^{^1F_3^1F_3} \\ &+ V_{NN\Delta\Delta}^{^1F_3^1F_3} G_{\Delta\Delta} T_{\Delta\Delta NN}^{^1F_3^1F_3} + V_{NN\Delta\Delta}^{^1F_3^5P_3} G_{\Delta\Delta} T_{\Delta\Delta NN}^{^5P_3^1F_3} \\ &+ V_{NN\Delta\Delta}^{^1F_3^5F_3} G_{\Delta\Delta} T_{\Delta\Delta NN}^{^5F_3^1F_3} + V_{NN\Delta\Delta}^{^1F_3^5H_3} G_{\Delta\Delta} T_{\Delta\Delta NN}^{^5H_3^1F_3}, \end{aligned} \quad (5.11)$$

which depends on four other T-matrices. Each of these is defined via a similar scattering equation, where one of them reads

$$\begin{aligned} T_{\Delta\Delta NN}^{^5P_3^1F_3} &= V_{\Delta\Delta NN}^{^5P_3^1F_3} + V_{\Delta\Delta NN}^{^5P_3^1F_3} G_{NN} T_{NNNN}^{^1F_3^1F_3} \\ &+ V_{\Delta\Delta\Delta\Delta}^{^5P_3^1F_3} G_{\Delta\Delta} T_{\Delta\Delta NN}^{^1F_3^1F_3} + V_{\Delta\Delta\Delta\Delta}^{^5P_3^5P_3} G_{\Delta\Delta} T_{\Delta\Delta NN}^{^5P_3^1F_3} \\ &+ V_{\Delta\Delta\Delta\Delta}^{^5P_3^5F_3} G_{\Delta\Delta} T_{\Delta\Delta NN}^{^5F_3^1F_3} + V_{\Delta\Delta\Delta\Delta}^{^5P_3^5H_3} G_{\Delta\Delta} T_{\Delta\Delta NN}^{^5H_3^1F_3}. \end{aligned} \quad (5.12)$$

This scattering equation for the T-matrix contains the low-energy constant contributing to the potential

$$V_{\Delta\Delta\Delta\Delta}^{^5P_3^5P_3} = C_{^5P_3} pp' + V_{\Delta\Delta\Delta\Delta, OPE}^{^5P_3^5P_3} + V_{\Delta\Delta\Delta\Delta, TPE}^{^5P_3^5P_3}. \quad (5.13)$$

Since in these cases the fit algorithm is not able to find LECs which differ from an arbitrary starting value, we tested NLO LEC-values in the range $-10^7 \text{GeV}^{-4} \dots +10^7 \text{GeV}^{-4}$ and LO LEC-values in the range $-10^6 \text{GeV}^{-2} \dots +10^6 \text{GeV}^{-2}$ for two different cutoff parameters Λ . The results are shown in Figs. 5.5 to 5.7, where the red band depicts the variation of the cutoff parameter $\Lambda = 400 \dots 800 \text{MeV}$ with the LECs set to zero. The different values for the cutoff are shown in blue for $\Lambda = 500 \text{MeV}$ and in green for $\Lambda = 700 \text{MeV}$. Up to $T_{\text{lab}} = 100 \text{MeV}$ the change of the 1F_3 -, 3F_4 - and 3D_3 -phase shifts by varying the LECs is negligible. For higher T_{lab} the different lines split up, but still are within the band produced by changing the cutoff parameter except for one case in the 3F_4 -wave. For the

${}^3\text{H}_4$ - and the ${}^3\text{G}_3$ -wave and the two mixing angles (ϵ_3 and ϵ_4) the different choices of the LECs cannot be distinguished from each other.

Due to the small effects of the contact potentials involving deltas, we omit these contact potentials in the following.

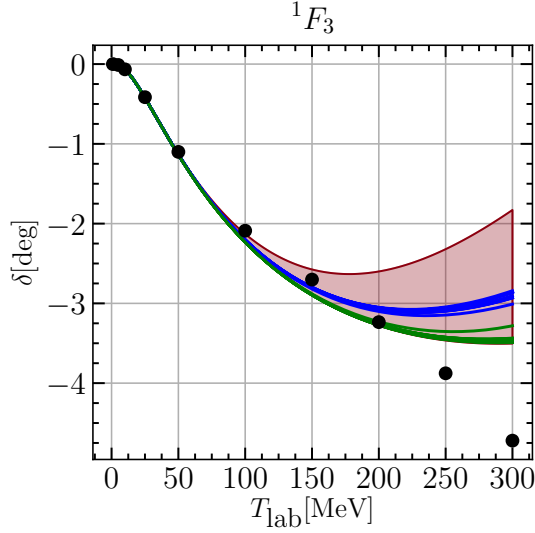


FIGURE 5.5: The NLO contact potential contributes to the $\Delta\Delta \rightarrow \Delta\Delta$ ${}^3\text{P}_3$ -wave and couples to the ${}^3\text{F}_3$ NN-channel. The variation of the LEC is shown for $\Lambda = 500$ MeV (blue) and $\Lambda = 700$ MeV (green). The red band depicts the variation of the cutoff Λ .

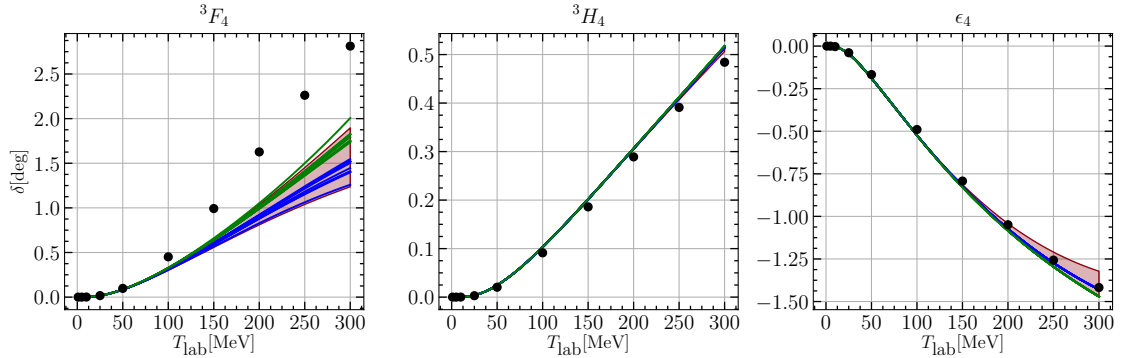


FIGURE 5.6: The NLO contact potential contributes to the $\Delta\Delta \rightarrow \Delta\Delta$ ${}^3\text{P}_4$ -wave and couples to the ${}^3\text{F}_4$ - ${}^3\text{H}_4$ coupled NN-channel. For notation see Fig. 5.5.

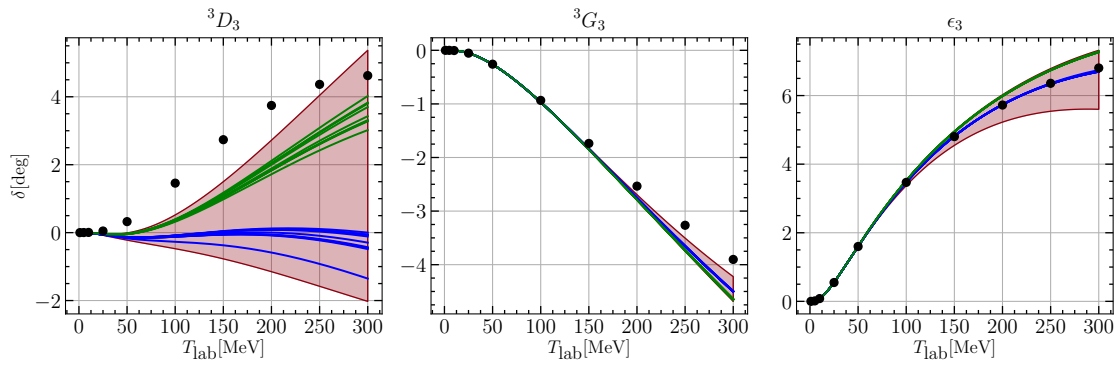


FIGURE 5.7: The LO contact potential contributes to the $\Delta\Delta \rightarrow \Delta\Delta$ 7S_3 -wave and couples to the 3D_3 - 3G_3 coupled NN-channel. For notation see Fig. 5.5.

PHASE SHIFTS

In this chapter, we present our results for phase shifts and mixing angles. In addition, we investigate the influence of $N\Delta$ -, ΔN - and $\Delta\Delta$ -coupled channels in the total coupled channel result. We present a comparison of the Kadyshevsky and the Lippmann-Schwinger equation and explore the next-to-next-to leading order purely nucleonic result and its differences and similarities to the explicit inclusion of the deltas and their coupled channels dynamics.

We compare all our results of the purely nucleonic and the coupled $N\Delta$ -, ΔN - and $\Delta\Delta$ -channels to the Nijmegen partial wave analysis [58].

6.1 PERIPHERAL PHASE SHIFTS

The peripheral phase shifts are independent of the NN-contact potential except for the 3F_2 -wave and ϵ_2 due to the mixing with 3P_2 . However, the influence of $C_{NNNN}^{3P_2}$ on the F-wave is nearly negligible, even at the highest energy $T_{\text{lab}} \simeq 300$ MeV.

6.1.1 *F-waves*

The F-wave phase shifts and the mixing angle ϵ_3 are shown in Fig. 6.1. Except for the 3F_2 -wave the coupled particle channel corrections are closer to the Nijmegen PWA result than the Δ -less case. The 1F_3 -wave is better described by the coupled channel potential at energies $T_{\text{lab}} < 170$ MeV, whereas for higher energies the deviation from the empirical PWA results increases. The 3F_3 phase shift improves substantially over the entire energy range $T_{\text{lab}} < 300$ MeV, whereas for the 3F_4 phase shift the corrections due to the coupled delta channels fill half of the gap between the purely nucleonic NLO calculation and the Nijmegen PWA for $T_{\text{lab}} > 50$ MeV. The mixing angle ϵ_3 can be reproduced very well. In the purely nucleonic calculation the data points lie at the lower edge of the band, whereas with coupled delta channels included the data points are located just in the middle of the band. In general the cutoff dependence for F-waves is rather weak. Note that by increasing the cutoff Λ , the interaction potentials get somewhat stronger and thus phase shifts tend to grow in magnitude.

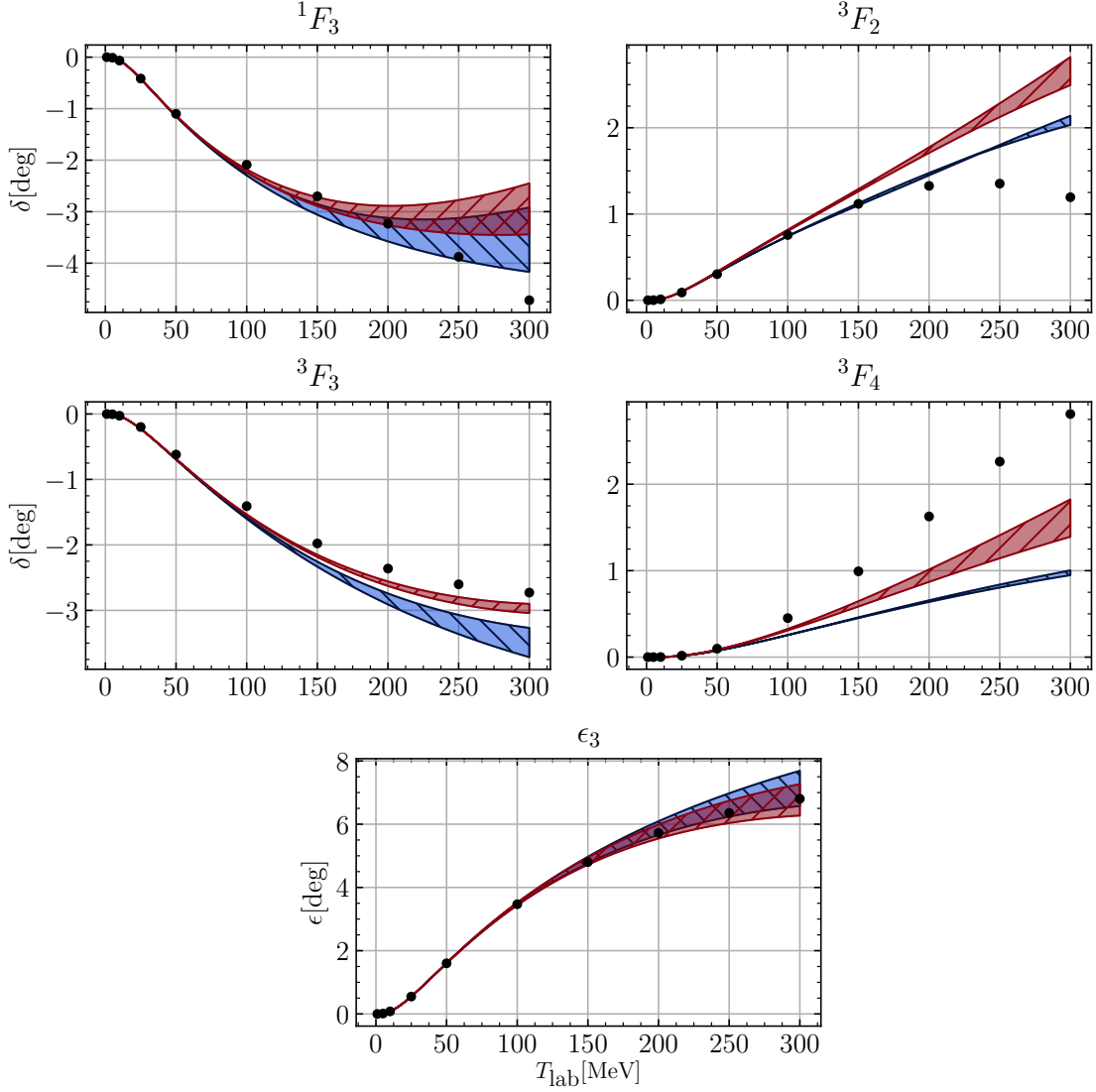


FIGURE 6.1: F-wave NN phase shifts and mixing angle ϵ_3 versus the nucleon lab kinetic energy T_{lab} for a cutoff variation $\Lambda = 450 \dots 700$ MeV. The blue band ($\backslash\backslash$ -hatching) and the red band ($/\!/$ -hatching) show the results of the calculation with chiral NN potentials only and with the full coupled (NN, $N\Delta$, ΔN , $\Delta\Delta$) channels at NLO, respectively. The filled circles stem from the Nijmegen PWA [58].

6.1.2 G-waves

The G-waves phase shifts and the mixing angle ϵ_4 are shown in Fig. 6.2. The coupled channel approach leads to some improvements in the waves 1G_4 , 3G_3 and 3G_4 at energies $T_{\text{lab}} > 200$ MeV. The 3G_5 phase shift changes from approximately -1.0° to a phase shift of -0.7° at 300 MeV lab energy, but it still does not reproduce the curvature behavior of the Nijmegen PWA. The reproduction of this delicate feature is observed only at higher

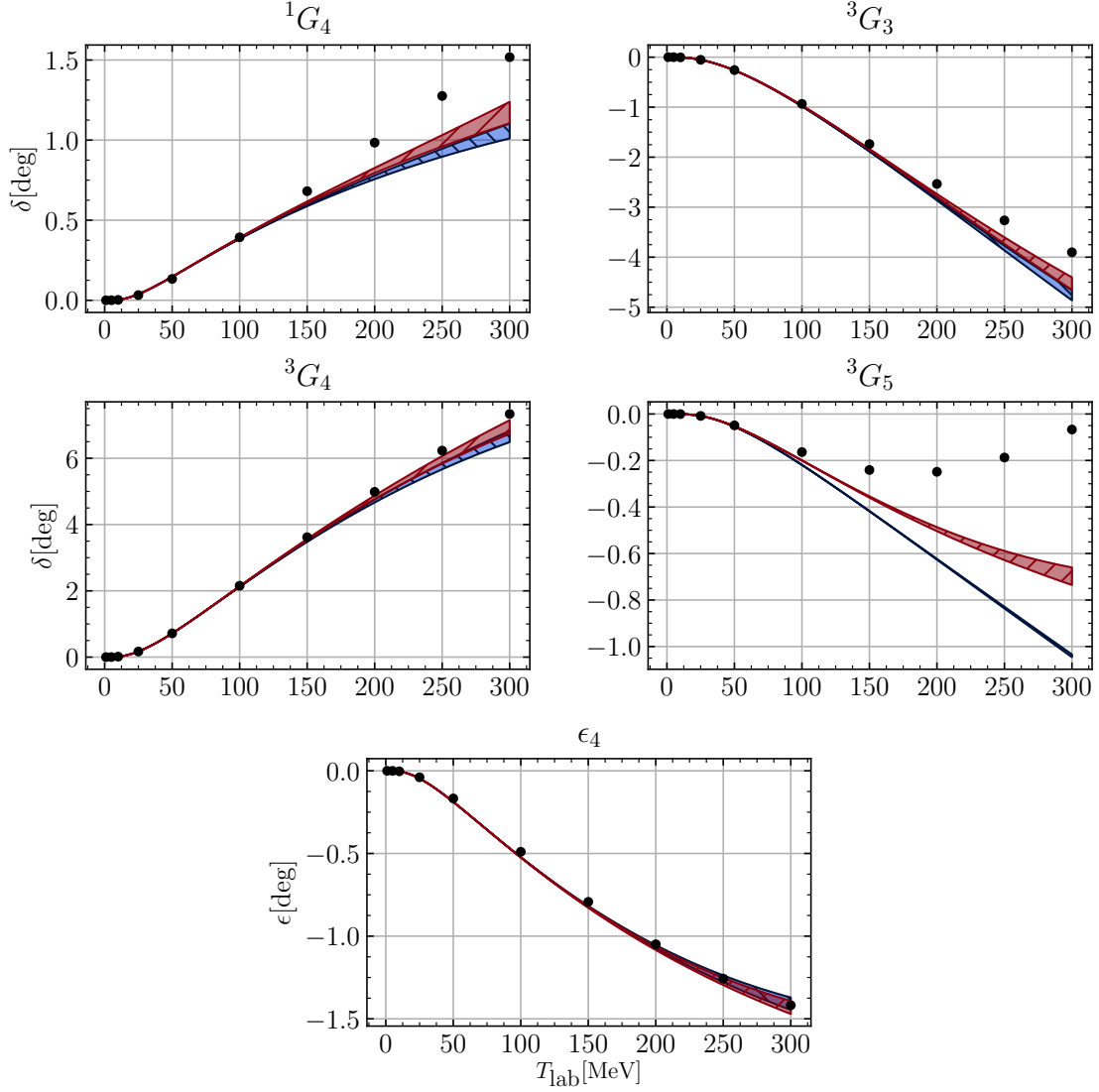


FIGURE 6.2: G-wave NN phase shifts and mixing angle ϵ_4 versus the nucleon lab kinetic energy T_{lab} for a cutoff variation $\Lambda = 450 \dots 700$ MeV. For notation see Fig. 6.1.

orders in the chiral expansion (see comparison of N2LO calculations with two different choices of $c_{1,3,4}$ parameters in Fig. 6.13). The cutoff dependence of the G-wave phase shifts decreased significantly compared to lower partial waves.

6.1.3 H-waves

For the H-waves the coupled channel approach leads to a slightly better agreement with the Nijmegen PWA for higher lab energies than the Δ -less phase shifts except for ${}^3\text{H}_4$ as we show in Fig. 6.3. The mixing angle ϵ_5 is nearly unaffected by the coupled channels.

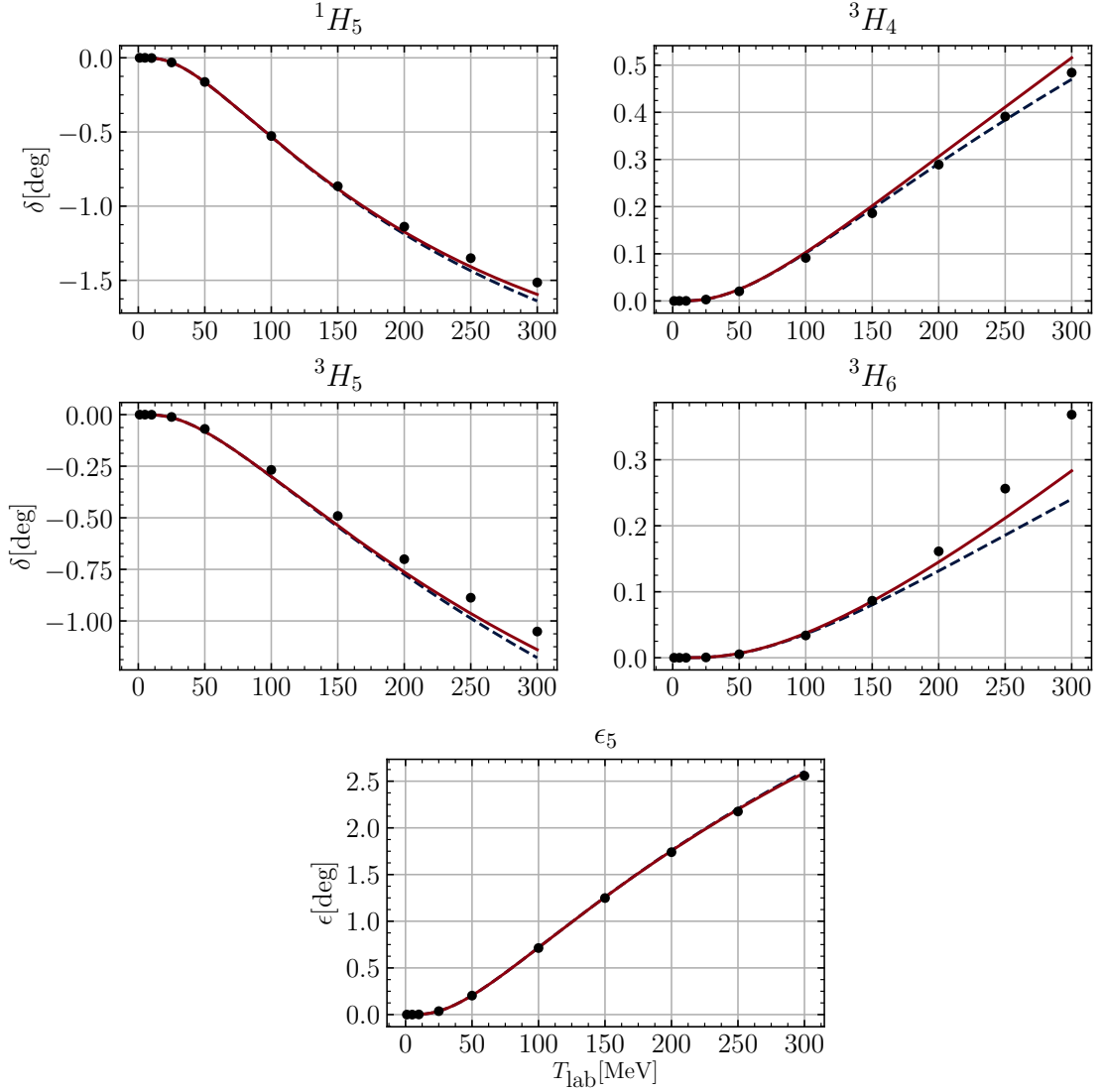


FIGURE 6.3: H-wave NN phase shifts and mixing angle ϵ_5 versus the nucleon lab kinetic energy T_{lab} for a cutoff variation $\Lambda = 450 \dots 700$ MeV. The dark blue (dashed) and red (solid) line show the results of the calculation with chiral NN potentials only and with the full coupled (NN, N Δ , Δ N, $\Delta\Delta$) channels at NLO, respectively. The filled circles stem from the Nijmegen PWA [58]. There is no visible cutoff dependence in these peripheral phase shifts.

Only ${}^3\text{H}_4$ can have a contribution from the contact potential $V_{\Delta\Delta\Delta\Delta}^{(2)}$, but it was shown in Section 5.2.3 that this effect is negligible.

6.1.4 *I-waves*

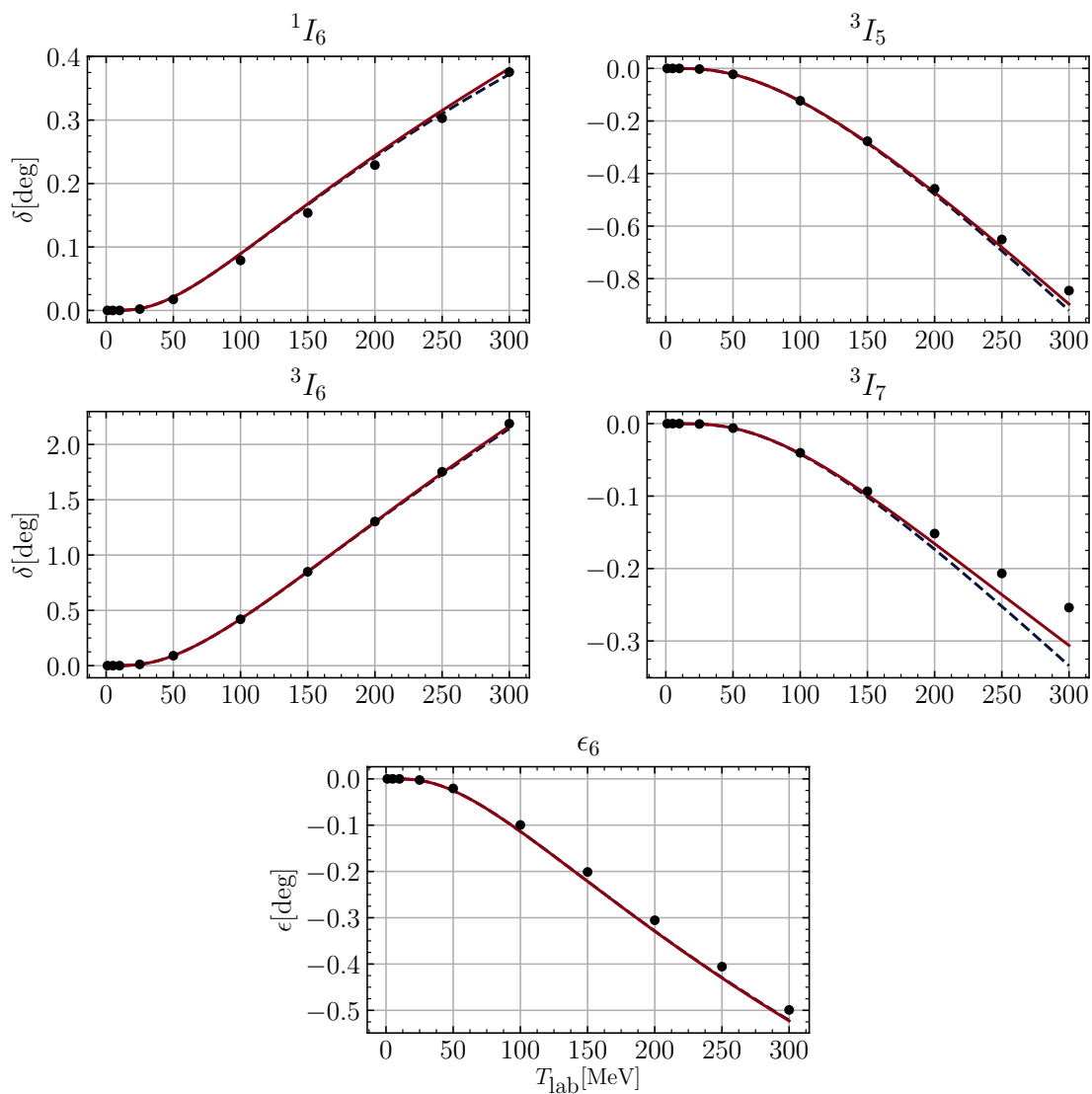


FIGURE 6.4: I-wave NN phase shifts and mixing angle ϵ_6 versus the nucleon lab kinetic energy T_{lab} for a cutoff variation $\Lambda = 450 \dots 700$ MeV. For notation see Fig. 6.3.

By including coupled channels, the I-waves in Fig. 6.4 show only very small deviations from the purely nucleonic chiral potentials. Due to the high orbital angular momentum $\ell = 6$ these phase shifts are mostly dominated by the one-pion exchange between nucleons.

Both the I- and H-waves and the corresponding mixing angles show no visible dependence on the cutoff parameter Λ .

6.2 PHASE SHIFTS IN LOW PARTIAL WAVES

In the partial waves with orbital angular momentum $\ell \leq 2$, the NN contact potentials at LO and NLO affect the interaction in the S- and P-waves and also in the 3D_1 -wave through the channel coupling ${}^3S_1 \leftrightarrow {}^3D_1$.

6.2.1 S-waves

With increasing ℓ in the peripheral partial waves, the cutoff dependence decreases rapidly. However, in the low partial waves the cutoff plays a major role but this regularization dependence is balanced in the S- and P-waves to a large extent by the NN contact potentials with their adjustable strength. The S-wave phase shifts are shown in Fig. 6.5. One has to perform separate fits in the coupled (NN, $N\Delta$, ΔN , $\Delta\Delta$)-channel approach and the purely nucleonic calculation in order to account for the differences of the 1π - and 2π -exchange potentials. Due to the strong influence of the NN low-energy constants the effect of the coupled particle channels is almost negligible, as one can see from the overlapping bands in Fig. 6.5. The fitted values of the low-energy constants can be found in Tables 5.3 and 5.4.

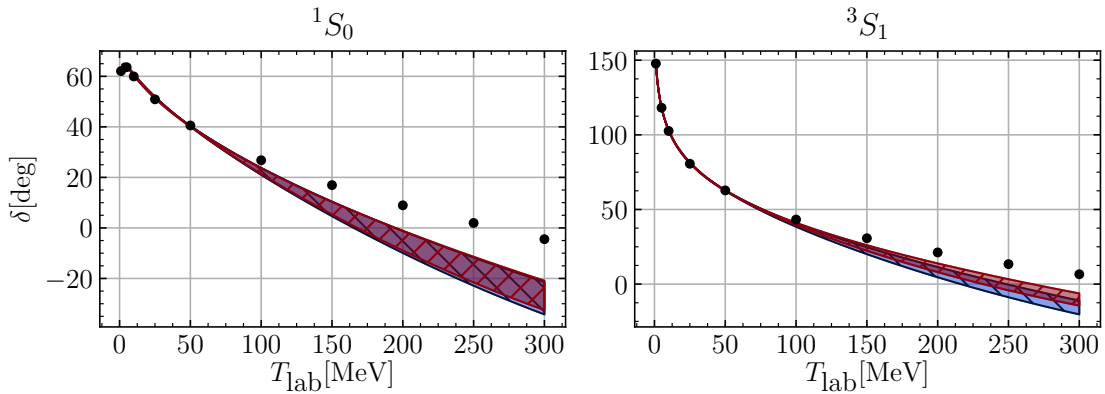


FIGURE 6.5: S-wave NN phase shifts versus the nucleon lab kinetic energy T_{lab} for a cutoff variation $\Lambda = 450 \dots 700$ MeV. The blue band ($\backslash\backslash$ -hatching) and the red band ($/\!/$ -hatching) show the results of the calculation with chiral NN potentials only and with the full coupled (NN, $N\Delta$, ΔN , $\Delta\Delta$) channels at NLO, respectively. The filled circles stem from the Nijmegen PWA [58].

6.2.2 P-waves

The P-wave phase shifts and the mixing angle ϵ_1 are shown in Fig. 6.6. They are also influenced by NN-contact potentials. The corresponding constants are listed in Tables 5.3 and 5.4. The 3P_0 -wave coupled $N\Delta$ channel result deviates a bit more from the Nijmegen

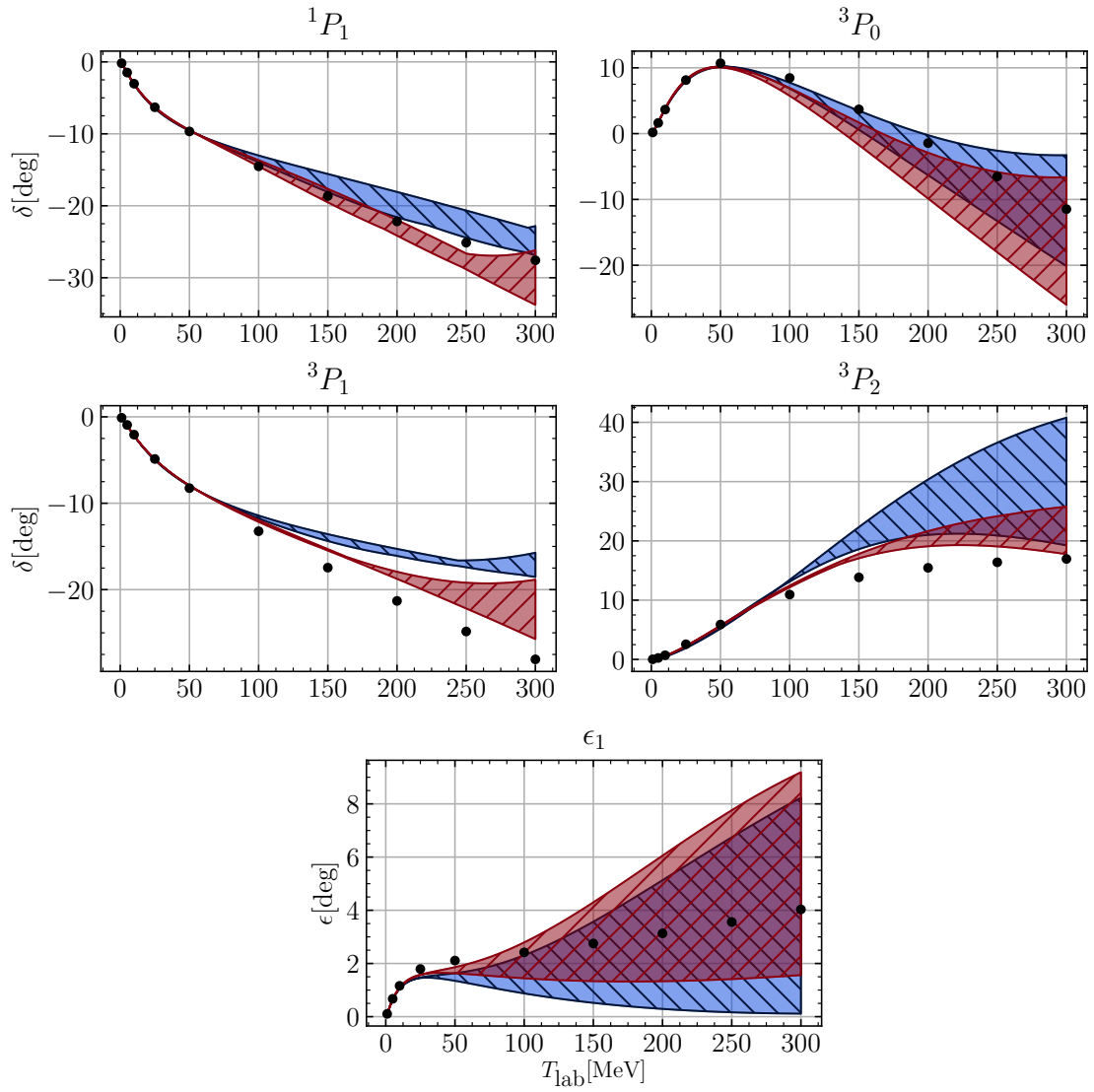


FIGURE 6.6: P-wave NN phase shifts and mixing angle ϵ_1 versus the nucleon lab kinetic energy T_{lab} for a cutoff variation $\Lambda = 450 \dots 700$ MeV. For notation see Fig. 6.5.

data points than that of the purely nucleonic calculation for $T_{\text{lab}} > 150$ MeV. In the 1P_1 -wave phase shift the coupled $N\Delta$ channels lead to a better agreement with the Nijmegen PWA up to $T_{\text{lab}} \approx 200$ MeV. The 3P_1 and the 3P_2 phase shifts receive corrections which move the rather narrow bands towards the data and the cutoff dependence is reduced significantly for the 3P_2 phase shift. At low lab energies $T_{\text{lab}} < 50$ MeV the mixing angle ϵ_1 comes out closer to the empirical values in the coupled channel approach, but with increasing energies the cutoff dependence of ϵ_1 grows in the same way for the calculation with and without coupled channels, such that the two bands overlap.

We show the influence of the variation of the NN-LEC $C_{NNNN}^{^3P_0} = -4623 \text{ GeV}^{-4}$ in Fig. 6.7, where we increased or decreased the value of the LEC by 100 GeV^{-4} , 500 GeV^{-4} , 1000 GeV^{-4} and 2000 GeV^{-4} . The four bands display the change from dark to light colors, respectively. The blue line shows the best fit to the data up to $T_{\text{lab}} = 100$ MeV. The data points at higher lab energy lie close to the $C_{NNNN}^{^3P_0} + 1000 \text{ GeV}^{-4}$ line. However, this boundary line does not describe the data in the best way for low lab energies T_{lab} .

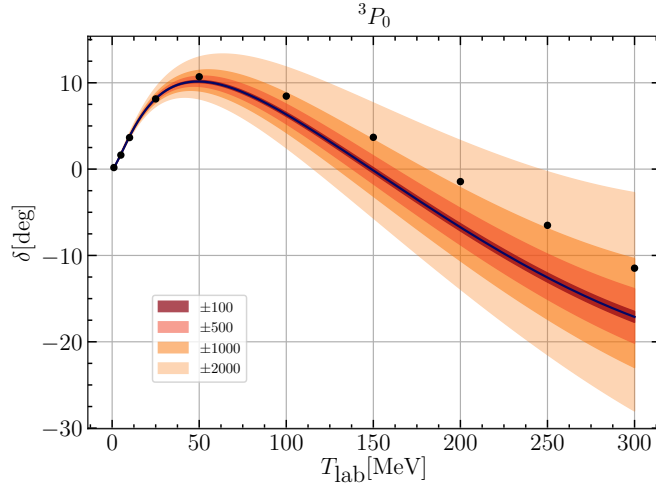


FIGURE 6.7: 3P_0 -wave: Variation of $C_{^3P_0}^{NNNN} = -4623 \text{ GeV}^{-4}$ by $\pm(100, 500, 1000, 2000) \text{ GeV}^{-4}$ as explained in the text. The blue line is the result of the fit.

6.2.3 D-waves

The D-wave phase shifts and the mixing angle ϵ_2 are shown in Fig. 6.8. Except for the 3D_1 phase shift, there is no influence of NN contact potentials on the D-waves. All corrections of the coupled $N\Delta$ channels tend into the right direction. For the 3D_2 -wave and the mixing angle ϵ_2 , the Nijmegen PWA results lie within the band obtained in the coupled $N\Delta$ channel approach. The bands resulting from the cutoff variation widen in most cases with increasing T_{lab} . Only for the 3D_1 phase shift, which is influenced by the part of the NN contact potential with low-energy constants $\tilde{C}^{^3S_1}$, $C^{^3S_1}$ and $C^{^3S_1-^3D_1}$ through the channel coupling $^3S_1 \leftrightarrow ^3D_1$, this cutoff dependence is strongly counterbalanced. The result of the coupled (NN, $N\Delta$, ΔN , $\Delta\Delta$) channel approach for the 3D_3 phase shift represents a

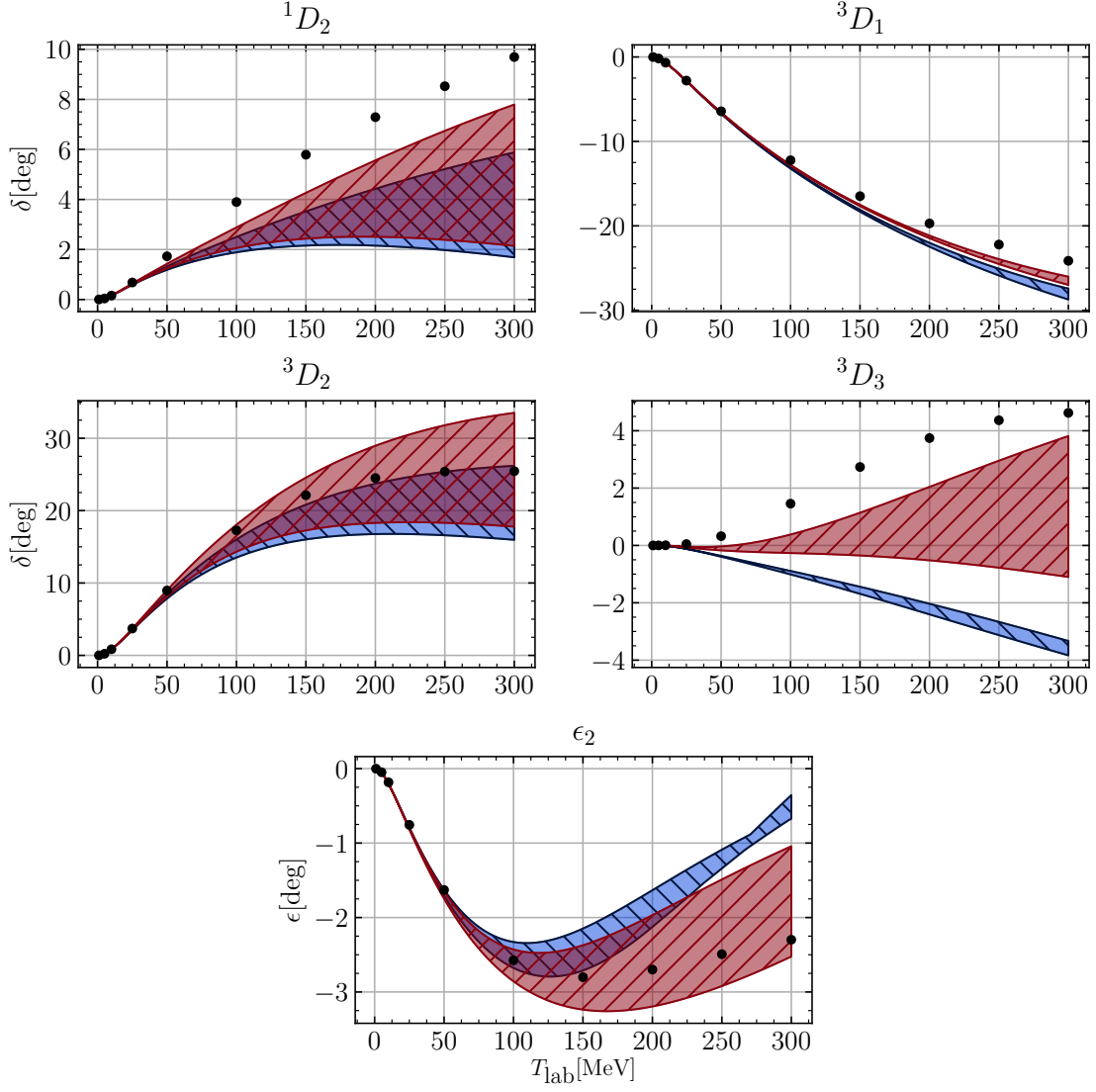


FIGURE 6.8: D-wave NN phase shifts and mixing angle ϵ_2 versus the nucleon lab kinetic energy T_{lab} for a cutoff variation $\Lambda = 450 \dots 700$ MeV. For notation see Fig. 6.5.

significant improvement over that of the calculation with the purely nucleonic chiral NN potential at NLO. Especially, for higher cutoffs $\Lambda > 650$ MeV the calculated phase shifts lie close to the empirical points from the Nijmegen PWA.

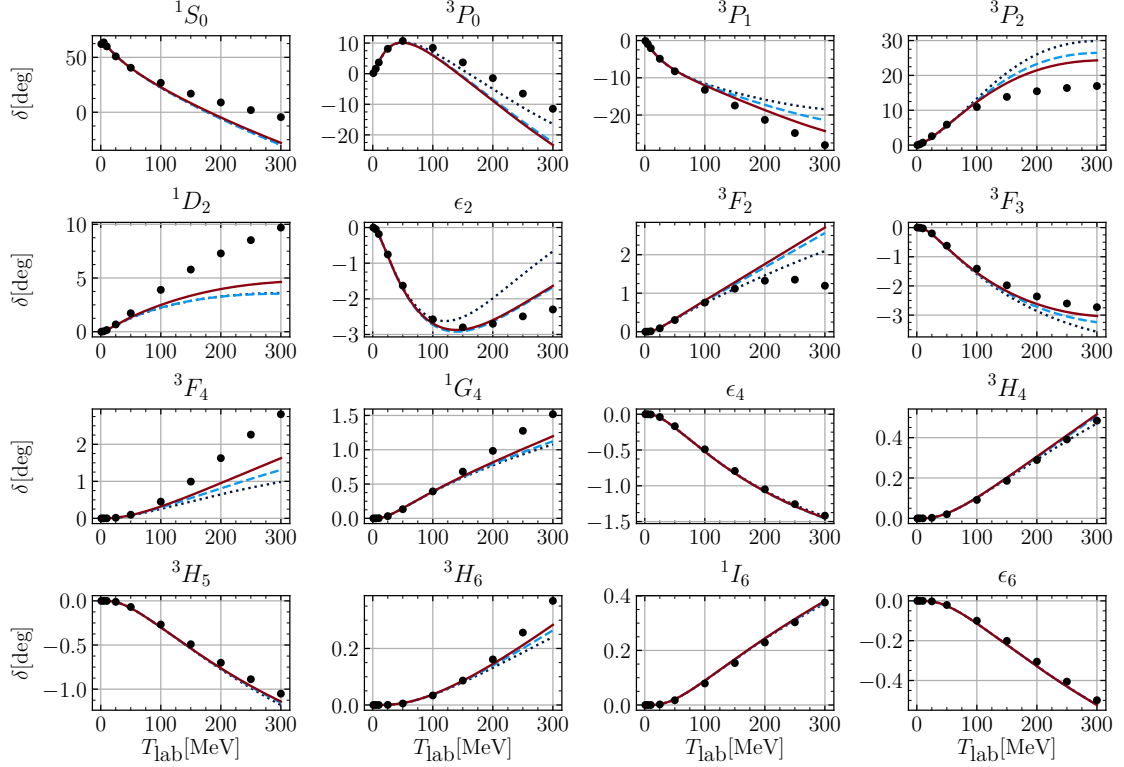
6.3 INFLUENCE OF THE $N\Delta$ -COUPLED CHANNELS


FIGURE 6.9: Contribution of NN coupled channels (blue dotted), additional $N\Delta$ (light blue dashed) and additional $\Delta\Delta$ coupled channels (red) in partial waves with isospin $I = 1$ for $\Lambda = 550$ MeV

The NN-waves with total isospin $I = 1$ are coupled to the $N\Delta$ - and $\Delta\Delta$ -channels. The contribution of the $N\Delta$ -channels to these waves and mixing angles is depicted in Fig. 6.9. For example, the addition in the 3P_0 -wave, the 3F_2 -wave and the mixing angle ϵ_2 is dominated by the $N\Delta$ -channels whereas in the 1D_2 -wave the $N\Delta$ -contribution is negligible. The 3P_1 -, 3P_2 -, 3F_3 - and 3F_4 -waves show an almost equal contribution from the $N\Delta$ - and $\Delta\Delta$ -channels. The S-wave and the partial waves with $j \geq 5$ show only little or no effect by switching on the coupled channels. In the isospin $I = 0$ NN-waves there exists only the coupled $\Delta\Delta$ channel. Results for these waves are shown in Fig. 6.10. Up to $j = 3$ and in the 3G -wave, the inclusion of the coupled channels shows a noticeable difference. It is important to note that these effects of the $\Delta\Delta$ -channel cannot be produced by the LECs acting in the lower partial waves.

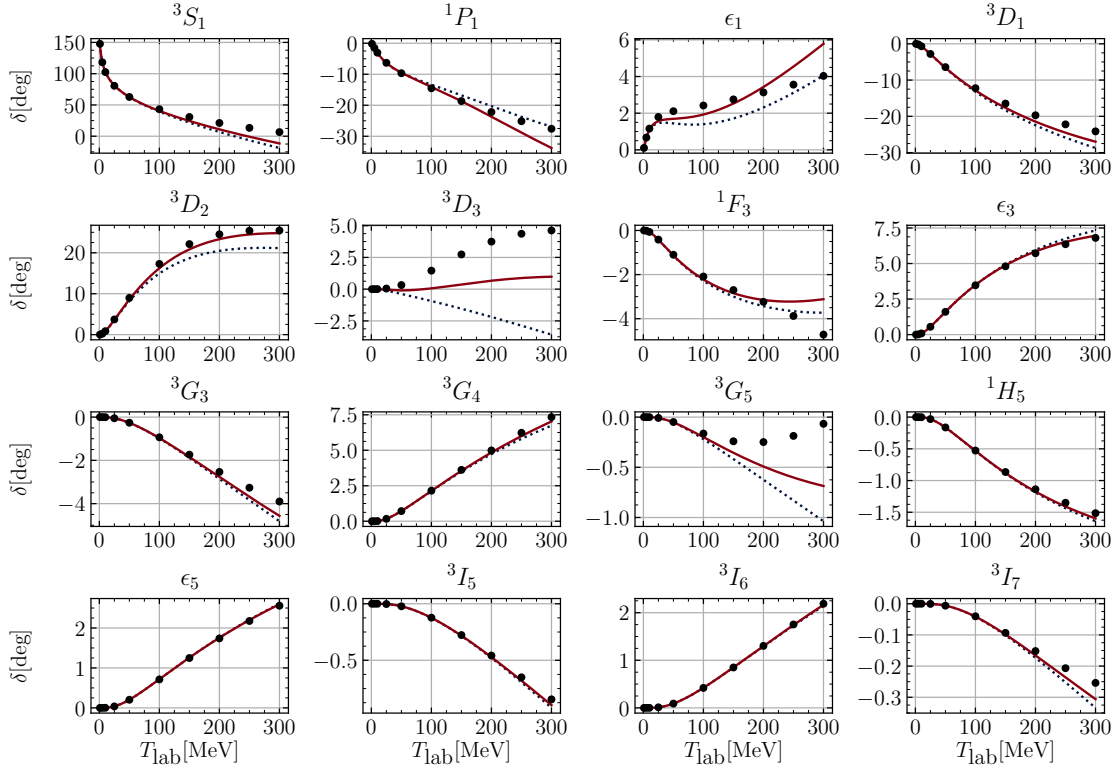


FIGURE 6.10: Contribution of NN coupled channels (blue dotted) and additional $\Delta\Delta$ coupled channels (red) in partial waves with isospin $I = 0$ for $\Lambda = 550$ MeV. The $N\Delta$ channels do not contribute to isospin $I = 0$.

6.4 COMPARISON OF RESULTS FOR TWO SCATTERING EQUATIONS

A comparison of the Kadyshevsky and the Lippmann-Schwinger equation for nucleon-nucleon scattering has been performed in Ref. [59] for phenomenological potentials. It was shown that the Kadyshevsky equation reproduces some features of other relativistic wave equations, e.g the Bethe-Salpeter equation [60].

We compare the Kadyshevsky equation (3.9) with the Lippmann-Schwinger equation for coupled channels (3.8) for the potential at next-to-leading order. The influence of the chosen scattering equation is shown in Fig. 6.11. The difference between these two equations in the purely nucleonic case is minor in most of the partial waves. In the coupled $N\Delta$ channel approach the Kadyshevsky equation leads to damped effects in the region of higher energy, compared to the Lippmann-Schwinger equation. In most of the partial waves the cutoff dependence decreases for the Kadyshevsky equation, the cutoff bands for selected waves are shown in Fig. 6.12.

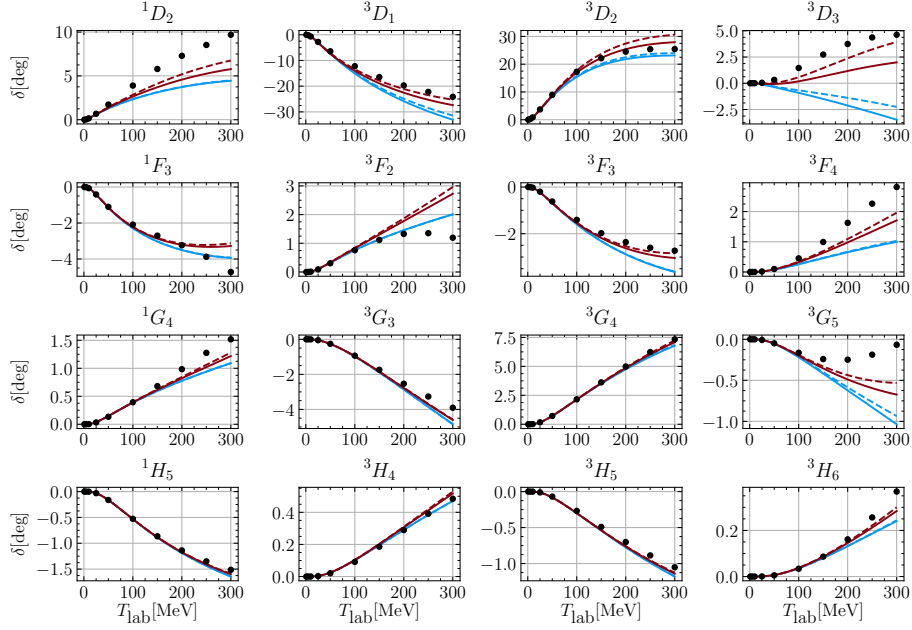


FIGURE 6.11: Selected partial waves for $\Lambda = 600$ MeV. Red curves: with coupled delta channels, light blue: without coupled delta channels, dashed lines: Lippmann-Schwinger equation, solid lines: Kadyshevsky equation.

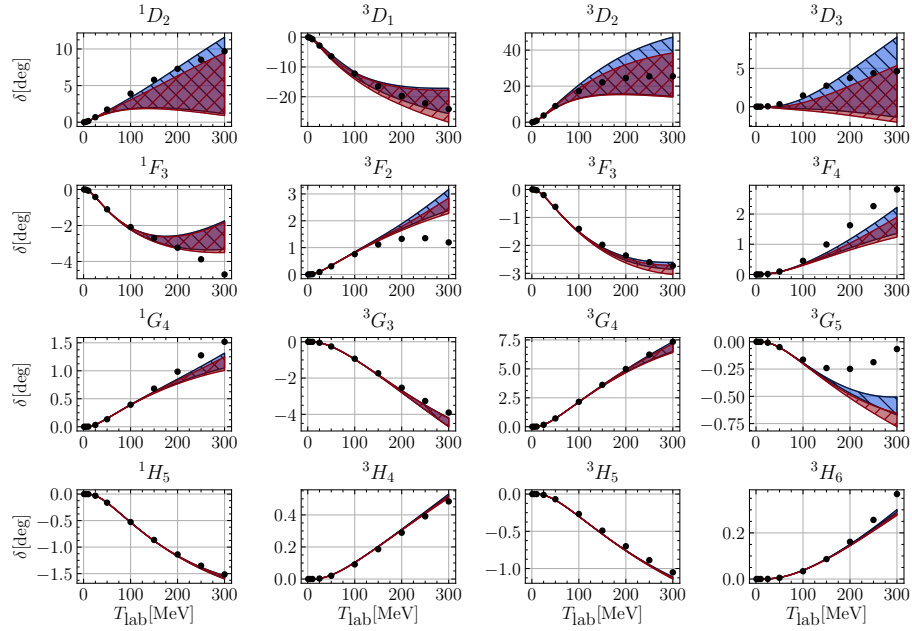


FIGURE 6.12: Selected partial waves for $\Lambda = 400 \dots 800$ MeV. Red bands with // hatching: Kadyshevsky with coupled channels, blue bands with \ hatching: Lippmann-Schwinger with coupled channels

6.5 NEXT-TO-NEXT-TO-LEADING ORDER EFFECTS

As shown Fig. 2.2 the effects of the $\Delta(1232)$ -resonance are hidden in the low-energy constants $c_{2,3,4}$ of higher derivative $2\pi NN$ -vertices of the pure NN-sector [12]. These additional Δ -isobar interactions at NLO in the coupled channel approach are transferred in the NN sector as a part of the pion-nucleon low-energy constants. We compare the Δ -less theory at N2LO to our coupled channel result.

At next-to-next-to-leading order we take the spectral functions from Ref. [12], which read

$$\begin{aligned}\text{Im } V_C &= \frac{3g_A^2}{64f_\pi^4} \left[2m_\pi^2(2c_1 - c_3) + \mu^2 c_3 \right] \frac{2m_\pi^2 - \mu^2}{\mu}, \\ \text{Im } W_T &= \frac{1}{\mu^2} \text{Im } W_S = \frac{g_A^2}{128f_\pi^4} c_4 \frac{4m_\pi^2 - \mu^2}{\mu}.\end{aligned}\quad (6.1)$$

The potentials $V_C(q)$ and $W_{S,T}(q)$ are again constructed through the regularized spectral representation in Eq. (3.21). We employ the πN -LECs c_i taken from the fit in Ref. [61], which were also used in Ref. [20]: $c_1 = (-0.81 \pm 0.15)\text{GeV}^{-1}$, $c_3 = (-4.69 \pm 1.34)\text{GeV}^{-1}$ and $c_4 = (3.40 \pm 0.04)\text{GeV}^{-1}$. In addition, we also consider a second set of values, that represent the parts arising solely from the $\Delta(1232)$ -resonance excitation, taken from Refs. [38, 62]: $c_1 = 0$, $c_3 = -2c_4 = -g_A^2/(2\Delta) = -2.84\text{GeV}^{-1}$, evaluating this relation for our choice of g_A . The pion-nucleon LEC c_1 is related to explicit chiral symmetry breaking and receives no contribution from the Δ -resonance. The results are shown in Fig. 6.13. The results of our coupled (NN, $N\Delta$, ΔN , $\Delta\Delta$) channel approach lie in between the NLO and N2LO calculations with purely nucleonic potentials for both choices of the low-energy constants $c_{1,3,4}$. As expected, the second set of LECs gives smaller changes of the phase shifts compared to NLO than the first set.

For the phase shifts in the partial waves 1F_3 , 3G_3 , 3G_4 , 3G_5 , 3H_6 , and in all I-waves, as well as for the mixing angles ϵ_3 and ϵ_4 , the coupled $N\Delta$ channel result agrees reasonably well with N2LO for set two. In the D-wave phase shifts the coupled $N\Delta$ channels are too weak compared to N2LO for set two. On the other hand, the pion-nucleon low-energy constants $c_{1,3,4}$ (set two) yield too strong effects in the $^3F_{2-}$, $^3F_{3-}$ and 3H_4 -waves, whereas the results of the coupled channel approach agree much better with the empirical phase shifts. The coupled (NN, $N\Delta$, ΔN , $\Delta\Delta$) channel dynamics generates (through infinite iterations) higher order corrections to the interaction strength represented by the low-energy constants $c_{3,4}$, and apparently these corrections go in the opposite direction. Such a reduction of the delta dynamics encoded in $c_{3,4}$ is favorable for some partial waves but unfavorable for others. This mixed findings point to the need for N3LO or even N4LO calculations [20–22] in order to get an accurate description of elastic nucleon-nucleon scattering in all partial waves.

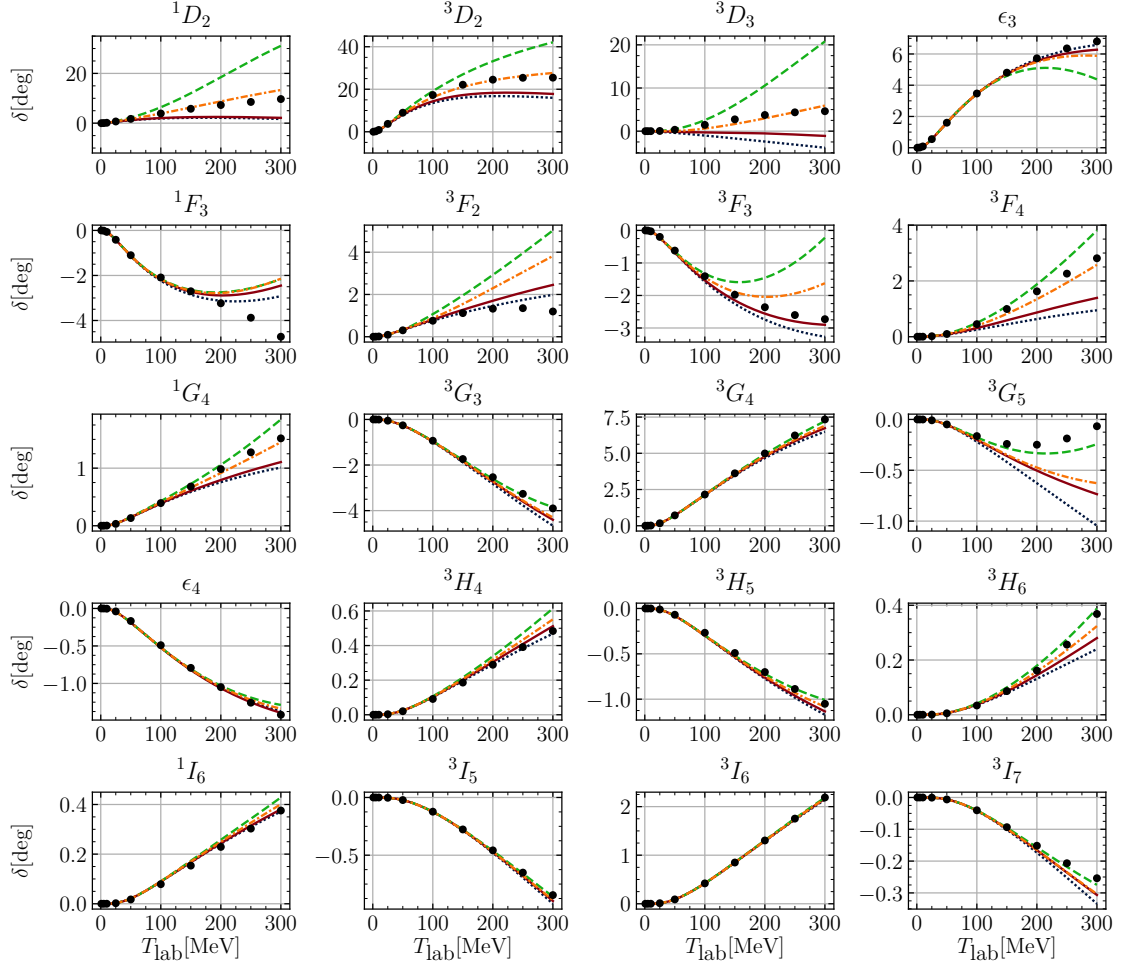


FIGURE 6.13: Selected NN phase shifts and mixing angles for a cutoff $\Lambda = 450$ MeV. Red solid curves: NLO calculation with coupled $N\Delta$ -channels, dark blue dotted curves: NLO calculation with chiral NN potentials only, green dashed curves: N2LO calculation with empirical low-energy constants $c_{1,3,4}$, orange dash-dotted curves: N2LO calculation with $c_1 = 0$, $c_3 = -2c_4 = -g_A^2/(2\Delta)$.

SUMMARY AND CONCLUSION

In this thesis, we have extended the chiral expansion of the two-nucleon potential at next-to-leading order by the inclusion of coupled (NN, $N\Delta$, ΔN , $\Delta\Delta$)-channels into the scattering equation. This extension requires the calculation of six additional one-pion exchange diagrams at leading order and about 60 two-pion exchange diagrams at next-to-leading order. Due to the small mass splitting of the nucleon and the delta, and the strong coupling of the delta to the πN -system, the delta is a natural candidate for an extension of the heavy baryon chiral effective field theory. This is a phenomenological extension, because the ΔN mass splitting is not related to explicit chiral symmetry breaking.

First, we have given a brief overview of QCD and the construction of chiral effective field theory. We have summarized the chiral Lagrangians including the Δ -isobar. Together with Weinberg's power counting scheme, we have identified the Feynman diagrams that are relevant for the calculation of the NN-potential. In addition, we have discussed scattering equations and regularization methods needed to obtain the T-matrix (or S-matrix) from the NN-potential. The Kadyshevsky equation, which is a scattering equation with relativistically corrected kinematics, is used together with a local regulator. This regulator acts already at the level of the spectral integrals and there are no subtractions needed for the 2π -exchange potential.

We have constructed the chiral one- and two-pion exchange potentials. The analytic expressions of the one-pion exchange potentials and of the two-pion exchange spectral functions for the seven different combinations of initial and final (NN, $N\Delta$, ΔN , $\Delta\Delta$)-states and the nine possible intermediate states have been given. The reducible components of the two-pion exchange planar box diagrams have been identified and excluded from the potential. The pertinent rule is: The irreducible parts of the $N\Delta$ and the $\Delta\Delta$ planar box diagram are equal and coincide with the negative of the $N\Delta$ crossed box diagram.

The NLO contact potentials have been derived and the low-energy constants have been identified in the spectroscopic notation. Only the purely nucleonic LECs have a one-to-one correspondence in the two notations. The relations between the other LECs in spectroscopic notation have been worked out. We have performed a fit of the NN LECs. As there are more LECs in the potentials which involve Δ -isobars, than data points for the fit, we omitted these LECs. In particular, the LECs arising from the potentials that include deltas, show only a subleading effect in the resulting phase shifts. Furthermore, the fitting procedure led to some undesired behavior after the delta LECs had been included as adjustable parameters in the fit.

We have solved the Kadyshevsky equation and the non-relativistic Lippmann-Schwinger equation with our coupled $N\Delta$ channel potential to obtain NN phase shifts and mixing angles for several cutoff parameters in the local regulator. We have found that in some of the partial waves and mixing angles, the N2LO contribution attributed to the Δ -isobar can be obtained already at NLO with coupled $N\Delta$ channels included. The inclusion of these coupled channels has also led to a reduction of the regularization cutoff dependence in some partial waves. Compared to the purely nucleonic results at next-to-leading order, the coupled $N\Delta$ channels improve in most partial waves the description of the empirical phase shifts and mixing angles, although the corrections by the inclusion of coupled $N\Delta$ channels are still too weak at higher lab energies, especially for 1D_2 , 3D_3 , 3F_4 , 3G_5 and 3H_6 .

This coupled channel approach can be continued also to higher orders in the chiral expansion. Then one has to consider also the $\pi\pi N\Delta$ vertex, which introduces the (shaded) triangle and football diagrams in Fig. 3.3. At N2LO one needs to find appropriate values for the pion-nucleon LECs, which do not contain contributions from hidden deltas any longer. It is worth to note that there exist no additional LECs for the (NN, $N\Delta$, $\Delta\Delta$) contact potentials at N2LO.

A

CONVENTIONS

A.1 GENERAL CONVENTIONS

- We use natural units, setting $c = \hbar = 1$.
- We use the Einstein summation convention: summation over repeated indices is implicitly understood.
- The metric tensor in Minkowski space is $g_{\mu\nu} = \text{diag}(1, -1, -1, -1)$.
- The contravariant components of the space-time four-vector x in Minkowski space are $x^\mu = (t, \mathbf{x})^T$ and its covariant components are $x_\mu = g_{\mu\nu}x^\nu = (t, -\mathbf{x})^T$.
- The Gell-Mann matrices λ_a forming a basis of the $\mathfrak{su}(3)$ Lie algebra are

$$\begin{aligned}\lambda_1 &= \begin{pmatrix} 0 & 1 & 0 \\ 1 & 0 & 0 \\ 0 & 0 & 0 \end{pmatrix}, & \lambda_2 &= \begin{pmatrix} 0 & -i & 0 \\ i & 0 & 0 \\ 0 & 0 & 0 \end{pmatrix}, & \lambda_3 &= \begin{pmatrix} 1 & 0 & 0 \\ 0 & -1 & 0 \\ 0 & 0 & 0 \end{pmatrix}, \\ \lambda_4 &= \begin{pmatrix} 0 & 0 & 1 \\ 0 & 0 & 0 \\ 1 & 0 & 0 \end{pmatrix}, & \lambda_5 &= \begin{pmatrix} 0 & 0 & -i \\ 0 & 0 & 0 \\ i & 0 & 0 \end{pmatrix}, & & \text{(A.1)} \\ \lambda_6 &= \begin{pmatrix} 0 & 0 & 0 \\ 0 & 0 & 1 \\ 0 & 1 & 0 \end{pmatrix}, & \lambda_7 &= \begin{pmatrix} 0 & 0 & 0 \\ 0 & 0 & -i \\ 0 & i & 0 \end{pmatrix}, & \lambda_8 &= \frac{1}{\sqrt{3}} \begin{pmatrix} 1 & 0 & 0 \\ 0 & 1 & 0 \\ 0 & 0 & -2 \end{pmatrix}\end{aligned}$$

They fulfill the following commutation relations

$$\left[\frac{\lambda_a}{2}, \frac{\lambda_b}{2} \right] = i f^{abc} \frac{\lambda_c}{2}, \quad \text{(A.2)}$$

with the totally antisymmetric structure constants f^{abc} . Up to permutations, their non-vanishing values are

$$f^{123} = 1, \quad f^{147} = f^{165} = f^{246} = f^{257} = f^{345} = f^{376} = \frac{1}{2}, \quad f^{458} = f^{678} = \frac{\sqrt{3}}{2}.$$

- The gamma matrices γ^μ read in Dirac representation

$$\gamma^0 = \begin{pmatrix} \mathbb{1}_2 & 0 \\ 0 & -\mathbb{1}_2 \end{pmatrix}, \quad \gamma^k = \begin{pmatrix} 0 & \sigma_k \\ -\sigma_k & 0 \end{pmatrix} \quad (\text{A.3})$$

where k runs from 1 to 3 and σ_k are the usual Pauli spin matrices.

- The Feynman slash abbreviates the 4×4 matrix $\not{a} = \gamma^\mu a_\mu$.

A.2 SPIN AND ISOSPIN MATRICES AND RELATIONS

This section collects the properties of the spin (transition) matrices σ^i , S^i , $S^{i\dagger}$ and Σ^i . All definitions and relations apply in exactly the same way for the isospin (transition) matrices τ^i , T^i , $T^{i\dagger}$ and Θ^i .

- The spin- $\frac{1}{2}$ matrices are the Pauli matrices σ^i

$$\sigma^1 = \begin{pmatrix} 0 & 1 \\ 1 & 0 \end{pmatrix}, \quad \sigma^2 = \begin{pmatrix} 0 & -i \\ i & 0 \end{pmatrix}, \quad \sigma^3 = \begin{pmatrix} 1 & 0 \\ 0 & -1 \end{pmatrix}. \quad (\text{A.4})$$

- The transition matrices for spin- $\frac{3}{2}$ to spin- $\frac{1}{2}$ read

$$\begin{aligned} S^1 &= \frac{1}{\sqrt{6}} \begin{pmatrix} -\sqrt{3} & 0 & 1 & 0 \\ 0 & -1 & 0 & \sqrt{3} \end{pmatrix}, \\ S^2 &= \frac{-i}{\sqrt{6}} \begin{pmatrix} \sqrt{3} & 0 & 1 & 0 \\ 0 & 1 & 0 & \sqrt{3} \end{pmatrix}, \\ S^3 &= \frac{1}{\sqrt{6}} \begin{pmatrix} 0 & 2 & 0 & 0 \\ 0 & 0 & 2 & 0 \end{pmatrix}. \end{aligned} \quad (\text{A.5})$$

and their hermitian conjugates $S^{i\dagger}$ serve for the reverse transition spin- $\frac{1}{2}$ to spin- $\frac{3}{2}$.

- The spin- $\frac{3}{2}$ matrices take the form

$$\begin{aligned} \Sigma^1 &= \begin{pmatrix} 0 & \sqrt{3} & 0 & 0 \\ \sqrt{3} & 0 & 2 & 0 \\ 0 & 2 & 0 & \sqrt{3} \\ 0 & 0 & \sqrt{3} & 0 \end{pmatrix}, \\ \Sigma^2 &= \begin{pmatrix} 0 & -\sqrt{3}i & 0 & 0 \\ \sqrt{3}i & 0 & -2i & 0 \\ 0 & 2i & 0 & -\sqrt{3}i \\ 0 & 0 & \sqrt{3}i & 0 \end{pmatrix}, \\ \Sigma^3 &= \begin{pmatrix} 3 & 0 & 0 & 0 \\ 0 & 1 & 0 & 0 \\ 0 & 0 & -1 & 0 \\ 0 & 0 & 0 & -3 \end{pmatrix}. \end{aligned} \quad (\text{A.6})$$

- We use additional spin-matrices defined in Ref. [57], which are symmetric in the multiple indices $i, j, k \in \{1, 2, 3\}$,

$$\begin{aligned}
 S^{ij\dagger} &= -\frac{1}{\sqrt{6}}(S^{i\dagger}\sigma^j + S^{j\dagger}\sigma^i) , \\
 S^{ij} &= -\frac{1}{\sqrt{6}}(\sigma^i S^j + \sigma^j S^i) , \\
 \Sigma^{ij} &= \frac{1}{8}(\Sigma^i \Sigma^j + \Sigma^j \Sigma^i - 10\delta^{ij}\mathbf{1}) = \delta^{ij}\mathbf{1} - \frac{3}{2}(S^{i\dagger}S^j + S^{j\dagger}S^i) , \\
 \Sigma^{ijk} &= \frac{1}{36\sqrt{3}}\left(5(\Sigma^i \Sigma^j \Sigma^k + \Sigma^k \Sigma^i \Sigma^j + \Sigma^j \Sigma^k \Sigma^i + \Sigma^i \Sigma^k \Sigma^j \right. \\
 &\quad \left. + \Sigma^j \Sigma^i \Sigma^k + \Sigma^k \Sigma^j \Sigma^i) - 82(\Sigma^i \delta^{jk} + \Sigma^j \delta^{ik} + \Sigma^k \delta^{ij})\right) . \tag{A.7}
 \end{aligned}$$

- The products of two matrices fulfill the following relations

$$\begin{aligned}
 \sigma^i \sigma^j &= \delta^{ij}\mathbf{1} + i\epsilon^{ijk}\sigma^k , \\
 S^{i\dagger}\sigma^j &= -\sqrt{\frac{3}{2}}S^{ij\dagger} - \frac{1}{2}i\epsilon^{ijk}S^{k\dagger} , \\
 \sigma^i S^j &= -\sqrt{\frac{3}{2}}S^{ij} - \frac{1}{2}i\epsilon^{ijk}S^k , \\
 S^{i\dagger}S^j &= \frac{1}{3}\delta^{ij}\mathbf{1} - \frac{1}{3}\Sigma^{ij} + \frac{1}{6}i\epsilon^{ijk}\Sigma^k , \\
 S^i S^{j\dagger} &= \frac{1}{3}(2\delta^{ij}\mathbf{1} - i\epsilon^{ijk}\sigma^k) , \\
 \Sigma^i S^{j\dagger} &= -\sqrt{\frac{3}{2}}S^{ij\dagger} + \frac{5}{2}i\epsilon^{ijk}S^{k\dagger} , \\
 S^i \Sigma^j &= -\sqrt{\frac{3}{2}}S^{ij} + \frac{5}{2}i\epsilon^{ijk}S^k , \\
 \Sigma^i \Sigma^j &= 5\delta^{ij}\mathbf{1} + 4\Sigma^{ij} + i\epsilon^{ijk}\Sigma^k , \\
 \Sigma^2 &= 15\mathbf{1} , \\
 \Sigma^i \Sigma^k \Sigma^i &= 11\Sigma^k , \tag{A.8}
 \end{aligned}$$

which are verified by using their explicit representations in Eqs. (A.4) to (A.6).

A.3 ISOSPIN MATRIX ELEMENTS

In isosinglet and isotriplet states one finds

$$\begin{aligned}
 \langle 0, 0 | \tau_1^a \otimes \tau_2^a | 0, 0 \rangle &= -3 & \langle 1, 1 | T_1^a \otimes T_2^{a\dagger} | 1, 1 \rangle &= -\frac{1}{3} \\
 \langle 1, 1 | \tau_1^a \otimes \tau_2^a | 1, 1 \rangle &= 1 & \langle 1, 1 | T_1^{a\dagger} \otimes \Theta_2^a | 1, 1 \rangle &= -2\sqrt{\frac{5}{3}} \\
 \langle 0, 0 | \Theta_1^a \otimes \Theta_2^a | 0, 0 \rangle &= -15 & \langle 0, 0 | T_1^{ab\dagger} \otimes T_2^{ab\dagger} | 0, 0 \rangle &= \frac{5\sqrt{2}}{3} \\
 \langle 1, 1 | \Theta_1^a \otimes \Theta_2^a | 1, 1 \rangle &= -11 & \langle 1, 1 | T_1^{ab\dagger} \otimes T_2^{ab\dagger} | 1, 1 \rangle &= -\frac{\sqrt{10}}{3} \\
 \langle 1, 1 | \tau_1^a \otimes T_2^{a\dagger} | 1, 1 \rangle &= 2\sqrt{\frac{2}{3}} & \langle 1, 1 | T_1^{ab} \otimes T_2^{ab\dagger} | 1, 1 \rangle &= -\frac{5}{3} \\
 \langle 1, 1 | \tau_1^a \otimes \Theta_2^a | 1, 1 \rangle &= -5 & \langle 1, 1 | T_1^{ab\dagger} \otimes \Theta_2^{ab} | 1, 1 \rangle &= -\sqrt{10} \\
 \langle 0, 0 | T_1^{a\dagger} \otimes T_2^{a\dagger} | 0, 0 \rangle &= -\sqrt{2} & \langle 0, 0 | \Theta_1^{ab} \otimes \Theta_2^{ab} | 0, 0 \rangle &= \frac{15}{2} \\
 \langle 1, 1 | T_1^{a\dagger} \otimes T_2^{a\dagger} | 1, 1 \rangle &= -\frac{\sqrt{10}}{3} & \langle 1, 1 | \Theta_1^{ab} \otimes \Theta_2^{ab} | 1, 1 \rangle &= \frac{3}{2},
 \end{aligned} \tag{A.9}$$

where the tensor product symbol \otimes indicates that the operators act in a product of two isospin-spaces.

A.4 NON-RELATIVISTIC EXPANSION

- The free Dirac spinors have the form

$$\bar{u}_i = \sqrt{\frac{E_i + M_N}{2M_N}} \left(\mathbf{1}, -\frac{\boldsymbol{\sigma} \cdot \mathbf{p}'}{E_i + M_N} \right), \quad u_j = \sqrt{\frac{E_j + M_N}{2M_N}} \left(\frac{\mathbf{1}}{E_j + M_N}, \boldsymbol{\sigma} \cdot \mathbf{p} \right), \tag{A.10}$$

with

$$E_i = \sqrt{M_N^2 + \mathbf{p}'^2}, \quad E_j = \sqrt{M_N^2 + \mathbf{p}^2}, \tag{A.11}$$

where M_N denotes the nucleon mass.

- The expansion of the baryon bilinears $(\bar{u}_3 \Gamma_1 u_1)$ or $(\bar{u}_4 \Gamma_2 u_2)$ in the inverse large nucleon mass up to order $\mathcal{O}(q^2)$ yields [11, 63]:

$$\begin{aligned}
 \bar{u}_i \mathbf{1} u_j &\approx 1 + \frac{p^2 + p'^2}{8M_N^2} - \frac{\boldsymbol{\sigma} \cdot \mathbf{p}' \boldsymbol{\sigma} \cdot \mathbf{p}}{4M_N^2}, \\
 \bar{u}_i \gamma^0 u_j &\approx 1 + \frac{p^2 + p'^2}{8M_N^2} + \frac{\boldsymbol{\sigma} \cdot \mathbf{p}' \boldsymbol{\sigma} \cdot \mathbf{p}}{4M_N^2}, \\
 \bar{u}_i \boldsymbol{\gamma} u_j &\approx \mathbf{0} + \frac{(\mathbf{p} + \mathbf{p}') + i(\mathbf{p} - \mathbf{p}') \times \boldsymbol{\sigma}}{2M_N},
 \end{aligned}$$

$$\begin{aligned}
 \bar{u}_i \gamma_5 u_j &\approx 0 + \frac{\boldsymbol{\sigma} \cdot (\mathbf{p} - \mathbf{p}')}{2M_N}, \\
 \bar{u}_i \gamma^0 \gamma_5 u_j &\approx 0 + \frac{\boldsymbol{\sigma} \cdot (\mathbf{p} + \mathbf{p}')}{2M_N}, \\
 \bar{u}_i \gamma \gamma_5 u_j &\approx \boldsymbol{\sigma} + \frac{p^2 + p'^2}{8M_N^2} \boldsymbol{\sigma} + \frac{\boldsymbol{\sigma} \cdot \mathbf{p}' \boldsymbol{\sigma} \boldsymbol{\sigma} \cdot \mathbf{p}}{4M_N^2}, \\
 \bar{u}_i \sigma^{0l} u_j &\approx 0 + i \frac{(p^l - p'^l) + i \epsilon^{lmn} (p^m + p'^m) \sigma^n}{2M_N}, \\
 \bar{u}_i \sigma^{kl} u_j &\approx \epsilon^{klm} \sigma^m + \epsilon^{klm} \frac{p^2 + p'^2}{8M_N^2} \sigma^m - \epsilon^{klm} \frac{\boldsymbol{\sigma} \cdot \mathbf{p}' \sigma^m \boldsymbol{\sigma} \cdot \mathbf{p}}{4M_N^2}. \tag{A.12}
 \end{aligned}$$

A.5 PROJECTORS ENTERING TWO-PION PHASE SPACE INTEGRALS

We list the projectors used to obtain the coefficients of interest from tensorial 2π -phase space integrals over l^μ , $l^\mu l^\nu$, $l^\mu l^\nu l^\rho$, and $l^\mu l^\nu l^\rho l^\sigma$ in Section 4.2.1.

$$\begin{aligned}
 Pr_{\tilde{A}_1} &= \frac{1}{\mu^2} q_\mu \\
 Pr_{\tilde{A}_2} &= \frac{1}{2\mu^2} q_\mu q_\nu + \frac{1}{2} v_\mu v_\nu - \frac{1}{2} g_{\mu\nu} \\
 Pr_{\tilde{B}_2} &= \frac{3}{2\mu^4} q_\mu q_\nu + \frac{1}{2\mu^2} v_\mu v_\nu - \frac{1}{2\mu^2} g_{\mu\nu} \\
 Pr_{\tilde{A}_3} &= \frac{1}{6\mu^2} (-q_\rho g_{\mu\nu} - q_\nu g_{\mu\rho} - q_\mu g_{\nu\rho}) + \frac{1}{2\mu^4} q_\mu q_\nu q_\rho + \frac{1}{6\mu^2} (q_\rho v_\mu v_\nu + q_\nu v_\mu v_\rho + q_\mu v_\nu v_\rho) \\
 Pr_{\tilde{B}_3} &= \frac{1}{2\mu^4} (-q_\rho g_{\mu\nu} - q_\nu g_{\mu\rho} - q_\mu g_{\nu\rho}) + \frac{5}{2\mu^6} q_\mu q_\nu q_\rho + \frac{1}{2\mu^4} (q_\rho v_\mu v_\nu + q_\nu v_\mu v_\rho + q_\mu v_\nu v_\rho) \\
 Pr_{\tilde{A}_4} &= \frac{1}{24} (g_{\mu\nu} g_{\rho\sigma} + g_{\mu\rho} g_{\nu\sigma} + g_{\mu\sigma} g_{\nu\rho}) \\
 &\quad + \frac{1}{24\mu^2} (-q_\rho q_\sigma g_{\mu\nu} - q_\nu q_\sigma g_{\mu\rho} - q_\mu q_\sigma g_{\nu\rho} - q_\nu q_\rho g_{\mu\sigma} - q_\mu q_\rho g_{\nu\sigma} - q_\mu q_\nu g_{\rho\sigma}) \\
 &\quad + \frac{1}{8\mu^4} q_\mu q_\nu q_\rho q_\sigma + \frac{1}{8} v_\mu v_\nu v_\rho v_\sigma \\
 &\quad + \frac{1}{24} (-v_\rho v_\sigma g_{\mu\nu} - v_\nu v_\sigma g_{\mu\rho} - v_\mu v_\sigma g_{\nu\rho} - v_\nu v_\rho g_{\mu\sigma} - v_\mu v_\rho g_{\nu\sigma} - v_\mu v_\nu g_{\rho\sigma}) \\
 &\quad + \frac{1}{24\mu^2} (q_\rho q_\sigma v_\mu v_\nu + q_\nu q_\sigma v_\mu v_\rho + q_\mu q_\sigma v_\nu v_\rho + q_\nu q_\rho v_\mu v_\sigma + q_\mu q_\rho v_\nu v_\sigma + q_\mu q_\nu v_\rho v_\sigma) \\
 Pr_{\tilde{B}_4} &= \frac{1}{24\mu^2} (g_{\mu\nu} g_{\rho\sigma} + g_{\mu\rho} g_{\nu\sigma} + g_{\mu\sigma} g_{\nu\rho}) \\
 &\quad + \frac{1}{8\mu^4} (-q_\rho q_\sigma g_{\mu\nu} - q_\nu q_\sigma g_{\mu\rho} - q_\mu q_\sigma g_{\nu\rho} - q_\nu q_\rho g_{\mu\sigma} - q_\mu q_\rho g_{\nu\sigma} - q_\mu q_\nu g_{\rho\sigma}) \\
 &\quad + \frac{5}{8\mu^6} q_\mu q_\nu q_\rho q_\sigma + \frac{1}{8\mu^2} v_\mu v_\nu v_\rho v_\sigma
 \end{aligned}$$

$$\begin{aligned}
 & + \frac{1}{24\mu^2} (-v_\rho v_\sigma g_{\mu\nu} - v_\nu v_\sigma g_{\mu\rho} - v_\mu v_\sigma g_{\nu\rho} - v_\nu v_\rho g_{\mu\sigma} - v_\mu v_\rho g_{\nu\sigma} - v_\mu v_\nu g_{\rho\sigma}) \\
 & + \frac{1}{8\mu^4} (q_\rho q_\sigma v_\mu v_\nu + q_\nu q_\sigma v_\mu v_\rho + q_\mu q_\sigma v_\nu v_\rho + q_\nu q_\rho v_\mu v_\sigma + q_\mu q_\rho v_\nu v_\sigma + q_\mu q_\nu v_\rho v_\sigma) \\
 Pr_{\tilde{C}_4} = & \frac{1}{8\mu^4} (g_{\mu\nu} g_{\rho\sigma} + g_{\mu\rho} g_{\nu\sigma} + g_{\mu\sigma} g_{\nu\rho}) \\
 & + \frac{5}{8\mu^6} (-q_\rho q_\sigma g_{\mu\nu} - q_\nu q_\sigma g_{\mu\rho} - q_\mu q_\sigma g_{\nu\rho} - q_\nu q_\rho g_{\mu\sigma} - q_\mu q_\rho g_{\nu\sigma} - q_\mu q_\nu g_{\rho\sigma}) \\
 & + \frac{35}{8\mu^8} q_\mu q_\nu q_\rho q_\sigma + \frac{3}{8\mu^4} v_\mu v_\nu v_\rho v_\sigma \\
 & + \frac{1}{8\mu^4} (-v_\rho v_\sigma g_{\mu\nu} - v_\nu v_\sigma g_{\mu\rho} - v_\mu v_\sigma g_{\nu\rho} - v_\nu v_\rho g_{\mu\sigma} - v_\mu v_\rho g_{\nu\sigma} - v_\mu v_\nu g_{\rho\sigma}) \\
 & + \frac{5}{8\mu^6} (q_\rho q_\sigma v_\mu v_\nu + q_\nu q_\sigma v_\mu v_\rho + q_\mu q_\sigma v_\nu v_\rho + q_\nu q_\rho v_\mu v_\sigma + q_\mu q_\rho v_\nu v_\sigma + q_\mu q_\nu v_\rho v_\sigma)
 \end{aligned} \tag{A.13}$$

In each case the coefficients in front of the tensors (built with $g_{\mu\nu}$, q_μ and v_μ) are found by solving systems of linear equations.

B

QUANTUM NUMBERS OF COUPLED CHANNELS

For each partial wave denoted by the total angular momentum j , the total isospin I and the parity π , the number of coupling channels n is given together with the set of quantum numbers for each channel. These channels are labeled by their angular momentum ℓ , their spin s and the number of Δ -isobars d in this channel.

1S_0

$$\begin{aligned} j &= 0, I = 1, \pi = 1, n = 4 \\ \ell & 0 \ 2 \ 0 \ 2 \\ s & 0 \ 2 \ 0 \ 2 \\ d & 0 \ 1 \ 2 \ 2 \end{aligned}$$

3P_0

$$\begin{aligned} j &= 0, I = 1, \pi = -1, n = 4 \\ \ell & 1 \ 1 \ 1 \ 3 \\ s & 1 \ 1 \ 1 \ 3 \\ d & 0 \ 1 \ 2 \ 2 \end{aligned}$$

3S_1 - 3D_1

$$\begin{aligned} j &= 1, I = 0, \pi = 1, n = 6 \\ \ell & 0 \ 2 \ 0 \ 2 \ 2 \ 4 \\ s & 1 \ 1 \ 1 \ 1 \ 3 \ 3 \\ d & 0 \ 0 \ 2 \ 2 \ 2 \ 2 \end{aligned}$$

1P_1

$$\begin{aligned} j &= 1, I = 0, \pi = -1, n = 4 \\ \ell & 1 \ 1 \ 1 \ 3 \\ s & 0 \ 0 \ 2 \ 2 \\ d & 0 \ 2 \ 2 \ 2 \end{aligned}$$

3P_1

$$\begin{aligned} j &= 1, I = 1, \pi = -1, n = 6 \\ \ell & 1 \ 1 \ 1 \ 3 \ 1 \ 3 \\ s & 1 \ 1 \ 2 \ 2 \ 1 \ 3 \\ d & 0 \ 1 \ 1 \ 1 \ 2 \ 2 \end{aligned}$$

3D_2

$$\begin{aligned}
 j &= 2, I = 0, \pi = 1, n = 4 \\
 \ell & 2 \quad 2 \quad 2 \quad 4 \\
 s & 1 \quad 1 \quad 3 \quad 3 \\
 d & 0 \quad 2 \quad 2 \quad 2
 \end{aligned}$$

 1D_2

$$\begin{aligned}
 j &= 2, I = 1, \pi = 1, n = 9 \\
 \ell & 2 \quad 2 \quad 0 \quad 2 \quad 4 \quad 2 \quad 0 \quad 2 \quad 4 \\
 s & 0 \quad 1 \quad 2 \quad 2 \quad 2 \quad 0 \quad 2 \quad 2 \quad 2 \\
 d & 0 \quad 1 \quad 1 \quad 1 \quad 1 \quad 2 \quad 2 \quad 2 \quad 2
 \end{aligned}$$

 3P_2 - 3F_2

$$\begin{aligned}
 j &= 2, I = 1, \pi = -1, n = 11 \\
 \ell & 1 \quad 3 \quad 1 \quad 3 \quad 1 \quad 3 \quad 1 \quad 3 \quad 1 \quad 3 \quad 5 \\
 s & 1 \quad 1 \quad 1 \quad 1 \quad 2 \quad 2 \quad 1 \quad 1 \quad 3 \quad 3 \quad 3 \\
 d & 0 \quad 0 \quad 1 \quad 1 \quad 1 \quad 1 \quad 2 \quad 2 \quad 2 \quad 2 \quad 2
 \end{aligned}$$

 3D_3 - 3G_3

$$\begin{aligned}
 j &= 3, I = 0, \pi = 1, n = 8 \\
 \ell & 2 \quad 4 \quad 2 \quad 4 \quad 0 \quad 2 \quad 4 \quad 6 \\
 s & 1 \quad 1 \quad 1 \quad 1 \quad 3 \quad 3 \quad 3 \quad 3 \\
 d & 0 \quad 0 \quad 2 \quad 2 \quad 2 \quad 2 \quad 2 \quad 2
 \end{aligned}$$

 1F_3

$$\begin{aligned}
 j &= 3, I = 0, \pi = -1, n = 5 \\
 \ell & 3 \quad 3 \quad 1 \quad 3 \quad 5 \\
 s & 0 \quad 0 \quad 2 \quad 2 \quad 2 \\
 d & 0 \quad 2 \quad 2 \quad 2 \quad 2
 \end{aligned}$$

 3F_3

$$\begin{aligned}
 j &= 3, I = 1, \pi = -1, n = 9 \\
 \ell & 3 \quad 3 \quad 1 \quad 3 \quad 5 \quad 3 \quad 1 \quad 3 \quad 5 \\
 s & 1 \quad 1 \quad 2 \quad 2 \quad 2 \quad 1 \quad 3 \quad 3 \quad 3 \\
 d & 0 \quad 1 \quad 1 \quad 1 \quad 1 \quad 2 \quad 2 \quad 2 \quad 2
 \end{aligned}$$

 3G_4

$$\begin{aligned}
 j &= 4, I = 0, \pi = 1, n = 5 \\
 \ell & 4 \quad 4 \quad 2 \quad 4 \quad 6 \\
 s & 1 \quad 1 \quad 3 \quad 3 \quad 3 \\
 d & 0 \quad 2 \quad 2 \quad 2 \quad 2
 \end{aligned}$$

 1G_4

$$\begin{aligned}
 j &= 4, I = 1, \pi = 1, n = 9 \\
 \ell & 4 \quad 4 \quad 2 \quad 4 \quad 6 \quad 4 \quad 2 \quad 4 \quad 6 \\
 s & 0 \quad 1 \quad 2 \quad 2 \quad 2 \quad 0 \quad 2 \quad 2 \quad 2 \\
 d & 0 \quad 1 \quad 1 \quad 1 \quad 1 \quad 2 \quad 2 \quad 2 \quad 2
 \end{aligned}$$

${}^3F_4-{}^3H_4$

$$j = 4, I = 1, \pi = -1, n = 12$$

ℓ	3	5	3	5	3	5	3	5	1	3	5	7
s	1	1	1	1	2	2	1	1	3	3	3	3
d	0	0	1	1	1	1	2	2	2	2	2	2

${}^3G_5-{}^3I_5$

$$j = 5, I = 0, \pi = 1, n = 8$$

ℓ	4	6	4	6	2	4	6	8
s	1	1	1	1	3	3	3	3
d	0	0	2	2	2	2	2	2

1H_5

$$j = 5, I = 0, \pi = -1, n = 5$$

ℓ	5	5	3	5	7
s	0	0	2	2	2
d	0	2	2	2	2

3H_5

$$j = 5, I = 1, \pi = -1, n = 9$$

ℓ	5	5	3	5	7	5	3	5	7
s	1	1	2	2	2	1	3	3	3
d	0	1	1	1	1	2	2	2	2

3I_6

$$j = 6, I = 0, \pi = 1, n = 5$$

ℓ	6	6	4	6	8
s	1	1	3	3	3
d	0	2	2	2	2

1I_6

$$j = 6, I = 1, \pi = 1, n = 9$$

ℓ	6	6	4	6	8	6	4	6	8
s	0	1	2	2	2	0	2	2	2
b	1	2	2	2	2	3	3	3	3

${}^1H_6-{}^3K_6$

$$j = 6, I = 1, \pi = -1, n = 12$$

ℓ	5	7	5	7	5	7	5	7	3	5	7	9
s	1	1	1	1	2	2	1	1	3	3	3	3
d	0	0	1	1	1	1	2	2	2	2	2	2

${}^3I_7-{}^3L_7$

$$j = 7, I = 0, \pi = 1, n = 8$$

ℓ	6	8	6	8	4	6	8	10
s	1	1	1	1	3	3	3	3
d	0	0	2	2	2	2	2	2

RELATIONS FOR LOW ENERGY CONSTANTS

C.1 DEFINITION OF LECS IN SPECTROSCOPIC NOTATION

In this chapter we list the relations for the LECS in the partial wave scheme. All of the constants below carry also the index of the potential specified in the headings, which we omitted here again for readability.

NN→ NN:

$$\begin{aligned}
\tilde{C}^{1S_0} &= 4\pi(C_S - 3C_T) \\
\tilde{C}^{3S_1} &= 4\pi(C_S + C_T) \\
C^{1S_0} &= \pi(4C_1 + C_2 - 12C_3 - 3C_4 - 4C_6 - C_7) \\
C^{3S_1} &= \frac{1}{3}\pi(12C_1 + 3C_2 + 12C_3 + 3C_4 + 4C_6 + C_7) \\
C^{1P_1} &= \frac{2}{3}\pi(4C_1 - C_2 - 12C_3 + 3C_4 - 4C_6 + C_7) \\
C^{3P_1} &= \frac{2}{3}\pi(4C_1 - C_2 + 4C_3 - C_4 + 4C_5 + 8C_6 - 2C_7) \\
C^{3P_0} &= \frac{2}{3}\pi(4C_1 - C_2 + 4C_3 - C_4 + 8C_5 - 12C_6 + 3C_7) \\
C^{3P_2} &= \frac{2}{3}\pi(4C_1 - C_2 + 4C_3 - C_4 - 4C_5) \\
C^{3D_1-3S_1} &= \frac{2}{3}\sqrt{2}\pi(4C_6 + C_7)
\end{aligned} \tag{C.1}$$

NN→ N Δ :

$$\begin{aligned}
C^{3P_0} &= \frac{2}{3\sqrt{3}}\pi(-16C_3 + 4C_4 - 4C_5 - 12C_6 + 3C_7) \\
C^{3P_1} &= \frac{1}{3\sqrt{6}}\pi(-32C_3 + 8C_4 - 4C_5 - 4C_6 + C_7) \\
C^{3P_2} &= \frac{1}{3\sqrt{6}}\pi(-32C_3 + 8C_4 + 4C_5 - 12C_6 + 3C_7) \\
C^{5P_1-3P_1} &= \frac{1}{3}\sqrt{\frac{5}{6}}\pi(4C_5 - 12C_6 + 3C_7)
\end{aligned}$$

$$\begin{aligned}
 C^{5P_2-3P_2} &= \frac{1}{\sqrt{6}}\pi(4C_5 + 4C_6 - C_7) \\
 C^{5D_0-1S_0} &= \sqrt{\frac{2}{3}}\pi(4C_6 + C_7) \\
 C^{5S_2-1D_2} &= \sqrt{\frac{2}{15}}\pi(4C_6 + C_7)
 \end{aligned} \tag{C.2}$$

$N\Delta \rightarrow N\Delta$:

$$\begin{aligned}
 \tilde{C}^{5S_2} &= 4\pi(C_1^{(0)} + 3C_2^{(0)}) \\
 C^{5S_2} &= \pi(4C_1 + C_2 + 12C_3 + 3C_4 + 4C_6 + C_7) \\
 C^{3P_0} &= -\frac{2}{3}\pi(4C_1 - C_2 - 20C_3 + 5C_4 + 8C_5 - 12C_{5-}) \\
 C^{3P_1} &= -\frac{1}{3}\pi(8C_1 - 2C_2 - 40C_3 + 10C_4 + 8C_5 - 12C_{5-} - 20C_6 + 5C_7) \\
 C^{3P_1-5P_1} &= \frac{\sqrt{5}}{3}\pi(4C_{5-} - 12C_6 + 3C_7) \\
 C^{5P_1} &= -\frac{1}{3}\pi(8C_1 - 2C_2 + 24C_3 - 6C_4 + 24C_5 - 12C_{5-} - 20C_6 + 5C_7) \\
 C^{3P_2} &= \frac{1}{3}\pi(-8C_1 + 2C_2 + 40C_3 - 10C_4 + 8C_5 - 12C_{5-} + 12C_6 - 3C_7) \\
 C^{3P_2-5P_2} &= \pi(4C_{5-} + 4C_6 - C_7) \\
 C^{5P_2} &= -\frac{1}{3}\pi(8C_1 - 2C_2 + 24C_3 - 6C_4 + 8C_5 - 4C_{5-} + 36C_6 - 9C_7) \\
 C^{5P_3} &= \frac{2}{3}\pi(-4C_1 + C_2 - 12C_3 + 3C_4 + 8C_5 - 4C_{5-}) \\
 C^{5S_2-3D_2} &= -\sqrt{\frac{6}{5}}\pi(4C_6 + C_7) \\
 C^{5S_2-5D_2} &= \sqrt{\frac{14}{5}}\pi(4C_6 + C_7)
 \end{aligned} \tag{C.3}$$

$NN \rightarrow \Delta\Delta$:

$$\begin{aligned}
 \tilde{C}^{1S_0} &= \frac{4}{3}\sqrt{2}\pi(-3C_2^{(0)} + 5C_3^{(0)}) \\
 \tilde{C}^{3S_1} &= -\frac{4}{3}\sqrt{10}\pi(C_2^{(0)} + C_3^{(0)}) \\
 C^{1S_0} &= \frac{\sqrt{2}}{9}\pi(-36C_3 - 9C_4 - 12C_6 - 3C_7 + 60C_8 + 15C_9 + 20C_{10} + 5C_{11}) \\
 C^{3S_1} &= -\frac{\sqrt{10}}{9}\pi(12C_3 + 3C_4 + 4C_6 + C_7 + 12C_8 + 3C_9 + 4C_{10} + C_{11}) \\
 C^{3P_0} &= -\frac{\sqrt{10}}{27}\pi(20C_{10} - 5C_{11} + 6(-4C_3 + C_4 - 4C_8 + C_9)) \\
 C^{1P_1} &= -\frac{2\sqrt{2}}{27}\pi(20C_{10} - 5C_{11} + 3(-12C_3 + 3C_4 - 4C_6 + C_7 + 20C_8 - 5C_9))
 \end{aligned}$$

$$\begin{aligned}
 C^{3P_1} &= \frac{1}{27} \sqrt{\frac{5}{2}} \pi (44C_{10} - 11C_{11} + 6(8C_3 - 2C_4 + 4C_6 - C_7 + 8C_8 - 2C_9)) \\
 C^{3P_2} &= \frac{1}{27\sqrt{10}} \pi (240C_3 - 60C_4 + 72C_6 - 18C_7 + 240C_8 - 60C_9 + 52C_{10} \\
 &\quad - 13C_{11}) \\
 C^{3P_1-5P_1} &= \frac{\sqrt{5}}{27} \pi (24C_6 - 6C_7 - 28C_{10} + 7C_{11}) \\
 C^{3P_2-7P_2} &= \frac{1}{9} \sqrt{\frac{7}{5}} \pi (24C_6 - 6C_7 + 4C_{10} - C_{11}) \\
 C^{3S_1-3D_1} &= -\frac{1}{9\sqrt{5}} \pi (28C_{10} + 7C_{11} + 8C_6 + 2C_7) \\
 C^{5S_2-1D_2} &= -\frac{1}{9\sqrt{10}} \pi (28C_{10} + 7C_{11} - 24C_6 - 6C_7) \\
 C^{7S_3-3D_3} &= \frac{1}{3\sqrt{30}} \pi (4C_{10} + C_{11} + 24C_6 + 6C_7) \\
 C^{1S_0-5D_0} &= -\frac{1}{9\sqrt{2}} \pi (28C_{10} + 7C_{11} - 24C_6 - 6C_7) \\
 C^{3S_1-3D_1} &= -\frac{1}{9\sqrt{5}} \pi (28C_{10} + 7C_{11} + 8C_6 + 2C_7) \\
 C^{3S_1-7D_1} &= \frac{1}{9} \sqrt{\frac{7}{10}} \pi (4C_{10} + C_{11} + 24C_6 + 6C_7) \tag{C.4}
 \end{aligned}$$

$N\Delta \rightarrow \Delta\Delta$:

$$\begin{aligned}
 \tilde{C}^{5S_2} &= 4\pi(-2\sqrt{3}C_2^{(0)} + \sqrt{2}C_3^{(0)}) \\
 C^{5S_2} &= \frac{1}{3} \pi (-24\sqrt{3}C_3 - 6\sqrt{3}C_4 - 8\sqrt{3}C_6 - 2\sqrt{3}C_7 + 3\sqrt{2}(4C_8 + C_9) \\
 &\quad + 4\sqrt{2}C_{10} + \sqrt{2}C_{11}) \\
 C^{3P_0} &= \frac{1}{18} \sqrt{\frac{5}{2}} \pi (32\sqrt{6}C_3 - 8\sqrt{6}C_4 + 8\sqrt{6}C_5 - 24\sqrt{6}C_6 + 6\sqrt{6}C_7 + 96C_8 - 24C_9 \\
 &\quad + 4C_{10} - C_{11}) \\
 C^{3P_1} &= \frac{1}{36} \sqrt{\frac{5}{2}} \pi (2(32\sqrt{6}C_3 - 8\sqrt{6}C_4 + 4\sqrt{6}C_5 + 28\sqrt{6}C_6 - 7\sqrt{6}C_7 + 96C_8 - 24C_9) \\
 &\quad + 92C_{10} - 23C_{11}) \\
 C^{3P_2} &= \frac{1}{36} \frac{1}{\sqrt{10}} \pi (320\sqrt{6}C_3 - 80\sqrt{6}C_4 - 40\sqrt{6}C_5 + 72\sqrt{6}C_6 - 18\sqrt{6}C_7 + 960C_8 - 240C_9 \\
 &\quad + 292C_{10} - 73C_{11}) \\
 C^{3P_1-5P_1} &= \frac{1}{72} \pi (-4\sqrt{3}(4C_5 + 12C_6 - 3C_7) + 84\sqrt{2}C_{10} - 21\sqrt{2}C_{11}) \\
 C^{3P_2-5P_2} &= \frac{1}{12\sqrt{30}} \pi (6\sqrt{2}(-4C_5 + 4C_6 - C_7) - 28\sqrt{3}C_{10} + 7\sqrt{3}C_{11}) \\
 C^{3P_2-7P_2} &= \frac{1}{6} \sqrt{\frac{7}{5}} \pi (2\sqrt{6}(-4C_6 + C_7) + 12C_{10} - 3C_{11})
 \end{aligned}$$

$$\begin{aligned}
 C^{5P_2-7P_2} &= \frac{1}{9}\sqrt{\frac{7}{5}}\pi(2\sqrt{6}(2C_5 - 12C_6 + 3C_7) + 4C_{10} - C_{11}) \\
 C^{5P_3-7P_3} &= \frac{1}{18}\pi(4\sqrt{3}(4C_5 + 12C_6 - 3C_7) - 4\sqrt{2}C_{10} + \sqrt{2}C_{11}) \\
 C^{1S_0-5D_0} &= \frac{1}{6\sqrt{2}}\pi(2\sqrt{6}(4C_6 + C_7) - 28C_{10} - 7C_{11}) \\
 C^{5S_2-3D_2} &= -\frac{1}{12\sqrt{5}}\pi(18\sqrt{2}(4C_6 + C_7) + 28\sqrt{3}C_{10} + 7\sqrt{3}C_{11}) \\
 C^{5S_2-5D_2} &= \frac{1}{12}\sqrt{\frac{7}{5}}\pi(12C_{10} + 3C_{11} - 2\sqrt{6}(4C_6 + C_7)) \\
 C^{5S_2-1D_2} &= \frac{1}{6\sqrt{10}}\pi(-28C_{10} - 7C_{11} + 2\sqrt{6}(4C_6 + C_7))
 \end{aligned} \tag{C.5}$$

$\Delta\Delta \rightarrow \Delta\Delta$:

$$\begin{aligned}
 \tilde{C}^{1S_0} &= \frac{2}{3}\pi(6C_1^{(0)} - 90C_2^{(0)} + 45C_3^{(0)} - 700C_4^{(0)}) \\
 \tilde{C}^{3S_1} &= 2\pi(2C_1^{(0)} - 22C_2^{(0)} + 3C_3^{(0)} + 140C_4^{(0)}) \\
 \tilde{C}^{5S_2} &= \frac{2}{3}\pi(6C_1^{(0)} - 18C_2^{(0)} - 27C_3^{(0)} - 140C_4^{(0)}) \\
 \tilde{C}^{7S_3} &= \frac{2}{3}\pi(6C_1^{(0)} + 54C_2^{(0)} + 9C_3^{(0)} + 20C_4^{(0)}) \\
 C^{1S_0} &= \frac{1}{18}\pi(72C_1 + 18C_2 - 1080C_3 - 270C_4 - 360C_6 - 90C_7 + 540C_8 \\
 &\quad + 135C_9 + 180C_{10} + 45C_{11} - 8400C_{12} - 2100C_{13} - 2800C_{14} - 700C_{15}) \\
 C^{3S_1} &= \frac{1}{6}\pi(24C_1 + 6C_2 - 264C_3 - 66C_4 - 88C_6 - 22C_7 + 36C_8 \\
 &\quad + 9C_9 + 12C_{10} + 3C_{11} + 1680C_{12} + 420C_{13} + 560C_{14} + 140C_{15}) \\
 C^{5S_2} &= \frac{1}{18}\pi(72C_1 + 18C_2 - 216C_3 - 54C_4 - 72C_6 - 18C_7 - 324C_8 \\
 &\quad - 81C_9 - 108C_{10} - 27C_{11} - 1680C_{12} - 420C_{13} - 560C_{14} - 140C_{15}) \\
 C^{7S_3} &= \frac{1}{18}\pi(72C_1 + 18C_2 + 648C_3 + 162C_4 + 216C_6 + 54C_7 + 108C_8 \\
 &\quad + 27C_9 + 36C_{10} + 9C_{11} + 240C_{12} + 60C_{13} + 80C_{14} + 20C_{15}) \\
 C^{3P_0} &= \frac{1}{9}\pi(-24C_1 + 6C_2 + 264C_3 - 66C_4 - 48C_5 + 360C_6 - 90C_7 - 36C_8 \\
 &\quad + 9C_9 - 96C_{10} + 24C_{11} - 1680C_{12} + 420C_{13} + 784C_{14} - 196C_{15}) \\
 C^{1P_1} &= \frac{1}{27}\pi(-72C_1 + 18C_2 + 1080C_3 - 270C_4 + 360C_6 - 90C_7 - 540C_8 \\
 &\quad + 135C_9 - 180C_{10} + 45C_{11} + 8400C_{12} - 2100C_{13} + 2800C_{14} - 700C_{15}) \\
 C^{3P_1} &= -\frac{1}{18}\pi(48C_1 - 12C_2 - 528C_3 + 132C_4 + 48C_5 + 96C_6 - 24C_7 + 72C_8 \\
 &\quad - 18C_9 - 60C_{10} + 15C_{11} + 3360C_{12} - 840C_{13} + 2464C_{14} - 616C_{15}) \\
 C^{5P_1} &= -\frac{1}{54}\pi(144C_1 - 36C_2 - 432C_3 + 108C_4 + 432C_5 - 1152C_6 + 288C_7
 \end{aligned}$$

$$\begin{aligned}
 & -648C_8 + 162C_9 + 36C_{10} - 9C_{11} - 3360C_{12} + 840C_{13} + 224C_{14} \\
 & - 56C_{15}) \\
 C^{1P_1-5P_1} &= \frac{4\sqrt{10}}{9}\pi(-12C_6 + 3C_7 + 56C_{14} - 14C_{15}) \\
 C^{3P_2} &= \frac{1}{90}\pi(-240C_1 + 60C_2 + 2640C_3 - 660C_4 + 240C_5 + 1152C_6 - 288C_7 \\
 & - 360C_8 + 90C_9 - 204C_{10} + 51C_{11} - 16800C_{12} + 4200C_{13} - 4256C_{14} \\
 & + 1064C_{15}) \\
 C^{7P_2} &= \frac{1}{135}\pi(-360C_1 + 90C_2 - 3240C_3 + 810C_4 - 1440C_5 + 1512C_6 - 378C_7 \\
 & - 540C_8 + 135C_9 + 36C_{10} - 9C_{11} - 1200C_{12} + 300C_{13} - 16C_{14} + 4C_{15}) \\
 C^{3P_2-7P_2} &= -\frac{2\sqrt{14}}{5}\pi(8C_6 - 2C_7 + 4C_{10} - C_{11} + 16C_{14} - 4C_{15}) \\
 C^{5P_3} &= \frac{1}{27}\pi(-72C_1 + 18C_2 + 216C_3 - 54C_4 + 144C_5 + 216C_6 - 54C_7 + 324C_8 \\
 & - 81C_9 + 72C_{10} - 18C_{11} + 1680C_{12} - 420C_{13} + 368C_{14} - 92C_{15}) \\
 C^{7P_3} &= \frac{1}{54}\pi(-144C_1 + 36C_2 - 1296C_3 + 324C_4 - 144C_5 - 1728C_6 + 432C_7 \\
 & - 216C_8 + 54C_9 - 180C_{10} + 45C_{11} - 480C_{12} + 120C_{13} - 352C_{14} \\
 & + 88C_{15}) \\
 C^{7P_4} &= \frac{1}{18}\pi(-48C_1 + 12C_2 - 432C_3 + 108C_4 + 144C_5 - 72C_8 \\
 & + 18C_9 - 12C_{10} + 3C_{11} - 160C_{12} + 40C_{13} - 32C_{14} + 8C_{15}) \\
 C^{1S_0-5D_0} &= \frac{4}{3}\pi(-12C_6 - 3C_7 + 56C_{14} + 14C_{15}) \\
 C^{3S_1-3D_1} &= -\frac{1}{15\sqrt{3}}\pi(-272C_6 - 68C_7 + 84C_{10} + 21C_{11} - 1344C_{14} - 336C_{15}) \\
 C^{3S_1-7D_1} &= -\frac{2\sqrt{7}}{5}\pi(8C_6 + 2C_7 + 4C_{10} + C_{11} + 16C_{14} + 4C_{15}) \\
 C^{5S_2-1D_2} &= \frac{4}{3\sqrt{5}}(-12C_6 - 3C_7 + 56C_{14} + 14C_{15}) \\
 C^{5S_2-5D_2} &= -\frac{1}{3}\sqrt{\frac{7}{10}}\pi(-48C_6 - 12C_7 + 12C_{10} + 3C_{11} + 64C_{14} + 16C_{15}) \\
 C^{7S_3-3D_3} &= -\frac{2\sqrt{3}}{5}\pi(8C_6 + 2C_7 + 4C_{10} + C_{11} + 16C_{14} + 4C_{15}) \\
 C^{7S_3-7D_3} &= \frac{1}{15\sqrt{3}}\pi(432C_6 + 108C_7 + 36C_{10} + 9C_{11} + 64C_{14} + 16C_{15}) \tag{C.6}
 \end{aligned}$$

C.2 RELATIONS FOR LECS IN SPECTROSCOPIC NOTATION

In the purely nucleonic sector, there are seven constants at next-to-leading order. These constants are contributing to seven matrix elements. For the contact interactions with one or more Δ -isobars the number of matrix elements is larger than the number of constants in the potential. Therefore, the following relations between the LECs at NLO in the partial wave naming scheme can be obtained from Eqs. (C.2) to (C.6).

NN \rightarrow N Δ :

$$\begin{aligned}
 15C^{3P_0} - 15C^{3P_1} - 3\sqrt{5}C^{5P_1-3P_1} + 10C^{5P_2-3P_2} &= 0 \\
 15C^{3P_1} + 3\sqrt{5}C^{5P_1-3P_1} + 5C^{5P_2-3P_2} - 15C^{3P_2} &= 0 \\
 \sqrt{5}C^{5D_0-1S_0} - 5C^{5S_2-1D_2} &= 0
 \end{aligned} \tag{C.7}$$

N Δ \rightarrow N Δ :

$$\begin{aligned}
 3\sqrt{35}C^{3S_1-3D_1} + 5C^{5S_2-5D_2} &= 0 \\
 \sqrt{35}C^{3S_1-5D_1} - 5C^{5S_2-5D_2} &= 0 \\
 \sqrt{7}C^{5S_2-3D_2} + \sqrt{3}C^{5S_2-5D_2} &= 0 \\
 \sqrt{5}(5C^{3P_0} - 5C^{3P_1} - C^{5P_1} + C^{5P_3}) - 10C^{3P_1-5P_1} &= 0 \\
 15C^{3P_1-5P_1} + \sqrt{5}(3C^{5P_1} - C^{3P_2-5P_2} - 5C^{5P_2} + 2C^{5P_3}) &= 0 \\
 \sqrt{5}C^{3P_1} - 4C^{3P_1-5P_1} - \sqrt{5}(C^{3P_2} + C^{5P_1} - C^{5P_2}) &= 0
 \end{aligned} \tag{C.8}$$

NN \rightarrow $\Delta\Delta$:

$$\begin{aligned}
 \sqrt{3}C^{3S_1-7D_1} - \sqrt{7}C^{7S_3-3D_3} &= 0 \\
 \sqrt{5}C^{1S_0-5D_0} - 5C^{5S_2-3D_2} &= 0 \\
 3\sqrt{2}C^{3S_1-3D_1} + \sqrt{7}C^{3S_1-7D_1} - 5C^{5S_2-3D_2} &= 0 \\
 3C^{1P_1-5P_1} + 2\sqrt{2}C^{3P_2} - 2\sqrt{2}C^{3P_0} - \sqrt{7}C^{3P_2-7P_2} &= 0 \\
 2C^{3P_0} + 3C^{3P_1} - 5C^{3P_2} &= 0
 \end{aligned} \tag{C.9}$$

N Δ \rightarrow $\Delta\Delta$:

$$\begin{aligned}
 \sqrt{5}C^{1S_0-5D_0} - 5C^{5S_2-1D_2} &= 0 \\
 \sqrt{10}C^{3S_1-5D_1} + 20C^{5S_2-1D_2} + 5\sqrt{14}C^{5S_2-5D_2} &= 0 \\
 4\sqrt{3}C^{5S_2-1D_2} + \sqrt{42}C^{5S_2-5D_2} - \sqrt{2}C^{5S_2-3D_2} &= 0 \\
 21\sqrt{10}C^{3P_1-5P_1} + 2\sqrt{7}(-10C^{3P_2-7P_2} + 3C^{5P_2-7P_2}) - 7\sqrt{2}C^{3P_2-5P_2} &= 0 \\
 56\sqrt{2}C^{3P_2-5P_2} + 10\sqrt{7}C^{3P_2-7P_2} + 2\sqrt{7}C^{5P_2-7P_2} + 7\sqrt{10}C^{5P_3-7P_3} &= 0 \\
 21\sqrt{2}C^{3P_1} + 98\sqrt{2}C^{3P_2-5P_2} + 2\sqrt{7}(4C^{3P_2-7P_2} + 3C^{5P_2-7P_2}) - 21\sqrt{2}C^{3P_2} &= 0 \\
 98C^{3P_0} + 38\sqrt{14}C^{3P_2-7P_2} - 21C^{3P_1} - 77C^{3P_2} - 45\sqrt{14}C^{5P_2-7P_2} &= 0
 \end{aligned} \tag{C.10}$$

$\Delta\Delta \rightarrow \Delta\Delta$:

$$\begin{aligned}
 & \sqrt{5}C^1S_0^{-5}D_0 - 5C^5S_2^1D_2 = 0 \\
 & 12\sqrt{14}C^5P_1 + 5 \left(8\sqrt{14}C^5P_2 + 40C^7P_2^{-3}P_2 + 9\sqrt{14}C^7P_4 \right) \\
 & \quad - \sqrt{14}(52C^5P_3 + 45C^7P_3) = 0 \\
 & 60\sqrt{10}C^1P_1^{-5}P_1 + 48C^3P_1 + 108C^5P_1 + 63C^7P_4 \\
 & \quad - 48C^3P_0 - 80C^5P_2 - 28C^5P_3 - 63C^7P_3 = 0 \\
 & 126C^5P_1 + 70C^5P_2 + 135C^7P_4 - 196C^5P_3 - 100C^7P_2 - 35C^7P_3 = 0 \\
 & 10C^3P_0 + 15C^3P_1 + 14C^5P_3 - 25C^3P_2 - 9C^5P_1 - 5C^5P_2 = 0 \\
 & 6\sqrt{7}C^3S_1^{-3}D_1 + 5\sqrt{70}C^5S_2^{-1}D_2 + 14\sqrt{5}C^5S_2^{-5}D_2 - 7\sqrt{2}C^3S_1^{-7}D_1 = 0 \\
 & \quad \sqrt{3}C^3S_1^{-7}D_1 + \sqrt{7}C^7S_3^{-3}D_3 = 0 \\
 & 4\sqrt{3}C^3S_1^{-7}D_1 + 3\sqrt{7}C^7S_3^{-7}D_3 - \sqrt{30}C^5S_2^{-5}D_2 = 0 \tag{C.11}
 \end{aligned}$$

The existence of these many relations is remarkable, but follows from the possible spin-structure of the NLO contact potentials.

BIBLIOGRAPHY

- [1] H. Yukawa, “On the Interaction of Elementary Particles I,” *Proc. Phys. Math. Soc. Jap.* **17** (1935) 48–57. [Prog. Theor. Phys. Suppl.1,1(1935)].
- [2] S. Weinberg, “Phenomenological Lagrangians,” *Physica* **A96** (1979) 327.
- [3] M. Taketani, “Meson theory. III,” *Prog. Theor. Phys. Suppl.* **3** (1956) 1.
- [4] J. W. Holt, N. Kaiser, and W. Weise, “Nuclear chiral dynamics and thermodynamics,” *Prog. Part. Nucl. Phys.* **73** (2013) 35–83, [arXiv:1304.6350 \[nucl-th\]](#).
- [5] J. Gasser and H. Leutwyler, “Chiral perturbation theory to one loop,” *Annals Phys.* **158** (1984) 142.
- [6] J. Gasser, M. E. Sainio, and A. Svarc, “Nucleons with chiral loops,” *Nucl. Phys.* **B307** (1988) 779–853.
- [7] S. Weinberg, “Nuclear forces from chiral Lagrangians,” *Phys. Lett.* **B251** (1990) 288–292.
- [8] S. Weinberg, “Effective chiral Lagrangians for nucleon-pion interactions and nuclear forces,” *Nucl. Phys.* **B363** (1991) 3–18.
- [9] C. Ordonez, L. Ray, and U. van Kolck, “The two nucleon potential from chiral Lagrangians,” *Phys. Rev.* **C53** (1996) 2086–2105, [arXiv:hep-ph/9511380](#).
- [10] U. van Kolck, “Few nucleon forces from chiral Lagrangians,” *Phys. Rev.* **C49** (1994) 2932–2941.
- [11] V. Bernard, N. Kaiser, and U.-G. Meißner, “Chiral dynamics in nucleons and nuclei,” *Int. J. Mod. Phys.* **E4** (1995) 193–346, [arXiv:hep-ph/9501384](#).
- [12] N. Kaiser, R. Brockmann, and W. Weise, “Peripheral nucleon-nucleon phase shifts and chiral symmetry,” *Nucl. Phys.* **A625** (1997) 758–788, [arXiv:nucl-th/9706045](#).
- [13] N. Kaiser, S. Gerstendörfer, and W. Weise, “Peripheral NN scattering: Role of delta excitation, correlated two pion and vector meson exchange,” *Nucl. Phys.* **A637** (1998) 395–420, [arXiv:nucl-th/9802071](#).
- [14] E. Epelbaum, W. Glöckle, and U.-G. Meißner, “Nuclear forces from chiral Lagrangians using the method of unitary transformation. 1. Formalism,” *Nucl. Phys.* **A637** (1998) 107–134, [arXiv:nucl-th/9801064](#).
- [15] E. Epelbaum, W. Glöckle, and U.-G. Meißner, “Nuclear forces from chiral Lagrangians using the method of unitary transformation. 2. The two nucleon system,” *Nucl. Phys.* **A671** (2000) 295–331, [arXiv:nucl-th/9910064](#).

- [16] N. Kaiser, “Chiral 2π exchange NN potentials: Two loop contributions,” *Phys. Rev.* **C64** (2001) 057001, [arXiv:nucl-th/0107064](#).
- [17] N. Kaiser, “Chiral 2π exchange NN potentials: Relativistic $1/M^2$ corrections,” *Phys. Rev.* **C65** (2002) 017001, [arXiv:nucl-th/0109071](#).
- [18] E. Epelbaum, W. Glöckle, and U.-G. Meißner, “The two-nucleon system at next-to-next-to-next-to-leading order,” *Nucl. Phys.* **A747** (2005) 362–424, [arXiv:nucl-th/0405048](#).
- [19] D. R. Entem and R. Machleidt, “Accurate charge dependent nucleon nucleon potential at fourth order of chiral perturbation theory,” *Phys. Rev.* **C68** (2003) 041001, [arXiv:nucl-th/0304018](#).
- [20] E. Epelbaum, H. Krebs, and U. G. Meißner, “Improved chiral nucleon-nucleon potential up to next-to-next-to-next-to-leading order,” *Eur. Phys. J.* **A51** (2015) 53, [arXiv:1412.0142 \[nucl-th\]](#).
- [21] E. Epelbaum, H. Krebs, and U. G. Meißner, “Precision nucleon-nucleon potential at fifth order in the chiral expansion,” *Phys. Rev. Lett.* **115** no. 12, (2015) 122301, [arXiv:1412.4623 \[nucl-th\]](#).
- [22] D. R. Entem, N. Kaiser, R. Machleidt, and Y. Nosyk, “Peripheral nucleon-nucleon scattering at fifth order of chiral perturbation theory,” *Phys. Rev.* **C91** no. 1, (2015) 014002, [arXiv:1411.5335 \[nucl-th\]](#).
- [23] D. R. Entem, N. Kaiser, R. Machleidt, and Y. Nosyk, “Dominant contributions to the nucleon-nucleon interaction at sixth order of chiral perturbation theory,” *Phys. Rev.* **C92** no. 6, (2015) 064001, [arXiv:1505.03562 \[nucl-th\]](#).
- [24] P. Reinert, H. Krebs, and E. Epelbaum, “Semilocal momentum-space regularized chiral two-nucleon potentials up to fifth order,” *Eur. Phys. J.* **A54** (2018) 86, [arXiv:1711.08821 \[nucl-th\]](#).
- [25] A. Bulla and P. U. Sauer, “Inclusion of π NN vertex into delta isobar dynamics,” *Few Body Syst.* **12** (1992) 141–174.
- [26] H. Pöpping, P. U. Sauer, and X.-Z. Zhang, “The two nucleon system above pion threshold: A force model with Δ -isobar and pion degrees of freedom,” *Nucl. Phys.* **A474** (1987) 557–607. [Erratum: *Nucl. Phys.*A550,563(1992)].
- [27] P. U. Sauer, “Three-nucleon forces,” *Int. J. Mod. Phys.* **E23** (2014) 1430015, [arXiv:1407.6841 \[nucl-th\]](#).
- [28] R. Machleidt, “The High precision, charge dependent Bonn nucleon-nucleon potential (CD-Bonn),” *Phys. Rev.* **C63** (2001) 024001, [arXiv:nucl-th/0006014](#).
- [29] A. Deltuva, R. Machleidt, and P. U. Sauer, “Realistic two baryon potential coupling two nucleon and nucleon delta isobar states: Fit and applications to three nucleon system,” *Phys. Rev.* **C68** (2003) 024005.

-
- [30] A. Deltuva, *Three-nucleon hadronic and electromagnetic reactions with Δ -isobar excitation*. PhD thesis, Universität Hannover, 2003.
<http://edok01.tib.uni-hannover.de/edoks/e01dh03/374454701.pdf>.
- [31] T. R. Hemmert, B. R. Holstein, and J. Kambor, “Chiral Lagrangians and $\Delta(1232)$ interactions: Formalism,” *J. Phys.* **G24** (1998) 1831–1859, [arXiv:hep-ph/9712496](https://arxiv.org/abs/hep-ph/9712496).
- [32] N. Fettes and U. G. Meißner, “Pion-nucleon scattering in an effective chiral field theory with explicit spin 3/2 fields,” *Nucl. Phys.* **A679** (2001) 629–670, [arXiv:hep-ph/0006299](https://arxiv.org/abs/hep-ph/0006299).
- [33] S. Scherer and M. R. Schindler, *A primer for chiral perturbation theory*. Springer Berlin Heidelberg, 2012.
- [34] R. Machleidt and D. R. Entem, “Chiral effective field theory and nuclear forces,” *Phys. Rept.* **503** (2011) 1–75, [arXiv:1105.2919](https://arxiv.org/abs/1105.2919) [[nucl-th](#)].
- [35] E. Epelbaum, H.-W. Hammer, and U.-G. Meißner, “Modern theory of nuclear forces,” *Rev. Mod. Phys.* **81** (2009) 1773–1825, [arXiv:0811.1338](https://arxiv.org/abs/0811.1338) [[nucl-th](#)].
- [36] **Particle Data Group** Collaboration, M. Tanabashi *et al.*, “Review of particle physics,” *Phys. Rev.* **D98** no. 3, (2018) 030001.
- [37] V. Baru, C. Hanhart, M. Hoferichter, B. Kubis, A. Nogga, and D. R. Phillips, “Precision calculation of the π^- deuteron scattering length and its impact on threshold π N scattering,” *Phys. Lett.* **B694** (2011) 473–477, [arXiv:1003.4444](https://arxiv.org/abs/1003.4444) [[nucl-th](#)].
- [38] V. Bernard, N. Kaiser, and U.-G. Meißner, “Aspects of chiral pion-nucleon physics,” *Nucl. Phys.* **A615** (1997) 483–500, [arXiv:hep-ph/9611253](https://arxiv.org/abs/hep-ph/9611253).
- [39] E. E. Jenkins and A. V. Manohar, “Baryon chiral perturbation theory using a heavy fermion Lagrangian,” *Phys. Lett.* **B255** (1991) 558–562.
- [40] H. Georgi, “An effective field theory for heavy quarks at low-energies,” *Phys. Lett.* **B240** (1990) 447–450.
- [41] V. Bernard, N. Kaiser, J. Kambor, and U.-G. Meißner, “Chiral structure of the nucleon,” *Nucl. Phys.* **B388** (1992) 315–345.
- [42] S. Weinberg, “Three body interactions among nucleons and pions,” *Phys. Lett.* **B295** (1992) 114–121, [arXiv:hep-ph/9209257](https://arxiv.org/abs/hep-ph/9209257).
- [43] H. P. Stapp, T. J. Ypsilantis, and N. Metropolis, “Phase shift analysis of 310 MeV proton-proton scattering experiments,” *Phys. Rev.* **105** (1957) 302–310.
- [44] B. A. Lippmann and J. Schwinger, “Variational principles for scattering processes. I,” *Phys. Rev.* **79** (1950) 469–480.
- [45] S. Petschauer, *Baryonic forces and hyperons in nuclear matter from $SU(3)$ chiral effective field theory*. Dissertation, Technische Universität München, 2016.
<http://mediatum.ub.tum.de/?id=1285353>.

- [46] S. Petschauer, J. Haidenbauer, N. Kaiser, U.-G. Meißner, and W. Weise, “Hyperons in nuclear matter from SU(3) chiral effective field theory,” *Eur. Phys. J.* **A52** (2016) 15, [arXiv:1507.08808 \[nucl-th\]](#).
- [47] V. G. Kadyshevsky, R. M. Mir-Kasimov, and N. B. Skatchkov, “Quasipotential approach and the expansion in relativistic spherical functions,” *Nuovo Cim.* **A55** (1968) 233–257.
- [48] V. G. Kadyshevsky, “Quasipotential type equation for the relativistic scattering amplitude,” *Nucl. Phys.* **B6** (1968) 125–148.
- [49] V. Baru, E. Epelbaum, J. Gegelia, and X. L. Ren, “Towards baryon-baryon scattering in manifestly Lorentz-invariant formulation of SU(3) baryon chiral perturbation theory,” *Physics Letters B* **798** (2019) 134987, [arXiv:1905.02116 \[nucl-th\]](#).
- [50] W. Glöckle, *The quantum mechanical few-body problem*. Texts and monographs in physics. Springer-Verlag, 1983.
- [51] T. A. Rijken, “Soft two pion exchange nucleon-nucleon potentials,” *Annals Phys.* **208** (1991) 253–298.
- [52] J. Golak, D. Rozpędzik, R. Skibiński, K. Topolnicki, H. Witała, W. Glöckle, A. Nogga, E. Epelbaum, H. Kamada, C. Elster, and I. Fachruddin, “A new way to perform partial wave decompositions of few-nucleon forces,” *Eur. Phys. J.* **A43** (2010) 241–250, [arXiv:0911.4173 \[nucl-th\]](#).
- [53] J. F. Donoghue, “On the marriage of chiral perturbation theory and dispersion relations,” in *International Workshop on Nuclear and Particle Physics: Chiral Dynamics in Hadrons and Nuclei Seoul, Korea, February 6-10, 1995*. 1995. [arXiv:hep-ph/9506205](#).
- [54] J. F. Donoghue, “Dispersion relations and effective field theory,” in *Advanced School on Effective Theories Almunecar, Spain, June 25-July 1, 1995*. 1996. [arXiv:hep-ph/9607351](#).
- [55] R. E. Cutkosky, “Singularities and discontinuities of Feynman amplitudes,” *J. Math. Phys.* **1** (1960) 429–433.
- [56] M. E. Peskin and D. V. Schroeder, *An Introduction to quantum field theory*. Addison-Wesley, Reading, USA, 1995.
- [57] J. Haidenbauer, S. Petschauer, N. Kaiser, U.-G. Meißner, and W. Weise, “Scattering of decuplet baryons in chiral effective field theory,” *Eur. Phys. J.* **C77** (2017) 760, [arXiv:1708.08071 \[nucl-th\]](#).
- [58] V. G. J. Stoks, R. A. M. Klomp, M. C. M. Rentmeester, and J. J. de Swart, “Partial-wave analysis of all nucleon-nucleon scattering data below 350 mev,” *Phys. Rev. C* **48** (1993) 792–815.

- [59] M. Bawin and J. P. Lavine, “Nucleon-nucleon scattering and the Kadyshevsky equation,” *Nucl. Phys.* **B49** (1972) 610–620.
- [60] E. E. Salpeter and H. A. Bethe, “A relativistic equation for bound state problems,” *Phys. Rev.* **84** (1951) 1232–1242.
- [61] P. Büttiker and U.-G. Meißner, “Pion nucleon scattering inside the Mandelstam triangle,” *Nucl. Phys.* **A668** (2000) 97–112, [arXiv:hep-ph/9908247](#).
- [62] H. Krebs, E. Epelbaum, and U.-G. Meißner, “Nuclear forces with delta-excitations up to next-to-next-to-leading order. I. Peripheral nucleon-nucleon waves,” *Eur. Phys. J.* **A32** (2007) 127–137, [arXiv:nucl-th/0703087](#).
- [63] S. Petschauer and N. Kaiser, “Relativistic SU(3) chiral baryon-baryon Lagrangian up to order q^2 ,” *Nucl. Phys.* **A916** (2013) 1–29, [arXiv:1305.3427 \[nucl-th\]](#).

DANKSAGUNG (ACKNOWLEDGMENTS)

Nach etwas mehr als dreieinhalb Jahren Arbeit an dieser Dissertation möchte ich gerne einigen Personen danken, ohne deren Unterstützung diese Arbeit nicht möglich gewesen wäre.

Zuerst gilt mein Dank Norbert Kaiser, der es mir seit meiner Bachelorarbeit ermöglicht hat im Bereich der chiralen effektiven Feldtheorie zu arbeiten und der mir auch die Arbeit an diesem spannenden Projekt ermöglicht hat. Ich möchte ihm für seine Hilfe und seinen Rat während dieser Arbeit danken. Außerdem bin ich sehr dankbar, dass ich die Möglichkeit hatte, an den DPG-Frühjahrstagungen teilzunehmen, auch wenn die diesjährige leider entfallen musste.

Des weiteren danke ich Wolfram Weise für viele hilfreiche und motivierende Diskussionen während unserer T39-Gruppenseminare.

Für finanzielle Unterstützung möchte ich dem chinesisch-deutschen CRC 110 “Symmetries and the Emergence of Structure in QCD” der DFG und der NSFC, dem Excellence Cluster UNIVERSE, dem Excellence Cluster ORIGINS, der TUM Graduate School und der Wilhelm und Else Heraeus-Stiftung danken.

Weiterer Dank gebührt Patrick Reinert, der mir seinen Code zur numerischen Berechnung der Phasenverschiebungen als Grundlage zur Verfügung gestellt und erläutert hat.

Ich danke all meinen gegenwärtigen und ehemaligen Bürokollegen, insbesondere Dominik Gerstung, Qibo Chen, Len Brandes, Bhawani Singh, Egor Streck, Corbinian Wellenhofer, Paul Springer und Stefan Petschauer für die gemeinsame Zeit und die angenehme Arbeitsatmosphäre. Außerdem danke ich Sebastian Steinbeißer für unsere unzähligen Diskussionen über Physik, Programmiersprachen und den Rest der Welt während einer Tasse Kaffee.

Mein besonderer Dank gilt Martin für seine Unterstützung und unsere wunderbare gemeinsame Zeit.

Zu guter Letzt möchte ich meinen Eltern aus tiefstem Herzen danken, dass sie mich all die Jahre unterstützt haben. Ohne euch wäre das alles nicht möglich gewesen!